Università degli Studi di Torino

Scuola di Dottorato in
Scienze della Natura e Tecnologie Innovative

Dottorato in
Scienze Farmaceutiche e Biomolecolari
(XXXII ciclo)

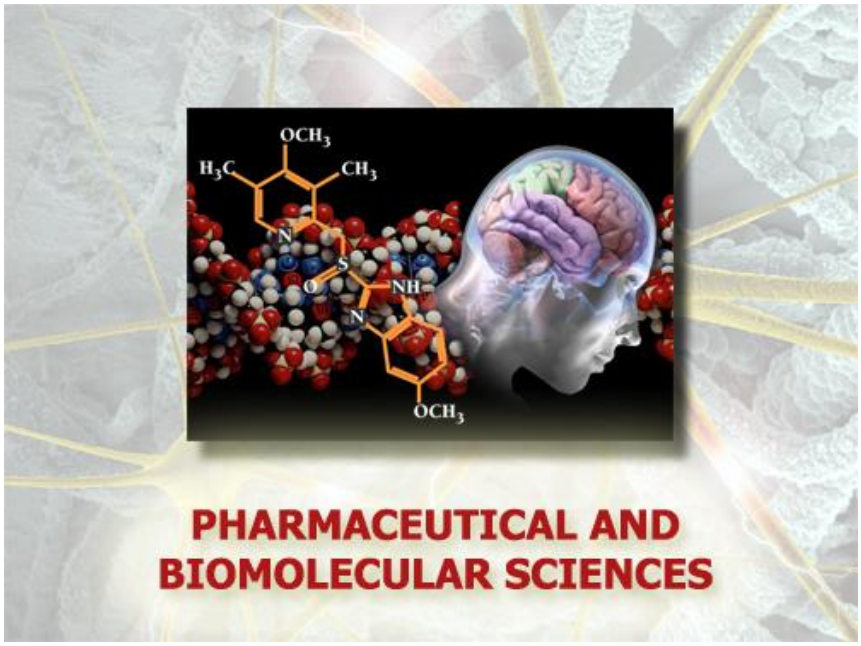

Process Development for the Adsorption/Desorption of Pharmaceuticals and Other Organic Pollutants from Industrial Wastewater

Candidato/a: Xinyu Ge **Tutor(s): Prof. Giancarlo Cravotto**

Università degli Studi di Torino

Dottorato in
Scienze Farmaceutiche e Biomolecolari

Tesi svolta presso il
Dipartimento di Scienza e Tecnologia del Farmaco

CICLO: XXXII

TITOLO DELLA TESI: Process development for the adsorption/desorption of pharmaceuticals and other organic pollutants from industrial wastewater

TESI PRESENTATA DA: Xinyu Ge

TUTOR(S): Professor Giancarlo Cravotto

COORDINATORE DEL DOTTORATO: Professor Gianmario Martra

ANNI ACCADEMICI: 2016/2019

SETTORE SCIENTIFICO-DISCIPLINARE DI AFFERENZA*: Chimica organica (CHIM/06)

Table of Contents

Preface

This thesis is an original intellectual product of the author, Xinyu GE, which is submitted to apply for the degree of Doctor in Pharmaceutical and Biomolecular Sciences at the University of Turin (Italy). The present research herein was conducted under the supervision of Prof. Giancarlo Cravotto and Dr. Zhilin Wu at the Department of Drug Science and Technology of the University of Turin (Italy), between October 2016 and October 2019.

This motivation for this research originated from my passion for developing superior wastewater treatment technologies based on the concept of green and circular economy. In today's society, the environmental pollution has become the leading risk issues and it needs urgently to develop efficient and low-cost treatment processes.

This doctoral study was funded by the University of Turin. This thesis has not been submitted for any other degree, diploma or other qualification at any other university. Two parts of the investigations have been published in the following peer journals: (1) X. Ge *et al.*, Cork wastewater purification in a cooperative flocculation adsorption process with microwave-regenerated activated carbon. *J. Hazard. Mater.* 360(2018) 412-419; (2) X. Ge *et al.*, Adsorptive recovery of Iopamidol from aqueous solution and parallel reuse of activated carbon: batch and flow study. *Ind. Eng. Chem. Res.* 58(2019) 7284-7295.

Acknowledgements

It is a real pleasure to have reached this moment after three years of doctoral study and the process of writing this thesis lately. Studying for a doctorate has been a truly life-changing experience for me and it would not have been possible to do without the support and guidance that I received from numerous people. Here I take this opportunity to express my sincere gratitude to the supervisor, committees, colleagues, families, and friends.

First of all, I would like to express my special gratitude to my supervisor Professor Giancarlo Cravotto, for his great support, valuable guidance, and consistent encouragement during the past three years. I am also very grateful for his scientific advice, knowledge, insightful discussions and suggestions. Many thanks to his concern and help during studying and living in Turin. And thanks for him, providing me the opportunity to grow and work in his research group. It is truly an honour to be his Ph.D. student.

I am also heartfelt gratitude to Dr. Zhilin Wu in our research group, he makes tremendous support and guidance for my Ph.D. research. Working with him has undoubtedly turned this tiring process into a real joy in Italy. His strong expertise, cautious optimistic, and patient guidance have all enlightened and accelerated my research. Each time I got stuck in something, he came up with the solution and encouraged me a lot.

My thanks also go out to all the support and guidance I received three months' internship in Prof. Dr. Kunz Werner group at the University of Regensburg (Germany). Also thanks for Frömel Bianca, Dr. Theresa, and Dr. Marcel helping me a lot during these three months in research and life aspects.

My sincere thanks also go to Prof. Maela Manzoli, who really helped me a lot in characterization materials, preparation presentation, and revision manuscripts. Without her support, it would not be possible to carry out some of the research. Thanks for her kind support, good suggestions and precious time. Also, special thanks to her concern for me in our laboratory.

I also thank my former postgraduate supervisor Prof. Zhansheng Wu. He has been helpful in providing good guidance for my postgraduate career and a chance, advice for doing Ph.D. in Italy.

Besides my supervisor, I would like to thank the rest of my thesis committees: Prof. Deorsola Fabio Alessandro (Polytechnic of Turin) and Dr. Francesco Zimbardi (Enea) for their insightful comments and suggestions, but also for useful questions helping me to widen my research view.

Special mention is given to the Department of Drug and Sciences and Doctoral School of the University of Turin, not only for providing the scholarship and funds that allowed me to undertake this research, but also for giving me the opportunities to attend conferences to meet so many interesting people.

I thank all the members of Professor Cravotto's group: Dr. László Jicsinszky supported me in experiment and data analysis. Dr. Katia Martina helped me in analysis using HPLC/UV; Stefano Mantegna and Dr. Giorgio Grillo supported me in experimental techniques in laboratory. Additionally, thanks for Dr. Emanuela Calcio Gaudino, Dr. Silvia Tabasso, Dr. Luisa Boffa, Veronika Gunjevic, Dr. María Jesús Morán Plata, Francesco Mariatti, Elisa Acciardo, Federica Calsolaro, Ana Luísa Soutelo Maria, Fabio Bucciol, Janet Menzio, Roberto Solarino and Mirko Sacco all kind help and accompany.

I would like to thank my friends Fan Yuan, Yang Jiahui, Masha Mishina, He Xiufang, Du Ziwei, Dong Xiaolu, Thao Anh and Monirul Islam Tutul for their concern and inspirations during this Ph.D.

Last, but not least, I would like to express appreciation to my family. Words cannot express how grateful to my mother and father for all of the sacrifices, consistent love and supports. I also thank my grandparents, aunt, uncle and young brother for great concern, support, and encouragement.

Acronyms and Abbreviations

Table A1. List of the acronyms of materials

Materials	Acronyms
Activated carbon	AC
Coconut powdered activated carbon	CPAC
Coconut granular activated carbon	CGAC
Granular activated carbon	GAC
Granular activated carbon (Merck)	MGAC
Powdered activated carbon	PAC
Peat powdered activated carbon	PPAC
Peat granular activated carbon	PGAC
Powdered activated carbon (Merck)	MPAC
Wood powdered activated carbon	WPAC

Table A2. List of the acronyms and abbreviations of parameters

Parameters	Acronyms and Abbreviations
UV absorbance at 254 nm	UV_{254}
Activated energy	$\boldsymbol{E_a}$
Adsorption capacity	q_e
Adsorption efficiency	*AE*
Chemical oxygen demand	COD
Desorption efficiency	*DE*
Dipole moment	μ
Dissociation constants	pKa
Enthalpy change	ΔH^0
Entropy change	ΔS^0
Formula weight	FW
Gibbs free energy change	ΔG^0
Mesopores volume	V_{meso}
Micropores volume	V_{micro}
Octanol/water partition coefficient	$logK_{ow}$
Polarizability	α
Polyphenols	PP
Removal efficiency	*RE*
Specific surface area	S_{BET}
Total dissolved solid	TDS
Total solid	TS
Total suspended solid	TSS
Water solubility	WS

Table A3. List of the acronyms and abbreviations of compounds and solvents

Compounds/Solvents	Acronyms and Abbreviations
Acetic acid	HOAc
Acetonitrile	ACN
Ammonia solution	NH_3 (aq)
Ceftiofur hydrochloride	CEF
Diethyl ether	Et_2O
Dihydrostreptomycin sulphate	DS
Dimethyl ketone (acetone)	DMK
Dimethylsulfoxide	DMSO
Ethanol	EtOH
Ethylene glycol	EG
Ferrous sulfate heptahydrate	$FeSO_4 \cdot 7H_2O$
gamma Valerolactone	GVL
Hydrogen chloride	HCl
Hydroquinone	HQ
Iopamidol	IOP
Marbofloxacin	MAR
Methanol	MeOH
Methyl ethyl ketone	MEK
N,*N*-Dimethylformamide	DMF
n-Butanol	*n*-BuOH
Non-polar solvents	NPS
n-Propanol	*n*-PrOH
Oxytetracycline	OXY
p-Chlorophenol	PCP
Phenol	PH
p-Hydroxybenzoic acid	PHBA
p-Nitrophenol	PNP
Polar aprotic solvents	PAS
Polar protic solvents	PPS
Potassium bromide	KBr
Sodium hydroxide solution	NaOH (aq)
Sulfamonomethoxine	SMMX
Urea solution	Urea (aq)
Iodinated contrast agents	ICAs

Table A4. List of the acronyms and abbreviations of characterization methods

Characterization methods	Acronyms and Abbreviations
Brunauer-Emmett-Teller	BET
Diffusion reflectance infrared Fourier transform spectroscopy	DRIFTS
Fourier transform infrared spectroscopy	FTIR
High performance liquid chromatography	HPLC
Point of zero charge	PZC
Proton nuclear magnetic resonance	NMR
Scanning electron microscope	SEM
Temperature programmed desorption	TPD
Thermogravimetric analysis	TGA
Transmission electron microscope	TEM
X-ray photoelectron spectroscopy	XPS

Table A5. List of the acronyms and abbreviations used in this study

Others	Acronyms and Abbreviations
Advanced oxidation processes	AOPs
Cork wastewater	CW
Internal diameter	I.D.
International Union of Pure and Applied Chemistry	IUPAC
Maximum residue limit	MRL
Microwave	MW
Microwave-assisted extraction	MAE
Orthogonal array testing	OAT
Relative standard deviation	RSD
Shaking	SK
Standing	ST
Ultrasound	US

Abstract

Water pollution caused by hazardous organic compounds represents a serious environmental issues. The emerging environmental contaminants, including pharmaceuticals and other organic pollutants, have drawn increasing attention, owing to their toxicity, persistence, long-range transport ability and bioaccumulation. Nowadays, the development of efficient, economically viable and environmentally friendly remediation technologies have been hot topics. Due to the high removal efficiency (*RE*), low cost, simple design, and easy operation toward noxious pollutants, the adsorption should be a preferred treatment process. Moreover, activated carbons (ACs) have been globally recognized as the oldest, widely used and most popular adsorbents in wastewater treatments. From economic and environmental viewpoints, there are two challenges about the adsorption process with ACs: the regeneration of spent ACs and recovery of high-value pollutants instead of only transferring the pollutants from liquid phase to adsorbents. With these backgrounds, this doctoral thesis aims at the development of highly efficient adsorption/desorption processes and innovative protocols for various wastewaters containing polyphenols (PP) and other corkwood extracts, phenolic compounds and X−ray contrast agent, as well as veterinary antibiotics. Specific processes involving purification/adsorptive removal, recovery of adsorbates via desorption, and regeneration of adsorbents were designed. This thesis study contains five parts:

(1) Treatment of industrial cork boiling wastewater containing chemical oxygen demand (COD) and PP at high contents. A novel combined method of flocculation/adsorption for cork wastewater (CW) purification and the efficient regeneration of spent ACs with microwave (MW) heating have been illustrated in Fig. A1. Overall effectiveness of flocculation/adsorption process was summarized as follows: 100% of UV_{254} (UV absorbance at 254 nm wavelength values), 98% of COD, 100% of PP, 58% of total solid (TS), 93% of total suspended solid (TSS), and 24% of total dissolved solid (TDS), while the characteristic colour of the CW completely disappeared. Additionally, the coconut powdered AC (CPAC) regenerated with MW calcination was recycled for five times without appreciable decrease in adsorption performance.

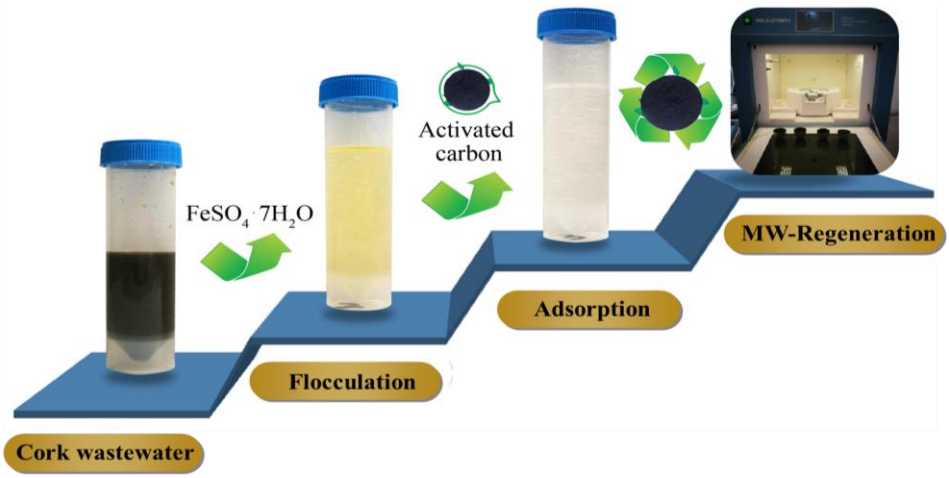

Fig. A1 CW purification using a cooperative flocculation/adsorption process with microwave-regenerated AC

(2) Adsorptive recovery of Iopamidol (IOP) from aqueous solution. An efficient adsorption/desorption process for recovery of high−value of IOP, and regeneration of the adsorbent via solvent elution in a semi-continuous flow mode have been demonstrated in Fig. A2. In a semi-continuous flow system, IOP was well adsorbed on the CPAC-column, hereafter, IOP was efficiently eluted and recovered using methanol. Moreover, the loaded-IOP CPAC was efficiently regenerated and reused in five adsorption/desorption cycles.

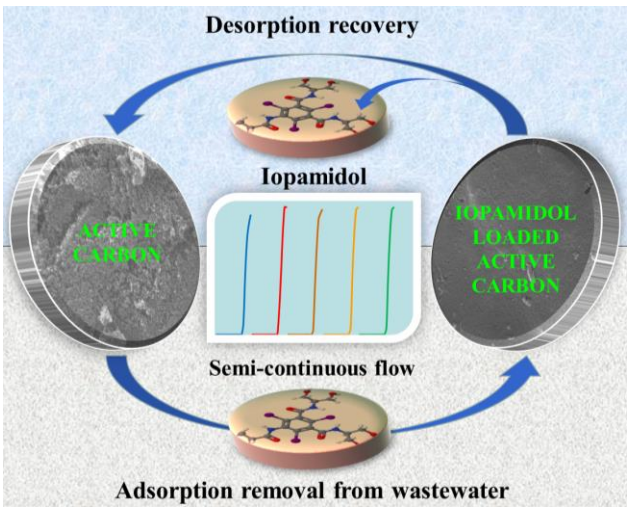

Fig. A2 Adsorptive recovery of IOP from aqueous solution and reuse of ACs in a semi-continuous flow system

(3) Desorption of phenolic compounds from ACs. As shown in Fig. A3, the desorption efficiency (*DE*) of phenols, including *p*-nitrophenol, *p*-chlorophenol, *p*-hydroxybenzoic acid, phenol and hydroquinone, from different ACs with various solvents under shaking (SK); as well as ultrasound (US), MW, and flow mode on desorption studies, thus we gain a deep insight into the feasibility and mechanism of phenols desorption. As a result, the basicity, polarity, and hydrogen bonds of solvents synergistically affect the desorption of phenols. The preferred solvents (Lewis basic solvents, acetic acid and alcohols) gave highly efficient elution. Increasing the alkaline or/and hydrogen bonding interactions, by adding ammonia or urea, enhanced the desorption in most solvents. Moreover, although sonication and MW-heating slightly improved desorption, complete desorption was easily achieved in a flow mode.

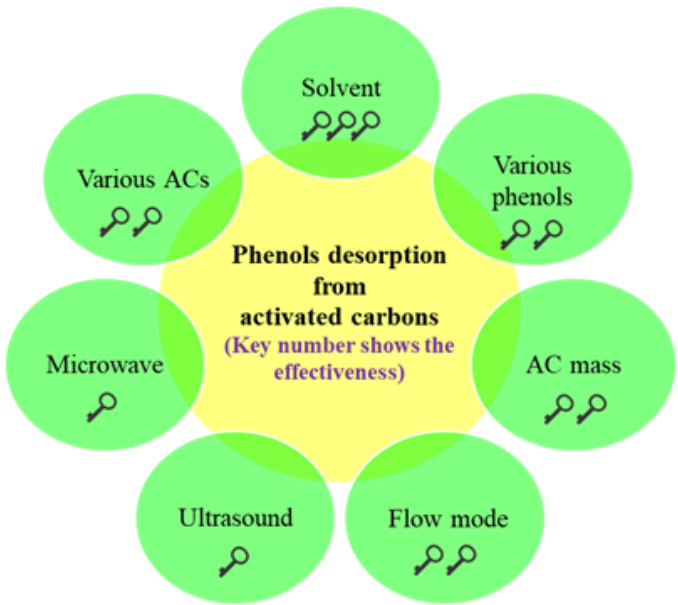

Fig. A3 Effects of various factors on the desorption of phenols from ACs

(4) Modification of ACs using various methods. Wood powdered AC (WPAC) was effectively modified by the oxidation with H_2O_2 under SK, US and MW heating (as shown in Fig. A4), as well as MW calcination (MWC), resulting in enhance the adsorption performance toward antibiotics. As compared with the oxidation with H_2O_2 under SK, US or MW heating accelerated the oxidation. Moreover, various ACs with MW calcination greatly enhanced adsorption efficiency (*AE*) for marbofloxacin (MAR) in aqueous solution.

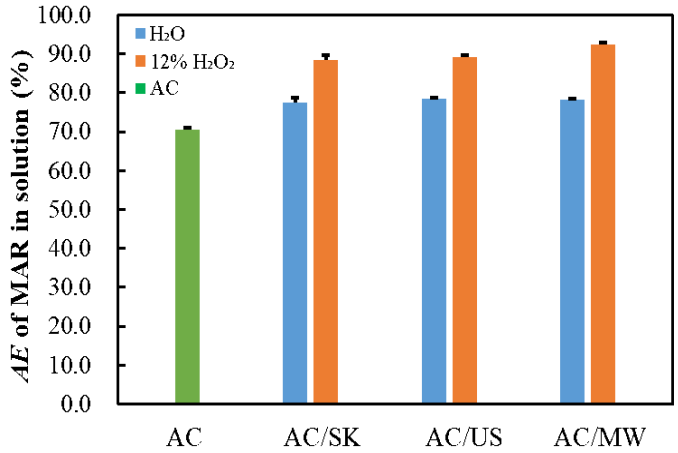

Fig. A4 *AE* values of MAR from aqueous solution by modified ACs under SK, US and MW

(5) Adsorptive removal of residual veterinary antibiotics in milk. The MAR from spiked−milk was removed in batch and flow systems to meet the maximum residue limit (MRL). In a flow mode, 325 mL of 1.0 μg mL^{-1} MAR-spiked milk was efficiently purified through 500 mg granular AC from Merck (MGAC) in a glass column. It was found that 0.066 μg mL^{-1} of MAR residue with 93.4% of *RE* were attained at the end to meet the MRL, as shown in Fig. A5.

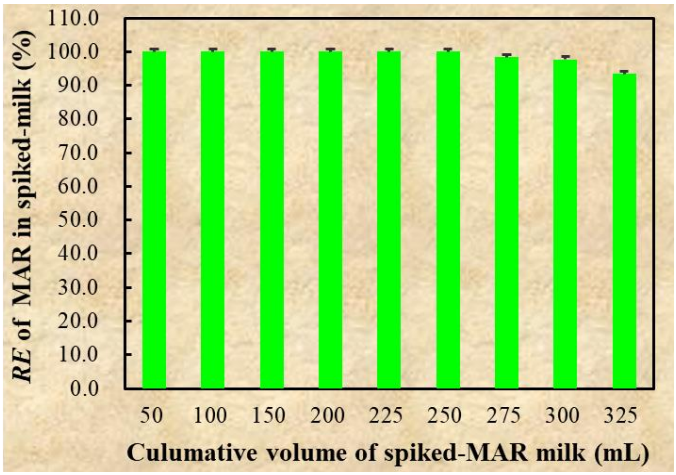

Fig. A5 Dependence of *RE* of MAR on the passed volume of spiked milk in flow mode

By the purification of CW, recovery of IOP, desorption of phenols, and modification of ACs for antibiotics removal; wastewater was efficiently purified; simultaneously valuable components such as IOP and phenols, as well as ACs were well recovered and reused. More importantly, the mechanisms of adsorption/desorption processes were further illustrated.

Chapter 1: Theoretical Part

1.1 Adsorption: fundamentals and applications

1.1.1 Definition of adsorption

Adsorption is the adhesion of atoms, ions or molecules from a gas, liquid or dissolved solid to a surface [1]. Specially, adsorption is a mass transfer process which involves the accumulation of substances at the interface of two phases, such as gas-solid or liquid-solid interface [2]. Adsorption process differs from absorption, adsorption does not actually involve taking in or absorbing of the liquid, gas or dissolved solid into the material, actually, it occurs when a gas or liquid solute makes a molecular or atomic film on the surface of a solid or liquid (Fig. 1.1) [3]. The term adsorption encompasses both processes, while desorption is the reverse of it. The substance being adsorbed is the adsorbate and the adsorbing material is termed the adsorbent. The properties of adsorbates and adsorbents are quite specific and depend upon their constituents [2]. Adsorption process is affected by the nature of the adsorbate and adsorbent, the presence of other pollutants, and experimental conditions (temperature, pH, concentration of pollutants, contact time and particle size of the adsorbent, etc.) [4].

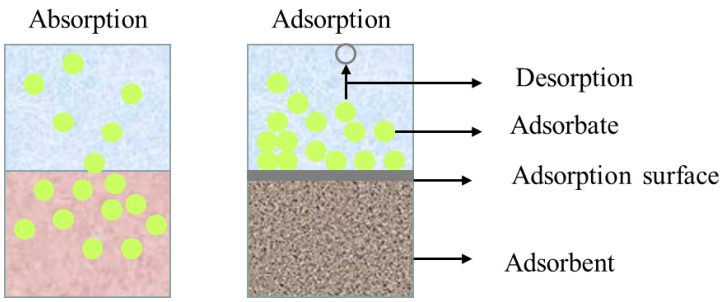

Fig. 1.1 The difference between absorption and adsorption

1.1.2 Mechanism of adsorption

Adsorption is a surface phenomenon in which soluble molecules from a solution are bonded onto a particular substrate [5]. Depending on the type of attractions between adsorbate and adsorbent, adsorption can be classified into two types: “physical adsorption,” also called “physisorption,” and “chemical sorption,” also called “chemisorption”, as shown in Fig. 1.2a.

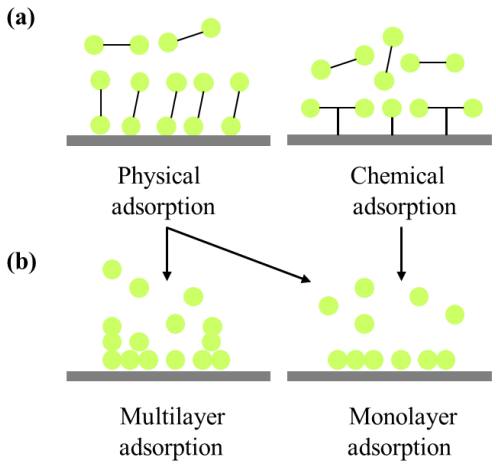

Fig. 1.2 (a) Physical adsorption and chemical adsorption; (b) Multilayer and monolayer adsorption

In physical adsorption, the weak forces such as electrostatic interactions and Van der Waals forces are involved. The strong chemical bonds like covalent bonds are formed between the surface and the adsorbed molecules in chemical adsorption. In this case of physisorption, the attraction interactions are weak, thus the process is reversible [2]. In contrast to physisorption, substances chemisorbed on solid surface are hardly removed and thus chemisorption is an irreversible process [3, 6]. Chemical adsorption is slower than physical adsorption and usually a monolayer (as shown in Fig. 1.2b: right), is formed on the adsorbent surface while physical adsorption occurs quickly and may be monolayer, or multilayer (as shown in Fig. 1.2b: left) [5], not all adsorbates are in contact with the surface layer of the adsorbent. As physical adsorption takes place, it begins as a monolayer. It can then become multilayer, and then, if the pores are close to the size of the molecules, more adsorption occurs until the pores are filled with adsorbate. Besides, the most important difference between physisorption and chemisorption is the magnitude of the enthalpy of adsorption. The change in adsorption enthalpy for physisorption is in the range from -20 to 40 kJ mol^{-1}, however, chemisorption is generally between -400 and -80 kJ mol^{-1} [6, 7]. Moreover, physisorption is performed at low temperatures, however, chemisorption occurs usually at temperatures much higher than the physisorption. The differences between physical and chemical adsorption are compared and summarized in Table 1.1 [8].

Table 1.1 Comparison between physical adsorption and chemical adsorption [8]

Physical adsorption	Chemical adsorption
Electrostatic interactions and Van der Waals forces are involved	Covalent bonds are formed between the surface and the adsorbed molecules
Fast	Slow
Reversible	Irreversible
Not very specific	It is specific
Multilayer/Monolayer	Monolayer
Activation energy is not required	Activation energy is required
It usually occurs at low temperature and decreases when temperature increase	High temperature is needed

Adapted with permission from reference 8, Copyright © 2018 Elsevier Inc.

For a given adsorption process, adsorption isotherm, kinetics and thermodynamic parameters studies are very important to evaluate the adsorption behaviour and mechanism. An adsorption isotherm presents the amount of solute adsorbed per unit weight of adsorbent as a function of the equilibrium concentration in the bulk solution at constant temperature [5]. As to a large amount of the previous adsorption studies, the adsorption isotherm is the most extensively employed method for representing the equilibrium states of an adsorption system, and evaluate the capacity of adsorbents for the adsorption of particular molecules [6]. It also provides important information regarding the magnitude of the enthalpy of adsorption and the relative adsorption ability. In particular, nitrogen adsorption-desorption isotherm of adsorbents can determinate the surface areas, pore volumes, and pore size distribution/average pore diameters of the adsorbent.

There are six types of adsorption isotherms for gas adsorption on the surface of solid adsorbents according to the International Union of Pure and Applied Chemistry (IUPAC) classification, as shown in Fig. 1.3 [9]. As shown in Fig. 1.3, Type I adsorption isotherm describes the adsorption of gas molecules to the adsorbents having micropores such as ACs and the surface of the adsorbent is covered with a monolayer of adsorbed molecules. Type II adsorption isotherm describes the adsorption of gas molecules to the macroporous adsorbents. Type III adsorption

isotherm refers to multilayer adsorption by weak interactions with low energy between adsorbed molecules and the adsorbent having macropores. Type IV and Type V adsorption isotherms models represent the multilayer adsorption together with capillary condensation to the mesoporous adsorbents. Type VI adsorption isotherm illustrates the stepwise formation of a multilayer on the surface of nonporous adsorbent [9, 10].

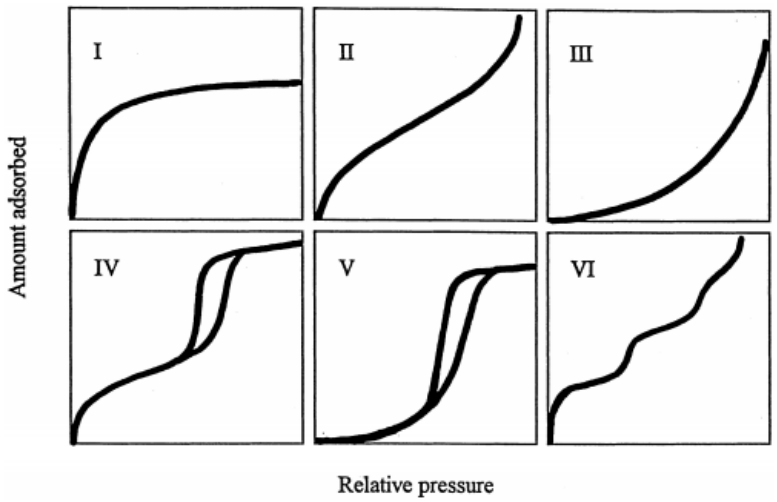

Fig. 1.3 Types of adsorption isotherms, according to the IUPAC classification [9]
Adapted with permission from reference 9. Copyright © 1998 Elsevier Science B.V.

Various adsorption isotherm models such as Langmuir, Freundlich, Temkin, Dubinin-Radushkevich, Harkins-Jura and Halsey, Redlich-Peterson, and Brunauer-Emmett-Teller are used for obtaining detailed information about the interactions between the surface of the adsorbents and molecules to be adsorbed [5, 6, 9]. Among Langmuir and Freundlich isotherms equations apply equally to physisorption as well as to chemisorption [6]. In 1916, Irving Langmuir published a new model isotherm for gases adsorbed to solids. It is a semi-empirical isotherm derived from a proposed kinetic mechanism [11]. It is based on four assumptions: (1) all of the adsorption sites are equivalent, and each site can only accommodate one molecule; (2) the surface is energetically homogeneous, and adsorbed molecules do not interact; (3) there are no phase transitions; (4) at the maximum adsorption, only a monolayer is formed; adsorption only occurs on localized sites on the surface, not with other adsorbates [5, 11]. It is noted that monolayer adsorption is generally described by Langmuir adsorption isotherm [12-14], but

the adsorption isotherms that can be represented by Langmuir adsorption isotherm, which are not necessarily monolayer adsorption [15]. In 1909, Herbert Freundlich gave an expression representing the isothermal variation of adsorption of a quantity of gas adsorbed by unit mass of solid adsorbent with pressure [16]. Freundlich equation is of greater significance for chemisorption, although some physical adsorption data have also been found to fit this equation [5]. However, monolayer or multilayer adsorption is not easy to be figured out by Freundlich equation, mainly depending on the coverage, which is related to the concentration of solution, temperature and other factors. Based in the adsorption thermodynamic equilibrium, Saha and Grappe studies revealed that the mechanism of adsorption can be attributed to two distinct phenomena: micropores filling for micropores adsorption, and surface layering for adsorption into larger pores [10].

Adsorption kinetics is the measure of the adsorption capacity with respect to time at a constant pressure or concentration and is employed to measure the diffusion of adsorbate in the pores [10]. Adsorption kinetics describes the adsorption rate, the equilibrium time of adsorption, and effective factors. Besides, the adsorption kinetics is the base to determine the performance of fixed-bed or any other flow systems [17]. While the adsorption of a compound to the surface of the adsorbent, the complete course of adsorption includes mass transfer and comprises three steps [17, 18, 19]: (1) transport in the bulk of the solution (external diffusion) and diffusion across the liquid film surrounding the sorbent particles (film diffusion); (2) diffusion in the liquid contained in the pores and/or the sorbate along the pore walls (internal diffusion or intra-particle diffusion); (3) adsorption and desorption with the particle and on the external surface or between the adsorbate and active sites.

In order to investigate the mechanism of adsorption and potential rate controlling steps such as mass transport and chemical reaction processes, the pseudo-first-order, pseudo-second-order kinetics models and Elovich equation were applied to study the kinetics of the adsorption process whereas the intraparticle diffusion model was further verified to determine the diffusion mechanism of the adsorption system [20]. Among pseudo-first-order and pseudo-second-order kinetics models follow with these assumption: (1) adsorption only occurs at specific binding sites, which are localized on the surface

of the adsorbent; (2) adsorption energy does not depend on the formation of a layer on the adsorbent surface; (3) the first-order equation or the second-order equation governs the rate of the adsorption process; (4) no interaction occurs between the adsorbed molecules on the surface of the adsorbent [21]. Weber and Morris have proposed intraparticle model to describe the adsorption process. Intraparticle diffusion of solute appears to control the rate of uptake, thus the rate is partially a function of the pore size distribution of the adsorbent, of the molecular size and configuration of the solute, and of the relative electrokinetic properties of adsorbate and adsorbent [22].

Thermodynamics studies are performed to investigate the temperature effect on the adsorption process. Various thermodynamics parameters such as enthalpy change (ΔH^0), Gibbs free energy change (ΔG^0), and entropy change (ΔS^0) are calculated to predict the nature of adsorption [7]. ΔH^0 is used to identify if the adsorption process is endothermic or exothermic. While $\Delta H^0 > 0$, the adsorption process is endothermic; $\Delta H^0 < 0$, the adsorption process is exothermic. ΔG^0 value indicates whether the adsorption process is spontaneous or not. If ΔG_0 value is negative, the adsorption takes places spontaneously. The positive ΔS^0 value suggests the organization of the adsorbate at the solid/solution interface becomes more random, while the negative ΔS^0 value suggests the opposite fact [23]. Arrhenius equation has a vast and important application in determining rate of chemical reactions and for calculation of energy of activation [20]. Moreover, the magnitude of activation energy (E_a) provides that the adsorption type is mainly either physisorption or chemisorption. Physisorption usually has lower E_a in the range of 5–40 kJ mol^{-1}, whereas higher activation energies (40–800 kJ mol^{-1}) suggest chemisorption [24].

1.1.3 Adsorption procedure

In practice, adsorption procedures include static adsorption and dynamic adsorption [25, 26]. In static adsorption (batch mode), a certain amount of adsorbent is mixed continuously with a specific volume of aqueous solution or wastewater until the pollutant in that solution has been decreased to a desired level [6]. The adsorbent is then removed and either discarded or regenerated for use with another volume of solution. The equilibrium and kinetics data obtained

in batch adsorption can provide information for the proper design and optimization of fixed-bed columns [25, 28].

In dynamic adsorption (flow mode) with a packed column of adsorbent, the contaminated fluid is fed continuously through the packed column, which ultimately becomes saturated state by loading contaminants (i.e., adsorbate) [27]. For the dynamic adsorption, it is vital to determine the breakthrough curve, providing the predominant information/technical support for the industrial applications [25, 29]. The dynamic adsorption is also a simple operation and effective treatment procedure in comparison with its batch-mode analogue. Furthermore, the adsorption in a flow system is able to handle large volumes with higher removal efficiency in wastewater treatment [25]. These advantages have driven us to investigate the adsorption/desorption processes of organic pollutants in flow systems.

1.1.4 Applications of adsorption

The word "adsorption" was coined in 1881 by German physicist Heinrich Kayser (1853–1940) [30]. After development, the adsorption has been present in many natural, physical, biological and chemical systems, and it is widely used in industrial applications such as heterogeneous catalysts, ACs, capturing and using waste heat to provide cold water for air conditioning and other process requirements (adsorption chillers), synthetic resins, increasing storage capacity of carbide-derived carbons and water purification [31]. Because water pollution is one of the most serious issues, the wastewater purification has received considerable attention [4, 32, 33]. Various treatment methods, such as coagulation [34], flotation [35], precipitation [36], ozonation [37-39], reverse osmosis [40], ion exchange [41], adsorption [6, 13-15, 19-25, 27] and advanced oxidation processes (AOPs) [27-32], have been employed for the purification of wastewaters. However, the shortcomings of the conventional methods, such as high operational and maintenance costs, generation of sludge/secondary pollutions, and complicated procedures have been found [42]. Comparatively, the adsorption process is considered as a better alternative in wastewater treatments, owing to its high removal efficiency, no formation of harmful by-products, potential of reuse as well as easy operation and scale-up.

1.2 Adsorbents: fundamental and applications

1.2.1 Characteristics and classification of adsorbents

Adsorbent, a solid substance used to collect solute molecules from a liquid or gas, plays a critical role in the adsorption. Usually, a variety of adsorbents are used in the various forms like spherical pellets, rods, granules and powder. Adsorbents mainly include activated alumina, silica gel, molecular sieve (zeolite), carbon-based porous material (ACs), and polymeric adsorbent. Most of adsorbents are manufactured such as ACs, but a few adsorbents like zeolites occur naturally. In general, adsorbents exhibit high abrasion resistance and thermal stability, as well as abundant pore structure, which results in high specific surface area and hence high adsorption capacity [6]. In the IUPAC classification, the pores on the surface of adsorbents are subdivided into three ranges: micropores (below 2 nm); mesopores (also known as transitional pores, 2-50 nm), and macropores (over 50 nm) [43]. Many adsorbents such as carbon materials [44], silica gels [45] and aluminas [46] are amorphous and contain complex networks of inter-connected micropores, mesopores and macropores. In contrast, the pores of zeolites have precise dimensions [47]. All these adsorbents can be categorized in a number of ways. Crini *et al.* classified them as conventional (zeolites, resins, derived from with coals) and non-conventional adsorbents (derived from industrial-, agricultural- and forest-waste) [48]. These conventional adsorbents are the preferred materials for the removal of contaminants, but the high cost restricted their industrial uses. As alternative, non-conventional low-cost adsorbents, mainly natural materials, green- or bio-sorbents were extensively employed [49-55]. In this study, the selective low-cost commercial porous ACs derived from wood, peat, and coconut shells were used. Moreover, various adsorption mechanisms of contaminants have been proposed based on the above classification of adsorbents, namely physisorption, chemisorption, ion-exchange and precipitation [48-50, 56].

1.2.2 Applications of adsorbents

Adsorbents have been extensively applied in various fields, including catalysis, separation and purification, biologic processes and medicine, as well as wastewater treatments [3]. Among many conventional adsorbents (zeolite, resin,

alumina, silica) and new adsorbents such as metal-organic framework (MOF), porous polymer and novel biosorbent, all have been largely reported and efficiently applied in wastewater treatments by adsorption processes [57-63]. For examples, Misaelides reported the application of natural zeolites to the environmental remediation, mainly based on their ion-exchange properties [57]. Sayari *et al.* specifically defined that there has been increasing interest in developing recyclable inorganic adsorbents, particularly for the efficient removal of organic pollutants from aqueous solutions [60]. Khan *et al.* summarized the recent literatures on the adsorptive removal of various hazardous compounds from wastewater by pristine or modified MOF materials [62]. Wang *et al.* presented a novel biosorbent efficiently adsorb of nine dyes in wastewaters [63].

1.3 Activated carbon: fundamental and applications

1.3.1 Activated carbon basics

AC includes a wide range of processed amorphous carbon-based material with highly developed porosity and an extended inter-particulate surface area [64]. Carbon is the major constituent of AC, it also contains other elements such as hydrogen, nitrogen, sulphur, and oxygen. AC is mainly produced from carbonaceous materials, such as coal (bituminous, subbituminous, and lignite), as well as agriculture and forests wastes (e.g. coconut, almond, hazelnut, wood, peat) [63, 65-73], etc. The carbonaceous material is converted to AC under a controlled atmosphere and temperature through two basic processes: (1) physical activation; (2) chemical activation [74]. The properties of AC prepared depend on the nature of the raw material, the activating agent, as well as the reaction conditions [6]. According to the shape of AC, AC is usually divided into two categories: powdered AC (PAC) and granular AC (GAC).

In general, physical characteristics of AC such as surface area and porosity (including pores size, pore volumes and pore size distribution) as well as chemical characteristics represented by pH, functional groups, etc. can affect the performance [75]. For example, the higher porosity provides a large surface area, which results in exceptional adsorptive properties. Depending on technology of production, the specific surface area of AC is in a very wide range from 500 to 3000 $m^2\ g^{-1}$ [76]. According to the IUPAC, AC comprises three types of pores:

macropores; mesopores; and micropores. Micropores generally contribute to the major part of the internal surface area and dominate the adsorption. Macro- and meso–pores is the passageway for adsorbates into the micropores of ACs. Macropores can be visualized using scanning electron microscopy (SEM), not of considerable importance to the adsorption process because their contribution to the surface area of the adsorbent is very small [6]. The pore size distribution and volume is highly important for the practical application, since the adsorption occurs that the pores of ACs are just a little larger than the adsorbate molecules, thus it is the pore volume with this size range that determines adsorption capacity [64]. The surface structure of AC consists of crystalline, porous and chemical structure. According to the crumpled-paper model, the schematic structure of AC is shown in Fig. 1.4 [77].

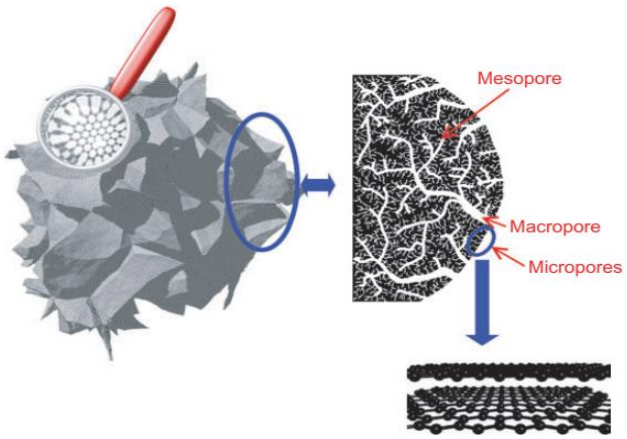

Fig. 1.4 Schematic structure of AC according to the crumpled-paper model (The distorted aromatic carbon sheets are loosely stacked, leading to macro-, meso- and micro-pores. The latter may be seen locally as being slit-shaped) [77]

The surface chemistry of AC essentially depends on their heteroatom content, mainly on their surface oxygen complex content. They determine the charge of the surface, its hydrophobicity, and the electronic density of the graphene layers. Moreover, surface functional groups and the delocalized electrons of the carbon structure also determine the acidic or basic characters [62]. The acidic character is closely related to the oxygen-containing surface groups [62, 78]. Generally, these groups are mainly present on the outer surface or edge of the basal plane and

contribute toward the chemical nature of the carbon. Thus, the content of oxygen on the surface significantly influences the adsorption capability [62].

The oxygen-containing surface groups is classified into three classes according to their chemical properties: acidic, basic, and neutral. Carboxylic, lactone, phenol, carbonyl, pyrones, ketones, chromene and ether groups observed on ACs surface are depicted in Fig. 1.5. Basicity of AC can be associated with: (1) resonating π-electrons of carbon aromatic rings that attract protons, and (2) basic surface functionalities (e.g. nitrogen-containing groups) that are capable of binding with protons [62, 79]. The certain oxygen-containing surface functionalities like chromene [80], ketone [81], and pyrone [82] also contribute to the carbon basicity (Fig. 1.5).

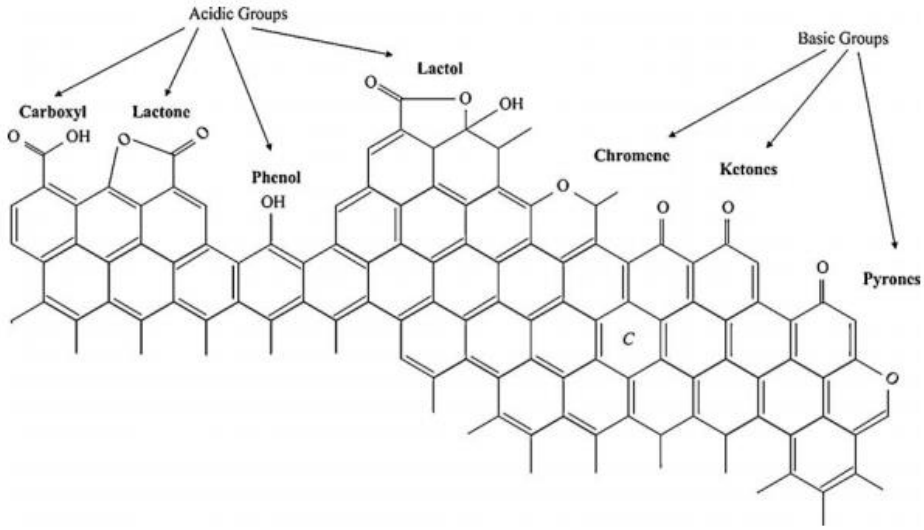

Fig. 1.5 Acidic and basic surface functionalities on a carbon basal plane [79]

Adapted with permission from reference 79. Copyright © 2004 Elsevier Ltd.

Possible structures of the nitrogen functionalities include the following: amide, imide, lactame, pyrrolic, and pyridinic groups [83], which are depicted in Fig. 1.6. However, the basic characteristic of AC arises primarily from delocalized-electrons of graphene layers [79]. The π-electrons of these graphene layers also act as Lewis base.

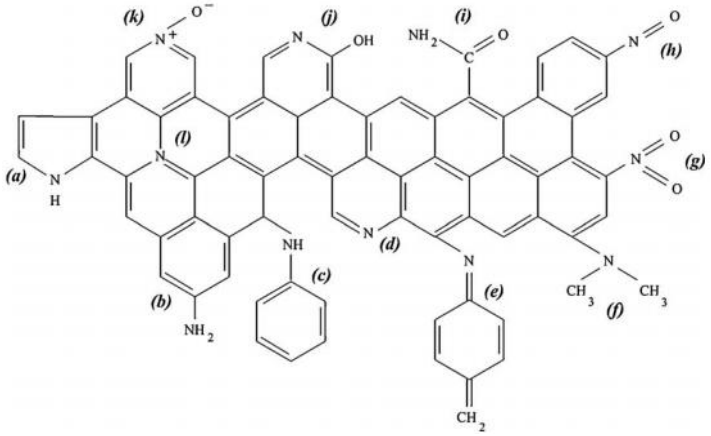

Fig. 1.6 Types of nitrogen surface functional groups: (a) pyrrole, (b) primary amine, (c) secondary amine, (d) pyridine, (e) imine, (f) tertiary amine, (g) nitro, (h) nitroso, (i) amide, (j) pyridone, (k) pyridine-N-oxide, (l) quaternary nitrogen [83]

Adapted with permission from reference 83. Copyright © 2009 Elsevier Ltd.

AC is used in methane and hydrogen storage [84], air purification [85], solvent recovery [86], decaffeination [87], gold purification [88], metal extraction [89], water purification [2, 5, 6, 12-15, 19, 20, 22-24, 33], sewage treatment [90], air filters in gas masks and respirators [32], as well as many other applications, etc. The most important application of AC adsorption is the purification of waste gas and wastewaters. AC is often an excellent and versatile adsorbent for treating pollutants owing to large surface area, well-developed pore structures and a variety of functional groups. More than 800 specific organic and inorganic chemical compounds have been identified in water [5].

In recent years, a number of adsorbents, such as ACs, silica zeolites and porous polymers have been widely employed in the treatment of polluted wastewaters with pharmaceuticals and other organic compounds, while ACs are one of the oldest and important adsorbents utilized for water and wastewater treatment worldwide [91]. The advantages of ACs, such as hydrophobicity, low-cost, and ability to regenerate [92], drive us to apply ACs for the purification of highly polluted wastewaters containing pharmaceuticals and other organic pollutants in this study.

1.3.2 Characterization of activated carbon

The physicochemical properties of ACs play an important role in the adsorption process [4, 75]. The surface structure, morphology and porosity properties are characterized by SEM, Transmission electron microscope (TEM) and N_2 adsorption-desorption isotherm.

The elements content was analysed by Element analyser. X-ray photoelectron spectroscopy (XPS) is used to determine the elemental composition and chemical states of the carbon surface [83]. Carbon-oxygen surface groups on carbons are the most important surface groups, which are analysed using physical, chemical, and physiochemical techniques, including desorption, neutralization with alkalis, zeta potential, thermometric, and spectroscopic methods. However, the precise nature of the chemical groups is not entirely demonstrated [6]. The point of zero charge (pH_{PZC}) values are determined by a mass titration method proposed by Noh and Schwarz [93]. The thermal stability of surface functional groups is characterized by Temperature programmed desorption (TPD) and Thermogravimetric analysis (TGA).

1.3.3 Modification of activated carbon

The physicochemical properties, such as surface functional groups, pore size distribution, pore volume and specific surface area, can be adjusted as needed. Therefore, the modification of adsorbents can gain prominence to increase their affinity, selectivity and capacity for certain contaminants and facilitate their removal in wastewaters [62, 94, 95]. The modification techniques are categorized as follows: (1) physical modification (heating); (2) chemical modification (acidic, base and impregnation of foreign compounds); (3) biological modification. In particle, MW treatment, the oxidation with ozone, hydrogen peroxide, plasma treatment, or other advance oxidation technologies have been prevalent strategies of modification [95-102]. Oxygen containing functionalities are created when the carbon surface is oxidized [103, 104]. Moreover, these oxidation treatments of AC affect the surface chemistry and porous structure, therefore, increasing or decreasing the adsorption performance for organic compounds.

MW heating is usually referred to as “dielectric heating”, as it is generated by the friction between molecules that is caused by interaction with the

electromagnetic field. As we know, AC is a good MW absorber. In recent years, the modification of AC by means of MW irradiation have been attracted great concern, with very promising results [98, 101, 102]. Compared with conventional heating, MW heating has the advantages of rapid temperature rise, uniform temperature distribution and saving of energy. Moreover, MW processing systems are also relatively compact, portable, maintainable and cost effective [105]. Liu *et al.* [98] and our previous studies [101, 102] indicated that the MW-assisted modification of ACs could benefit for adsorption of organic pollutants in solutions. In this study, the commercial ACs was modified with oxidation and MW treatments to enhance the adsorption capacity toward veterinary antibiotics from aqueous solutions. The advantage and disadvantage of these modification techniques are compared in Table 1.2 [95].

Table 1.2 Advantage and disadvantage of existing modification techniques

Modification category	Modification method	Advantage	Disadvantage
Physical	Heating	Increase BET surface area and pores volume	Oxygenated functional groups decomposition
Chemical	Acidic	Increase acidic functional groups	Decrease BET surface area and pores volume
	Basic	Increase the number of basic groups and more apolar surface	Reduce acidic functional groups
	Impregnation with metal / metal salt	Increase BET surface area and pore volume	High-costs
Biological	Microorganism adsorption	Convert a portion of the recalcitrant organics to biodegradable compounds	Hinder diffusion of adsorbate species due to thick films
Oxidative	Ozone/Hydrogen peroxide	Introduce oxygen-containing functional groups	Reduce BET surface area and pore volume
Dielectric heating	MW irradiation	Further carbonization of AC and change the pore structure	Oxygenated functional groups decomposition

Note: Brunauer-Emmett-Teller (BET).

1.3.4 Adsorption of organic pollutants using activated carbon

A variety of synthetic organic compounds are widely produced, used and discharged in chemical, pharmaceutical, and textile industries [106]. In recent years, the occurrence of emerging organic contaminants (e.g. pharmaceuticals, personal care products, endocrine disrupting chemicals, phenols, etc.) in the aquatic environment has been recognized as a serious problem [107-109]. These organic pollutants are compounds of great concern due to their toxicity, persistence, long-range transport ability and bioaccumulation [110].

The adsorption with ACs has been designated by the U.S. Environmental Protection Agency as one of the best available environmental control technologies [111], and it is currently the most frequently used technology for removing organic pollutants from aqueous industrial sludge, surface waters, drinking water and wastewater. The efficient removal of pharmaceuticals and other organic pollutants at trace and high concentration levels in wastewater was clearly evidenced [110, 112-114]. More importantly, no toxic or pharmacologically active products were generated by using AC adsorption [114]. Numerous studies on the adsorption of organics (aromatic compounds) in aqueous solutions have been published, but the intrinsic mechanisms should be better investigated to maximise the process effectiveness. The complex adsorption mechanism of aromatic compounds is proposed as follows: (1) Electrostatic and dispersive interactions between π electrons of the aromatic ring and π electrons of the graphene planes of the ACs surface; (2) Formation of a donor–acceptor complex involving carbonyl groups, which act as donors, and the aromatic ring of organic compounds, acting as acceptor; (3) Formation of hydrogen bridge bonds [113-117]. It is very significant to comprehensive investigation on specific pollutants to deeply understand the adsorption mechanism and promote the application of the adsorption process. Therefore, the pharmaceuticals including IOP and antibiotics, as well as phenols adsorption and desorption processes were studied in this study.

1.4 Desorption and regeneration of activated carbon

The desorption is the reverse process of adsorption, i.e., adsorbates are released from adsorbent [10], as shown in Fig. 1.1. The traditional adsorption is a

nondestructive process involving only a phase change of contaminants (from liquid onto adsorbents) [48], resulting in either secondary pollution or high post-treatment costs if the contaminants cannot be recovered or/and the adsorbents cannot be recycled/reused. From the economy and environmental viewpoint, the desorption process and regeneration of adsorbents are critical to the application of the adsorption process [49]. Therefore, the adsorption can render the wastewater treatment more economical and eco-friendly.

Since several decades, organic compounds from aqueous solutions and wastewaters have been efficiently removed by using ACs [103, 104, 106-110]. In recent years, the solvent elution [118, 119] and related aqueous thermal desorption [120, 121], ultrasonic desorption [122, 123], as well as microwave-assisted desorption [124, 125] have been well applied for the regeneration of spent ACs. Although the adsorption of organic compounds onto ACs is relatively simple, their desorption still poses a variety of challenges due to the high affinity of the compounds to the sorbent surface [126]. Himmelstein *et al.* and Parmele *et al.* have evaluated the economics of AC regeneration and concluded that solvent regeneration can be very competitive with thermal methods [118, 120, 126]. Sutlkno *et al.* stated that AC saturated with phenol has been regenerated with acetone extraction followed by low-pressure steaming in batch or continuous mode [127]. As compared to pyrolytic method, solvent elution requires relatively lower energy consumption and avoids loss of carbon, while enables the recovery of adsorbates [120].

The reversibility of adsorption process depends on the type of binding bonds, such as ionic, covalent bonding, or weak binding forces (Van der Waals' forces or a dipole-dipole interaction), formed between the adsorbent surface and the adsorbates [128]. Specifically, the desorption of adsorbates depends on the accessibility of the solvent to the micropores, the solubility and the adsorbate-carbon surface interactions. The reversible adsorption is attributed to adsorption as a result of Van der Waals forces and/or weak charge-transfer complexes that occur at the adsorption sites, since the adsorption energy is weaker in weaker in physical adsorption [129]. The high energy bonding of adsorbates to the specific functional groups on the active sites of carbon result in covalent bonding. Depending on the type of surface functional group and adsorbates, sufficiently strong bond can form irreversible adsorption.

Chemisorption appears to be the most logical explanation for irreversible adsorption [130, 131]. Thereby, the investigation on the desorption of organic compounds with solvent elution not only illustrates the feasibility of desorption, but also conversely demonstrates the adsorption mechanism.

ACs are effective in removing a large number of organic compounds from water and wastewater. However, the regeneration of spent ACs requires high-energy consumption and high costs [132]. Several methods, such as bio-regeneration [132, 133], thermal regeneration [134], solvent regeneration [120], oxidative regeneration [135] and MW irradiation regeneration [136-138], have been reported. Recently, the efficiency of applying MW heating technology to regenerate industrial waste carbons have been investigated [136-138]. The results are very promising due to the rapid heating of the carbons by MW energy. In addition, ACs regenerated using MW irradiation are long-lived and permit many reuse cycles [138]. For this purpose, the recovery of a high-value of X-ray contrast agent and phenols by desorption with elution and regeneration of ACs under MW irradiation were explored in this study.

1.5 Intensification of enabling technique on the adsorption and desorption processes

Ultrasound (US) is defined by the American National Standards Institute as "sound at frequencies greater than 20 kHz". Thus, US is the sonic wave ranged from about 20 kHz-10 MHz and is subdivided in three main regions: low frequency (20-100 kHz), high frequency (100-1000 kHz), and high frequency (1-10 MHz). Sonochemistry is the application of US to chemical reactions and processes [139]. Usually, the ultrasonic waves of 20-1000 kHz are used in sonochemistry [140]. The origin of sonochemistry is acoustic cavitation, which is the formation, growth and collapse of microbubbles in a liquid. The cavitation can be produced while the local pressure is lower than the vapor pressure of the liquid under sonication [141]. The sonication has been extensively used in the following fields: wastewater treatment [139, 142-144], food and beverages processing [145-147], etc. Under sonication, reaction rates and mass transfer have been significantly

enhanced. It offers the potential for shorter reaction cycles with cheaper reagents under mild conditions, leading to low-costs and perhaps smaller devices [139].

MWs are electromagnetic waves in the frequency range from 300 MHz to 30 GHz. In general, MW generators usually work at 2450 MHz. The electromagnetic energy of MWs is dissipated by substances through three different mechanisms: (1) magnetic losses in ferromagnetic materials; (2) ohmic losses in conducting materials; (3) electric losses caused by electromagnetic inhomogeneities like dipoles and ions [148]. MW-assisted technologies are recognized as a very promising technique to intensify chemical processes [125]. MWs have widely used in preparation, modification, regeneration of ACs, even for enhancing the adsorption and desorption of pollutants in wastewaters [125, 149, 150].

1.5.1 Adsorption and desorption under sonication

US has been proven to be a very useful tool to improve mass transfer process and breaking the affinity between adsorbate and adsorbent [151]. The roles of sonication on adsorption and desorption behaviours of organic compounds have been reported [123, 151, 152]. Hamdaoui *et al.* indicated that the adsorption of *p*-chlorophenol (PCP) onto GAC under sonication is lower than the adsorption under silent conditions; while the desorption is accelerated by increased US intensity due to improvement of diffusion in pores [123]. Schueller and Yang demonstrated that the improvement of sonication on the mass-transfer coefficient and adsorption amounts during the adsorption of phenol onto AC and polymeric resin. Meanwhile, the sonication enhanced the surface diffusivity and decreased the activation energy for surface diffusion to promote the desorption of phenol [152]. Juang *et al.* proved that the initial rate of adsorption and the final amount of desorption are both enhanced by sonication [153]. In this study, the US was used to further verify the enhancement of sonication on the desorption efficiency of PC with solvents.

1.5.2 Microwave-assisted adsorption and desorption

In 1980s, Roussy *et al.* have experimentally studied the dehydration of 13X zeolite with MW heating [154]. They proved that the molecules are directly desorbed by MW irradiation. In the few years, there are various reports about microwave-assisted extraction (MAE) from biomass [146, 155-159], MAE is a

process that removes solutes from a solid matrix into a solvent. Letellier and Budzinski presented that MW assisted extraction of organic compounds at atmospheric pressure is fast and requires less solvent consumption [159]. Robers *et al.* successfully applied MW irradiation for the regeneration of various adsorbents utilized in industry and previously exhausted with different odorous compounds. The adsorbents loaded with any of the odorous substances were fully regenerated under US with water and MW irradiation [160]. MW-assisted desorption strongly depends on the electromagnetic properties of adsorbent and solvents. One can subdivide two mechanisms, the MW-selective and the MW thermal mechanism [150]. However, a little is known about MW-assisted adsorption in aqueous solution and desorption of pharmaceuticals and other organic compounds. Thus, MW heating was used to regenerate the spent ACs and enhance the desorption of phenols with a variety of solvents in this study.

References

[1] "Glossary". The brownfields and land revitalization technology support center, Retrieved, 2009.

[2] De Gisi, S., Lofrano, G., Grassi, M., Notarnicola, M. Characteristics and adsorption capacities of low-cost sorbents for wastewater treatment: a review. Sustainable Materials and Technologies, 9(2016) 10-40.

[3] Saini, V. K., Shankar, A. How to improve selectivity of a material for adsorptive separation applications. Handbook of Environmental Materials Management, 2018, 1-37.

[4] Ali, I., Gupta, V. K. Advances in water treatment by adsorption technology. Nature Protocols, 1(2006) 2661.

[5] Ruthven, D. M. Principles of adsorption and adsorption processes. John Wiley & Sons, 1984.

[6] Bansal, R. C., Goyal, M. Activated carbon adsorption. CRC press, 2005.

[7] Meroufel, B., Benali, O., Benyahia, M., Benmoussa, Y., Zenasni, M. A. Adsorptive removal of anionic dye from aqueous solutions by Algerian kaolin: Characteristics, isotherm, kinetic and thermodynamic studies. Journal of Materials and Environmental Science, 4(2013) 482-491.

[8] Bushra, R., Ahmed, A., Shahadat, M. Mechanism of adsorption on nanomaterials. In Advanced Environmental Analysis, 2016, 90-111.

[9] Donohue M.D., Aranovich G.L. Classification of Gibbs adsorption isotherms. Advances in Colloid and Interface Science, 76 (1998) 137–152.

[10] Saha, D., Grappe, H. A. Adsorption properties of activated carbon fibers. In Activated Carbon Fiber and Textiles Woodhead Publishing. 2017, 143-165.

[11] Langmuir, I. The adsorption of gases on plane surfaces of glass, mica and platinum. Journal of the American Chemical Society, 40(1918) 1361-1403.

[12] Bulut, Y., Aydın, H. A kinetics and thermodynamics study of methylene blue adsorption on wheat shells. Desalination, 194(2006) 259-267.

[13] Tan, I. A. W., Ahmad, A. L., Hameed, B. H. Adsorption of basic dye on high-surface-area activated carbon prepared from coconut husk: Equilibrium, kinetic and thermodynamic studies. Journal of Hazardous Materials, 154(2008) 337-346.

[14] Hameed, B. H., Din, A. M., Ahmad, A. L. Adsorption of methylene blue onto bamboo-based activated carbon: kinetics and equilibrium studies. Journal of Hazardous Materials, 141(2007) 819-825.

[15] Al-Degs, Y. S., El-Barghouthi, M. I., El-Sheikh, A. H., Walker, G. M. Effect of solution pH, ionic strength, and temperature on adsorption behavior of reactive dyes on activated carbon. Dyes and Pigments, 77(2008) 16-23.

[16] Freundlich, H. Capillary chemistry, a representation of the chemistry of colloids and related areas. Academic publishing company, 1909.
[17] Qiu, H., Lv, L., Pan, B. C., Zhang, Q. J., Zhang, W. M., Zhang, Q. X. Critical review in adsorption kinetic models. Journal of Zhejiang University-Science A, 10(2009) 716-724.
[18] Ho, Y. S., Ng, J. C. Y., McKay, G. Kinetics of pollutant sorption by biosorbents. Separation and Purification Methods, 29(2000) 189-232.
[19] Tan, K. L., Hameed, B. H. Insight into the adsorption kinetics models for the removal of contaminants from aqueous solutions. Journal of the Taiwan Institute of Chemical Engineers, 74(2017) 25-48.
[20] Tan, I. A. W., Ahmad, A. L., Hameed, B. H. Adsorption isotherms, kinetics, thermodynamics and desorption studies of 2, 4, 6-trichlorophenol on oil palm empty fruit bunch-based activated carbon. Journal of Hazardous Materials, 164(2009) 473-482.
[21] Lagergren, S. In theory, so-called adsorption gelosterous substance. Royal Swedish Academy of Sciences. Documents, 24 (1898) 1-39.
[22] Weber, W. J., Morris, J. C. Kinetics of adsorption on carbon from solution. Journal of the Sanitary Engineering Division, 89(1963) 31-60.
[23] Liu, Q. S., Zheng, T., Wang, P., Jiang, J. P., Li, N. Adsorption isotherm, kinetic and mechanism studies of some substituted phenols on activated carbon fibers. Chemical Engineering Journal, 157(2010) 348-356.
[24] Hameed, B. H., Ahmad, A. A., Aziz, N. Isotherms, kinetics and thermodynamics of acid dye adsorption on activated palm ash. Chemical Engineering Journal, 133(2007) 195-203.
[25] Ahmed, M. J., Hameed, B. H. Removal of emerging pharmaceutical contaminants by adsorption in a fixed-bed column: a review. Ecotoxicology and Environmental Safety, 149(2018) 257-266.
[26] Xu, Z., Cai, J. G., Pan, B. C. Mathematically modeling fixed-bed adsorption in aqueous systems. Journal of Zhejiang University Science A, 14(2013) 155-176.
[27] Dichiara, A. B., Weinstein, S. J., Rogers, R. E. On the choice of batch or fixed bed adsorption processes for wastewater treatment. Industrial & Engineering Chemistry Research, 54(2015) 8579-8586.
[28] Kizito, S., Wu, S., Wandera, S. M., Guo, L., Dong, R. Evaluation of ammonium adsorption in biochar-fixed beds for treatment of anaerobically digested swine slurry: experimental optimization and modeling. Science of the Total Environment, 563(2016) 1095-1104.
[29] Zuo, L., Ai, J., Fu, H., Chen, W., Zheng, S., Xu, Z., Zhu, D. Enhanced removal of sulfonamide antibiotics by KOH-activated anthracite coal: batch and fixed-bed studies. Environmental Pollution, 211(2016) 425-434.

[30] Kayser, H. (1881). The compression of gases on surfaces in relation to pressure and temperature. Annalen der Physik, 250 (1881) 450-468.
[31] Hussain, A., Bhattacharya, A. (Eds.). Advanced design of wastewater treatment plants: emerging research and opportunities: emerging research and opportunities. IGI Global, 2019.
[32] Noll, K. E. Adsorption technology for air and water pollution control. CRC Press, 1991.
[33] Singh, N. B., Nagpal, G., Agrawal, S. Water purification by using adsorbents: a review. Environmental Technology & Innovation, 11(2018) 187-240.
[34] Jiang, J. Q. The role of coagulation in water treatment. Current Opinion in Chemical Engineering, 8(2015) 36-44.
[35] Rubio, J., Souza, M. L., Smith, R. W. Overview of flotation as a wastewater treatment technique. Minerals Engineering, 15 (2002) 139-155.
[36] Thoma, G. J., Bowen, M. L., Hollensworth, D. Dissolved air precipitation/solvent sublation for oil-field produced water treatment. Separation and Purification Technology, 16(1999) 101-107.
[37] Langlais, B., Reckhow, D. A., Brink, D. R. (Eds.). Ozone in water treatment: application and engineering. Routledge, 2019.
[38] Glaze, W. H. Drinking-water treatment with ozone. Environmental Science & Technology, 21(1987) 224-230.
[39] Glaze, W. H., Kang, J. W., Chapin, D. H. The chemistry of water treatment processes involving ozone, hydrogen peroxide and ultraviolet radiation, 1987, 335-352.
[40] Vourch, M., Balannec, B., Chaufer, B., Dorange, G. Treatment of dairy industry wastewater by reverse osmosis for water reuse. Desalination, 219(2008) 190-202.
[41] Rengaraj, S., Kyeong-Ho Yeon, and Seung-Hyeon Moon. Removal of chromium from water and wastewater by ion exchange resins. Journal of Hazardous Materials, 87 (2001) 273-287.
[42] A. Bhatnagar, M. Sillanpää, A. Witek-Krowiak, Agricultural waste peels as versatile biomass for water purification-a review. Chemical Engineering Journal, 270 (2015) 244–271.
[43] IUPAC (International Union of Pure and Applied Chemistry). Physical chemistry division commission on colloid and surface chemistry, subcommittee on characterization of porous solids: recommendations for the characterization of porous solids (Technical Report). Pure and Applied Chemistry, 66(1994) 1739-1758.
[44] Chuenchom, L., Kraehnert, R., Smarsly, B. M. Recent progress in soft-templating of porous carbon materials. Soft Matter, 8(2012) 10801-10812.

[45] Egeblad, K., Christensen, C. H., Kustova, M., Christensen, C. H. Templating mesoporous zeolites. Chemistry of Materials, 20(2007) 946-960.
[46] Dacquin, J. P., Dhainaut, J., Duprez, D., Royer, S., Lee, A. F., Wilson, K. An efficient route to highly organized, tunable macroporous–mesoporous alumina. Journal of the American Chemical Society, 131(2009) 12896-12897.
[47] Burton, A. W., Ong, K., Rea, T., Chan, I. Y. On the estimation of average crystallite size of zeolites from the Scherrer equation: a critical evaluation of its application to zeolites with one-dimensional pore systems. Microporous and Mesoporous Materials, 117(2009) 75-90.
[48] Crini, G., Lichtfouse, E., Wilson, L. D., Morin-Crini, N. Conventional and non-conventional adsorbents for wastewater treatment. Environmental Chemistry Letters, 17(2019) 195-213.
[49] Crini, G., Lichtfouse, E., Wilson, L. D., Morin-Crini, N. Adsorption-oriented processes using conventional and non-conventional adsorbents for wastewater treatment. In Green Adsorbents for Pollutant Removal Springer, 2018, 23-71.
[50] Crini, G. Non-conventional adsorbents for dye removal. Green Chemistry for Dyes Removal from Wastewater: Research Trends and Applications, 2015, 359-407.
[51] Hernandez-Ramirez, O., Holmes, S. M. Novel and modified materials for wastewater treatment applications. Journal of Materials Chemistry, 18(2008) 2751-2761.
[52] László, K., Bóta, A., Nagyu, L. G. Characterization of activated carbons from waste materials by adsorption from aqueous solutions. Carbon, 35(1997) 593-598.
[53] Gergova, K., Petrov, N., Eser, S. Adsorption properties and microstructure of activated carbons produc Mohan, D., Singh, K. P., Singh, V. K. Removal of hexavalent chromium from aqueous solution using low-cost activated carbons derived from agricultural waste materials and activated carbon fabric cloth. Industrial & Engineering Chemistry Research, 44(2005) 1027-1042.
[54] Mohan, D., Singh, K. P., Singh, V. K. Removal of hexavalent chromium from aqueous solution using low-cost activated carbons derived from agricultural waste materials and activated carbon fabric cloth. Industrial & Engineering Chemistry Research, 44(2005) 1027-1042.
[55] Sivakumar, V., Asaithambi, M., Sivakumar, P. Physico-chemical and adsorption studies of activated carbon from agricultural wastes. Advances in Applied Science Research, 3(2012) 219-226.
[56] Davis, T. A., Volesky, B., Mucci, A. A review of the biochemistry of heavy metal biosorption by brown algae. Water Research, 37(2003) 4311-4330.

[57] Misaelides, P. Application of natural zeolites in environmental remediation: A short review. Microporous and Mesoporous Materials, 144(2011) 15-18.
[58] Elwakeel, K. Z. Environmental application of chitosan resins for the treatment of water and wastewater: a review. Journal of Dispersion Science and Technology, 31(2010) 273-288.
[59] Gupta, V. K., Agarwal, S., Saleh, T. A. Synthesis and characterization of alumina-coated carbon nanotubes and their application for lead removal. Journal of Hazardous Materials, 185(2011) 17-23.
[60] Sayari, A., Hamoudi, S., Yang, Y. Applications of pore-expanded mesoporous silica. 1. Removal of heavy metal cations and organic pollutants from wastewater. Chemistry of materials, 17(2005) 212-216.
[61] Nasef, M. M., Nallappan, M., Ujang, Z. Polymer-based chelating adsorbents for the selective removal of boron from water and wastewater: A review. Reactive and Functional Polymers, 85(2014) 54-68.
[62] Khan, N. A., Hasan, Z., Jhung, S. H. Adsorptive removal of hazardous materials using metal-organic frameworks (MOFs): a review. Journal of Hazardous Materials, 244 (2013) 444-456.
[63] Wang, M. X., Zhang, Q. L., Yao, S. J. A novel biosorbent formed of marine-derived Penicillium janthinellum mycelial pellets for removing dyes from dye-containing wastewater. Chemical Engineering Journal, 259 (2015) 837-844.
[64] Koehlert, K. Activated carbon: fundamentals and new applications. Chemical Engineering, 7(2018) 32-40.
[65] Liu, D., Wu, Z., Ge, X., Cravotto, G., Wu, Z., Yan, Y. Comparative study of naphthalene adsorption on activated carbon prepared by microwave-assisted synthesis from different typical coals in Xinjiang. Journal of the Taiwan Institute of Chemical Engineers, 59(2016) 563-568.
[66] Önal, Y., Akmil-Başar, C., Eren, D., Sarıcı-Özdemir, Ç., Depci, T. Adsorption kinetics of malachite green onto activated carbon prepared from Tunçbilek lignite. Journal of Hazardous Materials, 128((2006) 150-157.
[67] Carrott, P. J. M., Carrott, M. R. Lignin–from natural adsorbent to activated carbon: a review. Bioresource Technology, 98 (2007) 2301-2312.
[68] Uraki, Y., Tamai, Y., Ogawa, M., Gaman, S., Tokura, S. Preparation of activated carbon from peat. BioResources, 4(2009) 205-213.
[69] Singh, C. K., Sahu, J. N., Mahalik, K. K., Mohanty, C. R., Mohan, B. R., Meikap, B. C. Studies on the removal of Pb (II) from wastewater by activated carbon developed from Tamarind wood activated with sulphuric acid. Journal of Hazardous Materials, 153(2008) 221-228.

[70] Yang, K., Peng, J., Srinivasakannan, C., Zhang, L., Xia, H., Duan, X. Preparation of high surface area activated carbon from coconut shells using microwave heating. Bioresource Technology, 101(2010) 6163-6169.
[71] Li, W., Peng, J., Zhang, L., Yang, K., Xia, H., Zhang, S., Guo, S. H. Preparation of activated carbon from coconut shell chars in pilot-scale microwave heating equipment at 60 kW. Waste Management, 29(2009) 756-760.
[72] Hashemian, S., Salari, K., Yazdi, Z. A. Preparation of activated carbon from agricultural wastes (almond shell and orange peel) for adsorption of 2-pic from aqueous solution. Journal of Industrial and Engineering Chemistry, 20(2014) 1892-1900.
[73] Imamoglu, M., Tekir, O. Removal of copper (II) and lead (II) ions from aqueous solutions by adsorption on activated carbon from a new precursor hazelnut husks. Desalination, 228(2008) 108-113.
[74] Mohammad-Khah, A., Ansari, R. Activated charcoal: preparation, characterization and applications: a review article. International Journal of ChemTech Research, 1(2009) 859-864.
[75] Ahmed, M. J., Theydan, S. K. Physical and chemical characteristics of activated carbon prepared by pyrolysis of chemically treated date stones and its ability to adsorb organics. Powder Technology, 229 (2012) 237-245.
[76] Volfkovich, Y. M., Filippov, A. N., Bagotsky, V. S. Structural properties of porous materials and powders used in different fields of science and technology. Springer, 2014.
[77] Oberlin, A. High-resolution TEM studies of carbonization and graphitization. Chemistry and physics of carbon, 22(1989).
[78] Ania, C. O., Parra, J. B., Pis, J. J. Oxygen-induced decrease in the equilibrium adsorptive capacities of activated carbons. Adsorption Science & Technology, 22(2004) 337-351.
[79] Montes-Morán, M. A., Suárez, D., Menéndez, J. A., Fuente, E. On the nature of basic sites on carbon surfaces: an overview. Carbon, 42(2004) 1219-1225.
[80] Garten, V. A., Weiss, D. E., Willis, J. B. A new interpretation of the acidic and basic structures in carbons. II. The chromene-carbonium ion couple in carbon. Australian Journal of chemistry, 10(1957) 309-328.
[81] Contescu, A., Vass, M., Contescu, C., Putyera, K., Schwarz, J. A. Acid buffering capacity of basic carbons revealed by their continuous pK distribution. Carbon, 36(1998) 247-258.
[82] Boehm, H. P. Surface oxides on carbon and their analysis: a critical assessment. Carbon, 40(2002) 145-149.
[83] Pietrzak, R. XPS study and physico-chemical properties of nitrogen-enriched microporous activated carbon from high volatile bituminous coal. Fuel, 88(2009) 1871-1877.

[84] Sun, Y., Liu, C., Su, W., Zhou, Y., Zhou, L. Principles of methane adsorption and natural gas storage. Adsorption, 15(2009) 133-137.
[85] Ao, C. H., Lee, S. C. Indoor air purification by photocatalyst TiO_2 immobilized on an activated carbon filter installed in an air cleaner. Chemical Engineering Science, 60(2005) 103-109.
[86] Ruhl, M. J. Recover VOCs via adsorption on activated carbon. Chemical Engineering Progress, United State, 89(1993).
[87] Katz, S. N. U.S. Patent No. 4,324,840. Washington, DC: U.S. Patent and Trademark Office, 1982.
[88] Bolisetty, S., Mezzenga, R. Amyloid-carbon hybrid membranes for universal water purification. Nature Nanotechnology, 11(2016) 365-371.
[89] Tuzen, M., Saygi, K. O., Soylak, M. Solid phase extraction of heavy metal ions in environmental samples on multiwalled carbon nanotubes. Journal of Hazardous Materials, 152(2008) 632-639.
[90] Vyrides, I., Stuckey, D. C. Saline sewage treatment using a submerged anaerobic membrane reactor (SAMBR): effects of activated carbon addition and biogas-sparging time. Water Research, 43(2009) 933-942.
[91] Mishra, A. K. Smart materials for waste water applications. John Wiley & Sons, 2016.
[92] Plaza, M. G., García, S., Rubiera, F., Pis, J. J., Pevida, C. Post-combustion CO_2 capture with a commercial activated carbon: comparison of different regeneration strategies. Chemical Engineering Journal, 163(2010) 41-47.
[93] Noh, J.S., Schwarz, J.A. Estimation of the point of zero charge of simple oxides by mass titration. Journal of Colloid and Interface Science, 130 (1989) 157–164.
[94] Figueiredo, J. L., Pereira, M. F. R., Freitas, M. M. A., Orfao, J. J. M. Modification of the surface chemistry of activated carbons. Carbon, 37(1999) 1379-1389.
[95] Yin, C. Y., Aroua, M. K., Daud, W. M. A. W. Review of modifications of activated carbon for enhancing contaminant uptakes from aqueous solutions. Separation and Purification Technology, 52(2007) 403-415.
[96] Carabineiro, S. A. C., Thavorn-Amornsri, T., Pereira, M. F. R., Figueiredo, J. L. Adsorption of ciprofloxacin on surface-modified carbon materials. Water Research, 45(2011) 4583-4591.
[97] De la Puente, G., Pis, J. J., Menéndez, J. A., Grange, P. Thermal stability of oxygenated functions in activated carbons. Journal of Analytical and Applied Pyrolysis, 43(1997) 125-138.
[98] Liu, Q. S., Zheng, T., Li, N., Wang, P., Abulikemu, G. Modification of bamboo-based activated carbon using microwave radiation and its effects on

the adsorption of methylene blue. Applied Surface Science, 256(2010) 3309-3315.

[99] Menéndez, J. A., Phillips, J., Xia, B., Radovic, L. R. On the modification and characterization of chemical surface properties of activated carbon: in the search of carbons with stable basic properties. Langmuir, 12(1996) 4404-4410.

[100] Gokce, Y., Aktas, Z. Nitric acid modification of activated carbon produced from waste tea and adsorption of methylene blue and phenol. Applied Surface Science, 313 (2014) 352-359.

[101] Ge, X., Wu, Z., Wu, Z., Yan, Y., Cravotto, G., Ye, B. C. Microwave-assisted modification of activated carbon with ammonia for efficient pyrene adsorption. Journal of Industrial and Engineering Chemistry, 39(2016) 27-36.

[102] Ge, X., Wu, Z., Wu, Z., Yan, Y., Cravotto, G., Ye, B. C. Enhanced PAHs adsorption using iron-modified coal-based activated carbon via microwave radiation. Journal of the Taiwan Institute of Chemical Engineers, 64(2016) 235-243.

[103] Ermolenko, I. N., Lyubliner, I. P., Gulko, N. V. Chemically modified carbon fibers and their applications, 1990.

[104] Jaramillo, J., Álvarez, P. M., Gómez-Serrano, V. Oxidation of activated carbon by dry and wet methods: Surface chemistry and textural modifications. Fuel Processing Technology, 91(2010) 1768-1775.

[105] Bhatnagar, A., Hogland, W., Marques, M., Sillanpää, M. An overview of the modification methods of activated carbon for its water treatment applications. Chemical Engineering Journal, 219(2013) 499-511.

[106] Lapworth, D. J., Baran, N., Stuart, M. E., Ward, R. S. Emerging organic contaminants in groundwater: a review of sources, fate and occurrence. Environmental Pollution, 163 (2012) 287-303.

[107] Heberer, T. Occurrence, fate, and removal of pharmaceutical residues in the aquatic environment: a review of recent research data. Toxicology Letters, 131(2002) 5-17.

[108] Dąbrowski, A., Podkościelny, P., Hubicki, Z., Barczak, M. Adsorption of phenolic compounds by activated carbon-a critical review. Chemosphere, 58(2005) 1049-1070.

[109] Yang, B., Ying, G. G., Zhao, J. L., Liu, S., Zhou, L. J., Chen, F. Removal of selected endocrine disrupting chemicals (EDCs) and pharmaceuticals and personal care products (PPCPs) during ferrate (VI) treatment of secondary wastewater effluents. Water Research, 46(2012) 2194-2204.

[110] Rashed, M. N. Adsorption technique for the removal of organic pollutants from water and wastewater. In Organic Pollutants-Monitoring, Risk and Treatment. 2013, 167-194.

[111] Derbyshire, F., Jagtoyen, M., Andrews, R., Rao, A., Martin-Gullon, I., Grulke, E. A. Carbon materials in environmental applications. Chemistry and Physics of Carbon, 2001, 1-66.

[112] Liu, Z. H., Kanjo, Y., Mizutani, S. Removal mechanisms for endocrine disrupting compounds (EDCs) in wastewater treatment–physical means, biodegradation, and chemical advanced oxidation: a review. Science of the Total Environment, 407(2009) 731-748.

[113] Radovic, L.R. (Ed.), Moreno-Castilla, C., Rivera-Utrilla, J. Carbon materials as adsorbents in aqueous solutions. Chemistry and Physics of Carbon. 2001, 227-406.

[114] Rivera-Utrilla, J., Sánchez-Polo, M., Ferro-García, M. Á., Prados-Joya, G., Ocampo-Pérez, R. Pharmaceuticals as emerging contaminants and their removal from water. A review. Chemosphere, 93(2013) 1268-1287.

[115] Moreno-Castilla, C. Adsorption of organic molecules from aqueous solutions on carbon materials. Carbon, 42(2004) 83-94.

[116] Stoeckli, F., Hugi-Cleary, D. On the mechanisms of phenol adsorption by carbons. Russian Chemical Bulletin, 50(2001) 2060-2063.

[117] Franz, M., Arafat, H. A., Pinto, N. G. Effect of chemical surface heterogeneity on the adsorption mechanism of dissolved aromatics on activated carbon. Carbon, 38(2000) 1807-1819.

[118] Himmelstein K. J., Fox R. D. Winter T. H. In-place regeneration of activated carbon. Chemical Engineering Progress, 69 (1973) 65-69.

[119] Parmele C. S., Alperin E. S. Exner J. H. Nondestructive regeneration of activated carbon a viable chemical engineering technology. Paper presented at the 19th Annual AIChE Meeting, New Orleans, 1981.

[120] Cooney, D. O., Nagerl, A., Hines, A. L. Solvent regeneration of activated carbon. Water Research, 17(1983) 403-410.

[121] Ledesma, B., Román, S., Sabio, E., Álvarez-Murillo, A. Aqueous thermal desorption as an effective way to regenerate spent activated carbons. The Journal of Supercritical Fluids, 85 (2014) 24-30.

[122] Hamdaoui, O., Naffrechoux, E., Suptil, J., Fachinger, C. Ultrasonic desorption of p-chlorophenol from granular activated carbon. Chemical Engineering Journal, 106(2005) 153-161.

[123] Hamdaoui, O., Naffrechoux, E., Tifouti, L., Pétrier, C. Effects of ultrasound on adsorption–desorption of p-chlorophenol on granular activated carbon. Ultrasonics Sonochemistry, 10(2003) 109-114.

[124] Chee, K. K., Wong, M. K., Lee, H. K. Microwave-assisted solvent elution technique for the extraction of organic pollutants in water. Analytica Chimica Acta, 330(1996) 217-227.

[125] Cherbański, R., Molga, E. Intensification of desorption processes by use of microwaves—an overview of possible applications and industrial perspectives. Chemical Engineering and Processing: Process Intensification, 48(2009) 48-58.
[126] Rege, S. U., Yang, R. T., Cain, C. A. Desorption by ultrasound: phenol on activated carbon and polymeric resin. AIChE Journal, 44(1998) 1519-1528.
[127] Sutikno, T., Himmelstein, K. J. Desorption of phenol from activated carbon by solvent regeneration. Industrial & Engineering Chemistry Fundamentals, 22(41983) 420-425.
[128] Ip, A. W. M., Barford, J. P., McKay, G. Reactive Black dye adsorption/desorption onto different adsorbents: effect of salt, surface chemistry, pore size and surface area. Journal of Colloid and Interface Science, 337(2009) 32-38.
[129] Çeçen, F., Aktas, Ö. Activated carbon for water and wastewater treatment: Integration of adsorption and biological treatment. John Wiley & Sons, 2011.
[130] Van der Aa, L. T. J., Rietveld, L. C., Van Dijk, J. C. Effects of ozonation and temperature on the biodegradation of natural organic matter in biological granular activated carbon filters. Drinking Water Engineering and Science, 4(2011) 25-35.
[131] Fang, C. S., Lai, P. M. Microwave regeneration of spent powder activated carbon. Chemical Engineering Communications, 147(1996) 17-27.
[132] Aktaş, Ö., Çeçen, F. Bioregeneration of activated carbon: a review. International Biodeterioration & Biodegradation, 59(2007) 257-272.
[133] Chudyk, W. A., Snoeyink, V. L. Bioregeneration of activated carbon saturated with phenol. Environmental Science & Technology, 18(1984) 1-5.
[134] Sabio, E., González, E., González, J. F., González-García, C. M., Ramiro, A., Ganan, J. Thermal regeneration of activated carbon saturated with p-nitrophenol. Carbon, 42(2004) 2285-2293.
[135] Muranaka, C. T., Julcour, C., Wilhelm, A. M., Delmas, H., Nascimento, C. A. Regeneration of activated carbon by (photo)-Fenton oxidation. Industrial & Engineering Chemistry Research, 49(2009) 989-995.
[136] X.Y. Ge, F. Tian, Z.L. Wu, Y.J. Yan, G. Cravotto, Z.S. Wu, Adsorption of naphthalene from aqueous solution on coal-based activated carbon modified by microwave induction: microwave power effects. Chemical Engineering and Processing: Process Intensification, 91 (2015) 67–77.
[137] F.K. Yuen, B.H. Hameed, Recent developments in the preparation and regeneration of activated carbons by microwaves. Advances in Colloid and Interface Science, 149 (2009) 19–27.

[138] Ania, C. O., Menéndez, J. A., Parra, J. B., Pis, J. J. Microwave-induced regeneration of activated carbons polluted with phenol. A comparison with conventional thermal regeneration. Carbon, 42(2004) 1383-1387.
[139] Adewuyi, Y. G. Sonochemistry: environmental science and engineering applications. Industrial & Engineering Chemistry Research, 40(2001) 4681-4715.
[140] Pollet, B. G. (Ed.), Ashokkumar, M. Introduction to Ultrasound, Sonochemistry and Sonoelectrochemistry. Springer Nature, 2019.
[141]Leong, T., Ashokkumar, M., Kentish, S. The fundamentals of power ultrasound: A review, Acoustics Australia, 39 (2011) 2-43.
[142] Wu, Z. L., Ondruschka, B., Cravotto, G. Degradation of phenol under combined irradiation of microwaves and ultrasound. Environmental Science & Technology, 42(2008) 8083-8087.
[143] Cravotto, G., Binello, A., Di Carlo, S., Orio, L., Wu, Z. L., Ondruschka, B. Oxidative degradation of chlorophenol derivatives promoted by microwaves or power ultrasound: a mechanism investigation. Environmental Science and Pollution Research, 17(2010) 674-687.
[144] Cravotto, G., Di Carlo, S., Curini, M., Tumiatti, V., Roggero, C. A new flow reactor for the treatment of polluted water with microwave and ultrasound. Journal of Chemical Technology & Biotechnology: International Research in Process, Environmental & Clean Technology, 82(2007) 205-208.
[145] Crudo, D., Bosco, V., Cavaglia, G., Mantegna, S., Battaglia, L. S., Cravotto, G. Process intensification in food industry: Hydrodynamic and acoustic cavitation for fresh milk treatment, Agro FOOD Industry Hi Tech, 25 (2014) 55-59.
[146] Cravotto, G., Boffa, L., Mantegna, S., Perego, P., Avogadro, M., Cintas, P. Improved extraction of vegetable oils under high-intensity ultrasound and/or microwaves. Ultrasonics Sonochemistry, 15(2008) 898-902.
[147] Li, Y., Fabiano-Tixier, A. S., Tomao, V., Cravotto, G., Chemat, F. Green ultrasound-assisted extraction of carotenoids based on the bio-refinery concept using sunflower oil as an alternative solvent. Ultrasonics Sonochemistry, 20(2013) 12-18.
[148] Bathen, D. Physical waves in adsorption technology-an overview. Separation and Purification Technology, 33(2003) 163-177.
[149] Turner, M. D., Laurence, R. L., Conner, W. C., Yngvesson, K. S. Microwave radiation's influence on sorption and competitive sorption in zeolites. AIChE Journal, 46(2000) 758-768.
[150] Reuß, J., Bathen, D., Schmidt-Traub, H. Desorption by microwaves: mechanisms of multicomponent mixtures. Chemical Engineering & Technology, 25(2002) 381-384.

[151] Hamdaoui, O., Naffrechoux, E. Adsorption kinetics of 4-chlorophenol onto granular activated carbon in the presence of high frequency ultrasound. Ultrasonics Sonochemistry, 16(2009) 15-22.
[152] Schueller, B. S., Yang, R. T. Ultrasound enhanced adsorption and desorption of phenol on activated carbon and polymeric resin. Industrial & Engineering Chemistry Research, 40(2001) 4912-4918.
[153] Juang, R. S., Lin, S. H., Cheng, C. H. Liquid-phase adsorption and desorption of phenol onto activated carbons with ultrasound. Ultrasonics Sonochemistry, 13(2006) 251-260.
[154] Roussy, G., Zoulalian, A., Charreyre, M., Thiebaut, J. M. How microwaves dehydrate zeolites. The Journal of Physical Chemistry, 88(1984) 5702-5708.
[155] Veggi, P. C., Martinez, J., Meireles, M. A. A. Fundamentals of microwave extraction. In microwave-assisted extraction for bioactive compounds. Springer, 2012, 15-52.
[156] Chemat, F., Cravotto, G. (Eds.). Microwave-assisted extraction for bioactive compounds: theory and practice. Springer Science & Business Media, 4(2012).
[157] Cravotto, G., Binello, A., Orio, L. Green extraction techniques. Agro FOOD Industry Hi-Tech, 22(2011) 57-59.
[158] Leonelli, C., Veronesi, P., Cravotto, G (Eds.). Microwave-assisted extraction: An introduction to dielectric heating. In microwave-assisted extraction for bioactive compounds, Springer, 2012, 1-14.
[159] Letellier, M., Budzinski, H. Microwave assisted extraction of organic compounds. Analusis, 27(1999) 259-270.
[160] Robers, A., Figura, M., Thiesen, P. H., Niemeyer, B. Desorption of odor-active compounds by microwaves, ultrasound, and water. AIChE Journal, 51(2005) 502-510.

Chapter 2: Activated Carbon and Characterization

2.1 Activated carbons

In this study, different types of commercial ACs were comprehensive investigated including adsorption, desorption behaviour and properties, as well as their regenerations after adsorption. Coconut-derived powdered AC (CPAC) was provided by ACEF SPA, Italy. Wood-derived powdered AC (WPAC), peat-derived powdered AC (PPAC), peat-derived granular AC (PGAC) and coconut-derived granular AC (CGAC) were purchased from Sigma-Aldrich. Besides, commercial granular AC (MGAC, Ref. 102514) and powdered AC (MPAC, Ref. 6412806) were also used in this study and purchased from Merck, Germany. All ACs were oven dried at 110°C for 4 h before use and stored in a vacuum desiccator.

All ACs used were characterized according to the following methods.

2.2 Characterization of activated carbons

In order to investigate the physicochemical characteristics of ACs, the following instruments and methods were used. These samples include the pristine ACs and ACs after adsorption, desorption, and regeneration at 800°C with microwave heating.

2.2.1 Scanning electron microscope

Scanning electron microscope (SEM) was used for characterization of the surface structure and morphology of ACs. Most of the samples were characterized using a ZEISS EVO 50 XVP microscope with a LaB_6 source, operating at 15 kV. Some samples were characterized with a field emission scanning electron microscopy (FESEM) analysis (QUANTA F250).

2.2.2 Transmission electron microscope

Transmission electron microscope (TEM) analyses were carried out using a side entry Jeol JEM 3010-UHR (300 kV), microscope equipped with a LaB_6 filament. The samples were deposited onto a copper grid and coated with a lacey carbon film for analysis. All digital micrographs were acquired using a (2 k × 2 k)-pixel

Gatan US1000 CCD camera with an OXFORD INCA instrument for atomic recognition via energy dispersive X-ray spectroscopy (EDS).

2.2.3 Porosity properties

The porosity properties were evaluated based on the adsorption/desorption isotherms at -196°C by means of an ASAP 2020 instrument (Micromeritics), in order to determine the total specific surface area using the Brunauer-Emmett-Teller (BET) method [161], mesoporous volume and average pore size were calculated using the Barrett-Joyner-Halenda (BJH) model [162], and micropores volume was obtained using the Density-Function-Theory (DFT) model of the ACs [163]. The samples were either in the form of a powder or granule (*ca.* 0.015-0.020 g), outgassed for about 48 hours at 100°C in vacuum (residual pressure 10^{-2} mbar) to completely remove atmospheric contaminants from the sample surfaces [164].

2.2.4 Diffusion reflectance infrared fourier transform spectroscopy and Fourier transform infrared spectroscopy

Diffusion reflectance infrared fourier transform spectroscopy (DRIFTS) is an important tool for the qualitative determination of characteristic functional groups. DRIFTS was acquired by using a Nicolet 6700 instrument equipped with a ThermoFisher Smart accessory and an MCT detector to give information of the surface functional groups, which were collected by averaging 1024 spectra with a spectral resolution of 4 cm^{-1}. The samples were measured in powder form in air with KBr. And the ratio of sample to KBr (w/w, mg/mg) is 1: 100-1: 200.

Fourier transform infrared spectroscopy (FTIR) was taken with a PHI5700 ESCA FTIR system using KBr disks prepared by mixing 0.5% of finely ground carbon sample in KBr. Pellet made of pure powder KBr was used as a reference sample for background measurements. The spectra were recorded from 4000 to 400 cm^{-1} at a resolution of 4 cm^{-1}.

2.2.5 X-ray photoelectron spectroscopy

X-ray photoelectron spectroscopy (XPS) of carbon samples were obtained with a model PHI 5700 ESCA X-ray photoelectron spectrometer. XPS was applied to determine the surface complexes on carbons. XPS analysis was conducted using

Mg Ka X-ray source (1253.6 eV) under a vacuum pressure of 10^6 Pa. The wide scans were conducted from 0 to 1000 eV with a pass energy of 50 eV. High-resolution scans of ACs were performed over the 524–544 eV range for O1s with the pass energy of 20 eV. High-resolution scans of ACs were performed over the 282-294 eV range for C1s with the pass energy of 40 eV.

XPS was employed to study the shifts of the binding energy (BE) of the O1s and C1s coordination atoms in the pristine samples. A curve-fitting based on the Gaussian-Lorentzian function after baseline subtraction using Shirley's method, was applied to the high-resolution spectra of C1s and O1s. Five components are considered to compose the C1s spectra with chemical shifts corresponding to: 284.6 eV (C-C/C-H), 286.0 eV (C-OH/C-O-C), 287.3 eV (C=O), 288.9 eV (COOH/COOR) and 290.3 eV (CO_3^{2-}, π-π*). Conversely, the deconvolution of the O1s spectra gave rise to four peaks at 531.2 eV (O=C), 532.4 eV (O-C), 533.3 eV (R-O-C=O), and 534.3 eV (C-OOH).

2.2.6 Thermogravimetric analysis

Thermogravimetric analysis (TGA) highlight that significant weight loss of sample before and after treatment. A TGA 400 (Perkin Elmer) was used to determine the weight loss of ACs, while thermal analysis was carried out at a heating speed of 10°C min^{-1} from room temperature to 800°C under Argon 5.0 (99.999%) atmosphere with 80 mL min^{-1} of flow rate.

2.2.7 Element analysis

Elemental analysis of carbon, hydrogen, nitrogen and sulphur was carried out using an elementary Analyser (Vario EL cube). The oxygen content was determined by difference.

2.2.8 Point of zero charge

The point of zero charge (PZC) is the pH at which the net surface charge is zero (pH_{PZC}). pH acid-base titration method was conducted with Microprocessor pH meter to determine the pH_{PZC} values of ACs.

References

[161] Brunauer, S., Emmett, P. H., Teller, E. Adsorption of gases in multimolecular layers. Journal of the American Chemical Society, 60(1938) 309-319.

[162] B. Nie, X. Liu, L. Yang, J. Meng, X. Li, Pore structure characterization of different rank coals using gas adsorption and scanning electron microscopy. Fuel, 158 (2015) 908-917.

[163] Ou, D. L., Chevalier, P. M., Mackinnon, I. A., Eguchi, K., Boisvert, R., Su, K. Preparation of microporous ORMOSILs by thermal degradation of organically modified siloxane resin. Journal of Sol-gel Science and Technology, 26(2003) 407-412.

[164] Mandizadeh, S., Sadri, M., Salavati-Niasari, M. Mechanosynthesis and characterization AFe_2O_4 (A: Ni, Cu, Zn)-activated carbon nanocomposite as an effective adsorbent for removal dodecanethiol. Microporous and Mesoporous Materials, 262(2018) 13-22.

Chapter 3: Cork Wastewater Purification and Microwave-Regenerated Activated Carbon

Abstract

Wastewater from cork processing industry presents a high content of organic compounds, such as PP, tannins, with low biodegradability and certain toxicity. The aim of this work is to develop a novel method, combing flocculation/adsorption, to purify cork wastewater (CW). Meanwhile, the spent CPAC was regenerated under MW irradiation. The flocculation treatment with $FeSO_4 \cdot 7H_2O$/NaOH provided high removal efficiencies (*RE*s): 90% of UV_{254}, 86% of COD, 81% of PP, 40% of TS, 62% of TSS, and 18% of TDS. After the flocculation and filtration, CPAC was used to further remove residues of TSS, TDS and dissolved organics. The effects of CPAC amount, pH value and adsorption time have been investigated. It was found that 250 mg is the optimum CPAC amount for the treatment of 50 mL sample at pH 3.5 for 10 min. Overall effectiveness of flocculation/adsorption process was summarized as follows: 100% of UV_{254}, 98% of COD, 100% of PP, 58% of TS, 93% of TSS, and 24% of TDS, while the characteristic colour of the CW after flocculation/adsorption completely disappeared. Additionally, the CPACs regenerated with MW heating maintained their performance and permitted five additional cycles without appreciable decrease in *RE*s of UV_{254}, COD and PP. This simple and scalable process could represent a promising treatment method for highly polluted industrial wastewaters containing organic matter, such as PP, phenolic acids and tannins.

3.1 Introduction

Industrial wastewater treatment is a complex problem due to the presence of a variety of compounds at high concentrations [165]. Based on our previous studies [166], cork boiling wastewater, as an example of the challenge on the treatment and reuse of a complex industrial wastewater, was further explored [167]. Cork is a natural, renewable and biodegradable material obtained from the outer bark of cork oak trees (*Quercus suber* L.), rich in numerous organic compounds (lignin, waxes, PP, etc.) [168], while its potential in the field of platform chemicals is still underestimated. Cork oak predominantly grows in Mediterranean countries (mainly Portugal and Spain) [169] and has a broad range of applications, in particular wine bottle corks. The boiling of cork planks is the

main processing step, along with producing a large amount of dark brown CW due to the high concentrations of PP, the other corkwood extracts such as phenolic acids and tannins [170, 171], as well as sugars and salts [169]. Interestingly, the drive toward developing circular economy has meant that wastewaters are currently attracting a great deal of attention as potential sources of nutrients and low-cost chemical feedstocks [172, 173]. Nevertheless, the sewage and CW highly polluted by PP and others should be treated before they are discharged into municipal sewers or subsequently reused. Accordingly, low-cost and highly effective strategies are of the utmost importance.

In general, CW displays low biodegradability, certain toxicity and reluctance to undergo purification by conventional treatments [170, 173]. Various physical and chemical methods such as coagulation/flocculation [174, 175], flotation [175], membrane filtration [171, 176], adsorption [177, 178] and AOPs [165, 166, 170, 171] have so far been used to improve COD removal and/or promote CW biodegradability. However, each technique has its own disadvantages such as low *RE*, high cost, generation of hazardous products, potential secondary pollution and complex treatments. Thus, it is necessary to develop a simple and more efficient combination process. As a pre-treatment process, flocculation is a simple and efficient method that removes the aggregates formed between flocculants and contaminants, however, lower *RE* of COD was found in CW treatment [179-181]. Adsorption using ACs has been applied both in single and combination with other processes to remove harmful organic compounds, such as polycyclic aromatic hydrocarbon [136, 103], pharmaceuticals [114, 182], dyes [183] and phenols [184], etc., owing to its high efficiency, easy operation, abundant developed internal pore structures and large specific surface area. To the best of our knowledge, although flocculation/adsorption combination was proven to be cheap, simple and highly effective, it has not yet been investigated for use in CW treatment [185]. Notably, the regeneration ability of the adsorbents is a key feature for the full-scale wastewater treatment (industrial applications). MW irradiation has been proposed as a potentially viable technique for regeneration of spent carbonaceous materials due to its fast volumetric heating [186].

The objective of this study is to evaluate the CW purification efficiency by combination of flocculation with adsorption using various ACs. The original CW was firstly pretreated by flocculation and filtration, and then the filtrate was

subjected to adsorption onto ACs. The effects of AC amount, pH value and adsorption time have been studied using a factorial experiment design. Moreover, the flocculation alone, adsorption alone, two-stage adsorption and combination of flocculation/adsorption methods have been compared. Adsorption on PACs and GACs were also studied. MW irradiation has been used to regenerate the exhausted carbons after adsorption, in order to reuse the CPAC. The indicators used to determine the *RE*s were as follows: UV_{254}, COD, PP, TS, TDS, and TSS. Additionally, ACs were characterized by SEM, TEM, porosity properties and TGA.

3.2 Experimental

3.2.1 Chemicals

The used flocculant, ferrous sulfate heptahydrate ($FeSO_4 \cdot 7H_2O$, ≥99.0%) was purchased from Riedel-de Haën. Sodium hydroxide (NaOH, 98%) and hydrochloric acid (HCl, 36%, w/w) were analytical grade and obtained from Sigma-Aldrich and Alfa Aesar, respectively, which were used to adjust the pH of solutions.

3.2.2 Setup

The information of experimental setups is listed in Table 3.1.

Table 3.1 The information of setups used in this study

Apparatus name	Type and Manufacturer	Application
Heating Magnetic Stirrer	AREX VELP Scientifica, Italy	Flocculation process
Liquid Phase Parallel Synthesizer	Heidolph Synthesis 1, Germany	Adsorption process
UV-Visible Spectrophotometer	Cary 60 UV-vis Spectrophotometer, USA	UV_{254} and PP analysis
COD test	Hanna HI839800 COD Test Tube Heater and a Photometer HI 83214 COD, USA	Quantify the content of organic compounds in water
Advance Microwave Synthesis Labstation	MicroSynth, Pyro, Milestone Srl, Italy	Regeneration process
pH Meter	pH 211, HANNA Instruments, USA	pH Measurement
Heating Oven	STF-F52, Falc, Italy	Drying

The main instruments used in this study are shown in Fig. 3.1.

Fig. 3.1 Synthesizer (left); UV-Vis spectrophotometer (middle); MicroSynth (right)

3.2.3 Methodology

3.2.3.1 Pre-treatment by flocculation

The original CW (hereafter denoted as S_0) used was provided by CICYTEX, Mérida (Spain). The barrel containing S_0 was shaken adequately prior to flocculation. Based on our previous research [166], 2.0 g of $FeSO_4 \cdot 7H_2O$ was added to 800 mL of S_0. The mixture was then stirred with 500 rpm at 30°C for 30 min using a magnetic stirrer. After mixing, the pH value was adjusted to *ca.* 9.5 by the addition of 2N NaOH solution, to attain flocculation. The sample was denoted as S_1 after pre-treatment by flocculation.

3.2.3.2 Post-treatment via adsorption on ACs

The effects of CPAC amount, pH value and adsorption time on the *RE*s of UV_{254} for S_1 were studied. The three factors and two levels of orthogonal array testing (OAT) were initially implemented. The effects of critical influence factors at selected levels were estimated through the OAT. Furthermore, the effects of factors at more levels were investigated in detail. In typical runs, 250 mg of CPAC was added into 50 mL of S_1 and shaken in a Liquid Phase Parallel Synthesizer with 450 rpm at 30°C for 10 min. The sample obtained after post-treatment via adsorption on CPAC was denoted S_2.

3.2.3.3 Microwave regeneration of CPAC

The regeneration of CPAC was performed in nickel crucibles fixed in the chamber of the MicroSynth, working at a frequency of 2.45 GHz and a maximum output power of 1500 W. In order to ensure sufficient pyrolysis of adsorbates on

the exhausted carbon, the temperature ramped from 25°C to 800°C in 12 min under N_2 atmosphere with flow rate of 10 NL h^{-1} and then the temperature maintained at 800°C for 3 min.

3.2.3.4 Analysis of water quality indicators

The indicators of water quality such as UV_{254}, COD, PP, TS, TDS and TSS were used to evaluate the *REs*. All experiments are duplicated and errors were shown by the difference between the higher measured value and the average value. If the errors are not visible in Figures, they are smaller than the symbols representing the average values. UV_{254} provides a quick measurement of the organic matter (specifically containing aromatic rings or unsaturated carbon bonds) in water. PP value is the total phenol contents in water. COD can be used to easily quantify the content of organics in water [183]. In this study, the better linear correlations between UV_{254} and COD (R^2 = 0.9885), as well as, UV_{254} and PP (R^2 = 0.9829) were also established (as shown in Supplementary Data (S), Fig. S3.1). Therefore, only UV_{254} was chosen as an indicator during the optimization of adsorption process conditions. Importantly, UV_{254}, PP and COD were detected for the critical treatments.

The UV absorbance of water samples at 254 nm was measured. The comparable UV_{254} values (expressed in cm^{-1}) and its *RE* were calculated in terms of the following equations:

$$UV_{254} = [A/b] \times D \quad (1)$$

$$RE\,(\%) = \frac{UV_{254} - UV_{254}'}{UV_{254}} \times 100\% \quad (2)$$

where *A* is the absorbency value, *b* is optical path of the quartz cuvette in cm and *D* is the dilution factor, UV_{254} is UV_{254} value before treatment, and UV_{254}' is UV_{254} value after treatment.

COD was measured in agreement with EPA 410.4 and ISO 15705:2002 standards. COD reagents and the medium-range EPA dichromate method (25 test vials, HI 93754B-25) were used to measure COD in the 0 to 1500 mg L^{-1} range. PP contents were determined using the Folin-Ciocalteu's reagent, as described by Cicco *et al.* [187]. The absorption of the final mixtures was measured at 725 nm in

1 cm cuvettes in the UV-Vis spectrophotometer described above. The *REs* of COD and PP also were calculated referring to equation (2).

For the TSS measurements, 50 mL of CW sample passed through a 0.45 μm filter membrane and the filter residue in the filter was oven dried to constant weight at 100 ± 2°C. TSS was then calculated by subtracting the weight of the filter. For the TDS measurements, the above filtrate was placed in an evaporating dish and then oven dried to constant weight at 100 ± 2°C. Likewise, TDS was calculated by subtracting the weight of the evaporating dish.

CW quality (S_0) is expressed with various parameters and listed in Table 3.2.

Table 3.2 Water quality of S_0

CW	Parameters						
	pH	UV_{254} (cm^{-1})	COD ($mg\ L^{-1}$)	PP ($mg\ L^{-1}$)	TS ($mg\ L^{-1}$)	TSS ($mg\ L^{-1}$)	TDS ($mg\ L^{-1}$)
S_0	6.4	35.2 [a]	2315.0	178.7	2818.0	1400.0	1418.0

[a] calculated in terms of the detection of the 50-fold-diluted CW.

3.3 Results and discussion

3.3.1 Efficiency of flocculation process

After flocculation, the mixture of CW and flocculant was then allowed to stand overnight at room temperature (**Fig. 3.2**). Afterward, the supernatant was decanted and the sediment was filtered to obtain the filtrate. The filtrate was merged with the supernatant to form the secondary sample (S_1).

Fig. 3.2 Appearance of the CW after flocculation process

(Flocculation conditions: 2.0 g of $FeSO_4 \cdot 7H_2O$ in 800 mL S_0 stirred with 500 rpm at 30°C and pH 9.5 (adjust with 2N NaOH) for 30 min, then stand overnight)

As seen in Fig. 3.2, a large amount of dark brown sediment of floc appeared while the addition of NaOH solution, and then a light yellow supernatant was observed after 30 min because of the solid-liquid separation. Minhalma and De Pinho indicated that the formation of bigger agglomerates by flocculation leads to a higher removal of organic matter, which is reflected in the decreasing values of total organic carbon (TOC) and PP in CW [175]. In this study, the UV_{254} value of CW decreased from 35.2 to 3.66 cm^{-1} after flocculation and the *RE* reached 90%. Meanwhile, the *RE* values of COD, PP, TS, TSS and TDS were 86%, 81%, 40%, 62% and 18%, respectively. Obviously, a certain amount of organic contaminants still presented in the supernatant and required further purification.

3.3.2 Preliminary investigation on the adsorption efficiency

The effects of pH value, CPAC amount and adsorption time on the *RE* of UV_{254} for the S_1 sample were studied in terms of OAT. The results are listed in Table 3.3.

Table 3.3 Adsorption results of S_1 onto CPAC with OAT design

Experiment number	Parameters			UV_{254} value (cm^{-1})	Visual effect
	pH	CPAC amount (mg)	Adsorption time (min)		
1	3.5	100	4	0.44	
2	3.5	200	8	0.26	
3	9.5	100	8	2.10	
4	9.5	200	4	1.73	
$\bar{A}_1$	0.35	1.20	1.10		
$\bar{A}_2$	1.90	0.99	1.20		
R	1.55	0.26	0.085		

Note: $\bar{A}_1$, $\bar{A}_2$ is average value under level 1 or level 2, representing the average UV_{254} value under level 2 for each factor; *R* is the range of $\bar{A}_1$ and $\bar{A}_2$, representing the impact extent or importance of one factor.

As shown in Table 3.3, pH value was verified as the most critical factor as compared with CPAC amount and adsorption time in terms of *R* value. In addition, pH 3.5 is significantly beneficial to the adsorption of S_1 as compared with pH 9.5. Under acidic conditions, dissolved PP compounds such as phenolic acids and tannins exist mostly in their unionized forms, causing increase of hydrophobicity and enhancing adsorption [188, 189]. Similarly, CPAC amount is the second important factor and adsorption time is a less important factor for the adsorption in accordance with *R* value. Furthermore, the color changes after adsorption reflects the difference among UV_{254} values (Table 3.3), indicating the superior decolorizing performance of CPAC [175, 185].

3.3.3 Influence of variables on the adsorption process

Of all the possible conditions, only two levels were chosen in the OAT, so the effect of factors at more levels was further studied in details. Thus the optimal conditions can be precisely achieved.

3.3.3.1 Effect of adsorption time

The effect of adsorption time on the *RE* of S_1 onto CPAC is shown in Fig. 3.3. It was found that UV_{254} value decreased from 3.66 to 0.77 cm^{-1} (79% of *RE*) after only 1 min, and then UV_{254} value further dropped till 3 min. After 3 min, the decrease became very slowly. As depicted in Fig. 3.3, the adsorption equilibrium was achieved after 10 min.

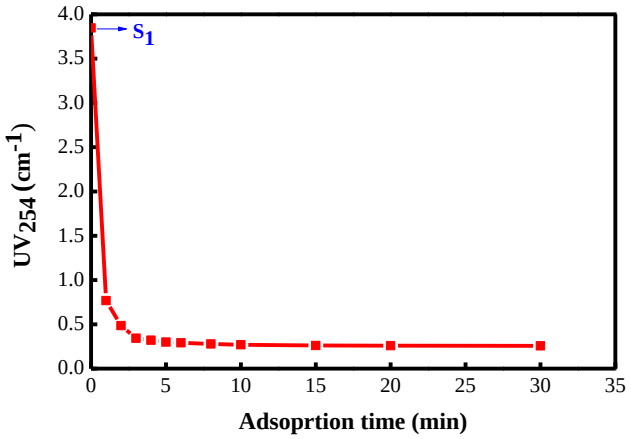

Fig. 3.3 Effect of adsorption time on S_1 adsorption onto CPAC (Adsorption conditions: 100 mg of CPAC in 50 mL S_1 shaken with 450 rpm at 30°C and pH 3.5 for 0-30 min)

The adsorption process onto AC in aqueous solutions includes: (1) diffusion across the boundary layer surrounding the AC particles; (2) mass transfer across the internal surface of the AC particle; (3) adsorption onto a suitable active site at longer adsorption times [190]. The adsorption onto CPAC has been shown to be very fast in this study. Meanwhile, large amounts of dark coloured components were removed by CPAC, leading to significant decrease in UV_{254} values after 10 min. Thus 10 min was chosen as the adsorption time for the following studies.

3.3.3.2 Effect of CPAC amount

The adsorption process is generally a surface phenomenon, which can be significantly affected by surface areas and the number of available active sites in relation to the amount or the mass of the adsorbent [191, 192]. The effect of CPAC amount on the UV_{254} value for S_1 adsorption was illustrated in in Fig. 3.4.

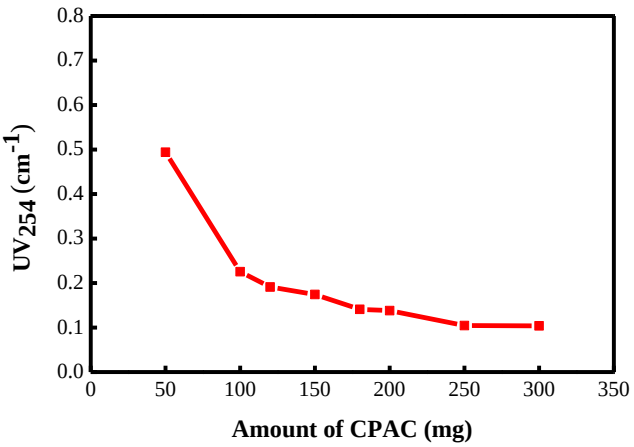

Fig. 3.4 Effect of CPAC amount on S_1 adsorption

(Adsorption conditions: 50-300 mg of CPAC in 50 mL S_1 shaken with 450 rpm at 30°C and pH 3.5 for 10 min)

The UV_{254} value clearly decreases as CPAC amount increases because of the presence of more active sites that are available for adsorption [193]. As shown in Fig. 3.4, the UV_{254} value using 250 mg CPAC is very close to the lowest value using 300 mg CPAC. Taking into consideration economical aspects, the optimization of adsorbent amount for the design of large-scale equipment is mandatory. 250 mg (5 mg mL^{-1}) was thus considered as the optimal CPAC amount for the adsorption of S_1 and was used in the subsequent experiments.

3.3.3.3 Effect of pH value

According to the findings of the preliminary study reported in Section 3.3.2, the pH value is the most factor affecting the performance of adsorption. The effect of pH value from 2.0 to 9.5 on adsorption of S_1 was further studied in details and the results are shown in Fig. 3.5.

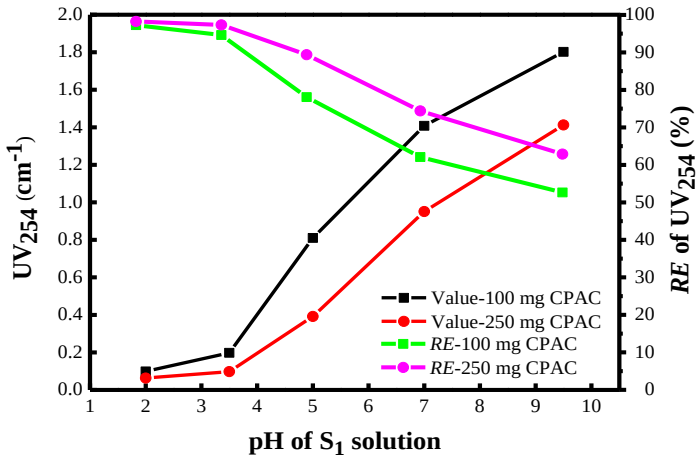

Fig. 3.5 Effect of pH value on S_1 adsorption

(Adsorption conditions: 100 or 250 mg CPAC in 50 mL S_1 shaken with 450 rpm at 30°C and pH 2-10 for 10 min)

As shown in Fig. 3.5, the UV_{254} value increases and the corresponding *RE* decreases as pH value increase from pH 2.0 to 9.5. It was again demonstrated that the acidic condition of wastewater is favourable for adsorption [188]. Moreover, the UV_{254} value and *RE* were very close between at pH 2.0 and pH 3.5. Thus pH 3.5 was then chosen as the optimal pH value for the subsequent experiments from environmental and economical perspectives.

3.3.4 Direct adsorption of cork wastewater

The original CW (S_0) was directly treated using the adsorption process with various amounts of CPAC. The effect of various amounts of CPAC on the UV_{254} values of CW is shown in Fig. 3.6. Obviously, the UV_{254} value decreased gradually as the CPAC amount increased.

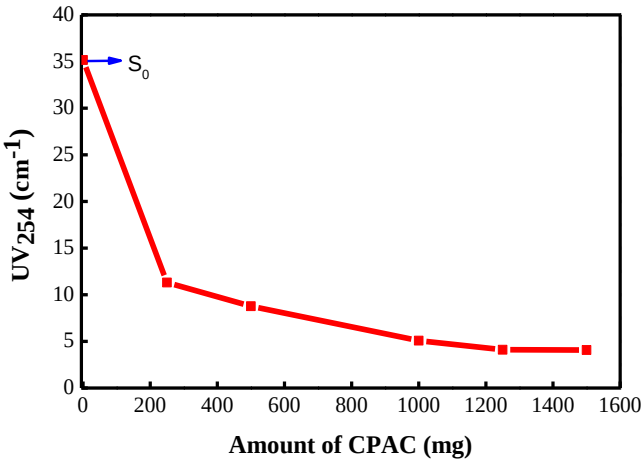

Fig. 3.6 Effect of CPAC amount on S_0 adsorption

(Adsorption conditions: 0-1500 mg of CPAC in 50 mL S_0 shaken with 450 rpm at 30°C and pH 6.4 for 10 min)

The optimal *RE* of UV_{254} value (88%) was achieved in the presence of 1250 mg of CPAC. This *RE* value is comparable with the *RE* (90%) achieved using the flocculation process. However, the decolorization effect observed after the direct adsorption onto CPAC was not as impressive, as shown in Fig. 3.7.

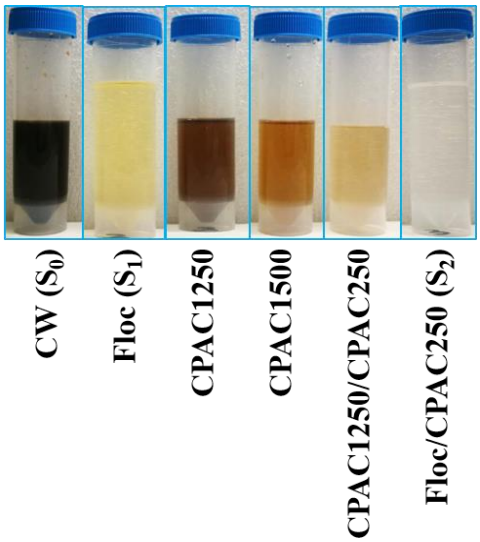

Fig. 3.7 Comparison of decolorization using a variety of treatments

(The meanings of abbreviations specified in Table 3.4)

3.3.5 Removal efficiency using various methods

3.3.5.1 Comparison of removal efficiency among various processes

In order to optimize the treatment process, various processes were examined according to the design shown in Table 3.4.

Table 3.4 Design of various processes based on CPAC adsorption

Processes	Step 1	Step 2
Floc	Flocculation	
CPAC1250	Adsorption with 1250 mg CPAC	-
CPAC1500	Adsorption with 1500 mg CPAC	-
CPAC1250-CPAC250	Adsorption with 1250 mg CPAC	Adsorption with 250 mg CPAC
Floc-CPAC250	Flocculation	Adsorption with 250 mg CPAC

Adsorption Conditions: CPAC in 50 mL S_0 or S_1 shaken with 450 rpm at 30°C for 10 min.

The UV_{254}, PP and COD values before and after treatments were measured to evaluate the *RE* values using various processes. The results are shown in Fig. 3.8.

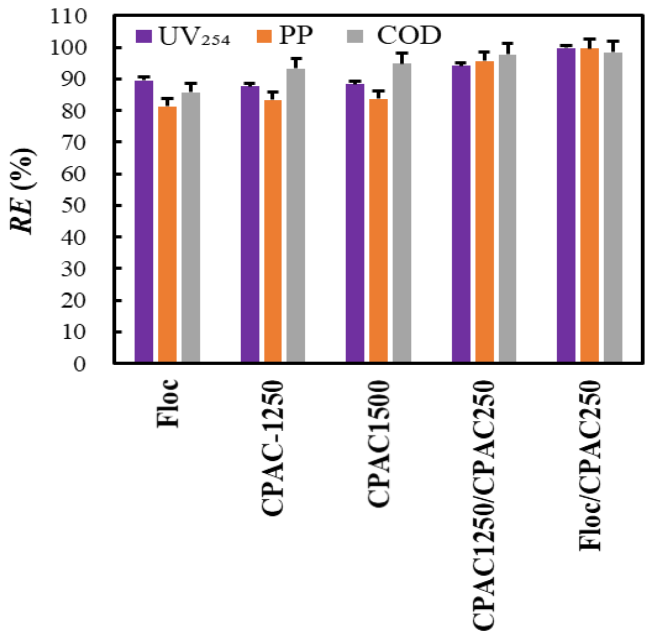

Fig. 3.8 Comparison of *RE* values obtained from various processes
(Flocculation conditions: 2.0 g of $FeSO_4 \cdot 7H_2O$ in 800 mL S_0 stirred with 500 rpm at 30°C and pH 9.5 for 30 min; Adsorption conditions: CPAC in 50 mL S_0 or S_1 shaken with 450 rpm at 30°C for 10 min)

As seen in Fig. 3.8, the *RE* values for S_0 after simple flocculation and after adsorption with 1250 mg and 1500 mg of CPAC are very similar, although wastewater colour after the flocculation process is lighter than that observed after adsorption with CPAC (Fig. 3.7). Using the identical amount of CPAC (1500 mg), the adsorption process for S_0 was designed to be two-stage adsorption (1250 mg CPAC and then 250 mg CPAC). Obviously, the *RE* using two-stage adsorption is higher than that using one-stage adsorption. In particular, the *RE* for the combination of flocculation and adsorption (Floc/CPAC250) was slightly higher than that of the two-stage adsorption (CPAC1250/CPAC250), which is also reflected in the colour change shown in Fig. 3.7. This feature suggests that the combined method (Floc/CPAC250) provides the best decolorization [189, 194]. In conclusion, the single flocculation or adsorption process cannot meet the discharge standards, while the highest *RE*s of UV_{254}, PP, COD and significant decolorization were achieved by cooperative flocculation/adsorption. Considering the dosage and unit price, $FeSO_4 \cdot 7H_2O$ is much more convenient than AC in the pre-treatment. The combined process, the flocculation as pre-treatment and the adsorption as post-treatment is therefore necessary to meet the discharge standards.

3.3.5.2 Comparing the removal efficiencies among onto various ACs

Various ACs were used to investigate the effects of ACs nature on the adsorption process. For the sake of comparing the physical properties of different ACs including CPAC, WPAC, PPAC and CGAAC (Section 2.1), the surface morphology was measured by SEM and shown in Figs. 3.9a-3.9d under magnification 2000×. Moreover, the *RE* values onto various ACs are shown in Fig. 3.10.

As shown in Fig. 3.9a, the particles of pristine CPAC showed a certain degree of roughening. In Fig. 3.9b, the particles of WPAC seem sharper while compared with CPAC; whereas PPAC surface does not show significantly difference from CPAC (Fig. 3.9c). On the other hand, CGAC (Fig. 3.9a) displays a rough and compact external surface (Fig. 3.9d) and similar features were observed inside the broken granules (Figure are not shown here). In addition, CPAC images from TEM under magnification 150000× and 300000× were depicted in Fig. S3.2. A large amount of pores on its surface were observed.

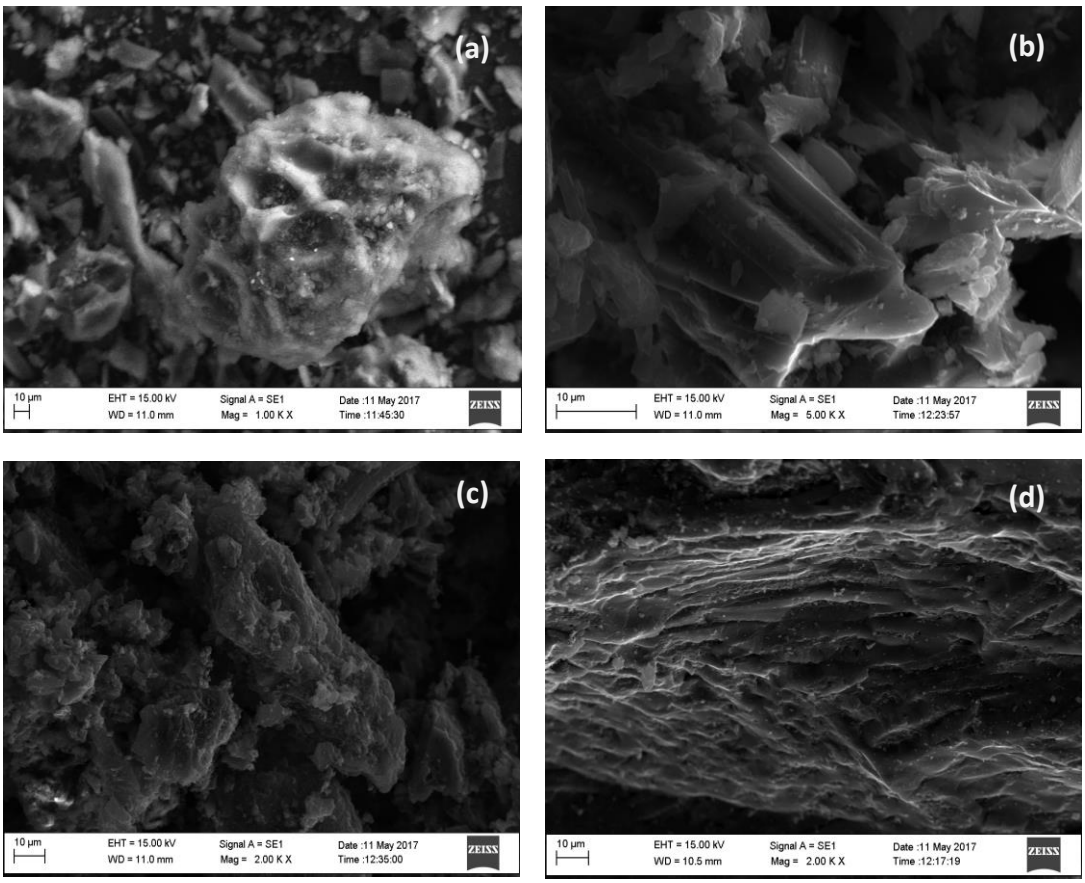

Fig. 3.9 SEM images of pristine CPAC (a); WPAC (b); PPAC (c); and CGAC (d)

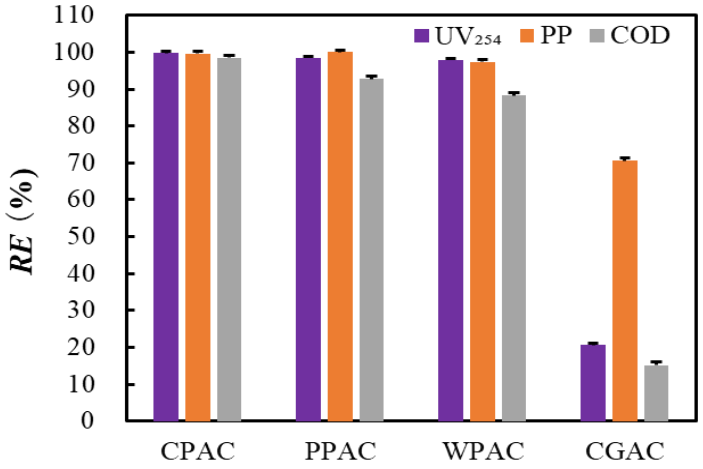

Fig. 3.10 Comparison of *RE* values onto various ACs

(Adsorption conditions: 250 mg of CPAC in 50 mL S_1 volume shaken with 450 rpm at 30°C for 10 min)

As shown in Fig. 3.10, all PACs showed similar *RE*s and higher than that of GAC after 10 min of adsorption time. In the previous study, PAC also showed higher COD removal than GAC in a cassava alcohol wastewater batch reactor experiment [185]. PACs have the rapid adsorption kinetics because of their small particle size and low surface area of carbon [195]. In this study, CPAC was the best and CGAC was the worst adsorbent because of the significant difference in BET surface area (S_{BET}), micropores volume (V_{micro}) and mesopores volume (V_{meso}), as show in Table 3.5. In practical applications, both the *RE* and cost are important factors, and the low-cost PAC should be chosen while wastewater quality can meet the discharge standards.

Table 3.5 Textural properties of ACs

Samples	S_{BET} ($m^2 g^{-1}$)	V_{micro} ($cm^3 g^{-1}$)	V_{meso} ($cm^3 g^{-1}$)	Pore diameter (D_p, nm)
CPAC	1951.3	1.76	1.57	3.95
PPAC	1012.6	0.75	0.61	3.46
WPAC	1504.5	1.17	0.75	3.28
CGAC	1014.8	0.45	0.06	1.90
PGAC	614. 0	0.36	0.14	2.47
5th Reg. CPAC	1810.6	1.76	1.58	4.17

3.3.5.3 Removal efficiency of TS, TSS and TDS

As shown in Table 3.2, S_0 contains high levels of TS, TDS and TSS. The TS can be effectively removed by flocculation with $FeSO_4 \cdot 7H_2O$ or $FeCl_3 \cdot 6H_2O$ [165], and the adsorption can further remove such matters [185]. The total *RE* (*TRE*) values of TS, TDS and TSS using flocculation and adsorption are depicted in Table 3.6.

Table 3.6 Removal efficiencies of TS, TDS, TSS using flocculation/adsorption

Sample	TS ($mg L^{-1}$)	*RE* (%)	TDS ($mg L^{-1}$)	*RE* (%)	TSS ($mg L^{-1}$)	*RE* (%)
S_0	2818.0	-	1418.0	-	1400.0	-
S_1	1695.0	40	1161.7	18	533.0	62
S_2	1173.5	31	1073.5	8	100.0	81
TRE	-	58	-	24	-	93

Flocculation conditions: 2.0 g $FeSO_4 \cdot 7H_2O$ in 800 mL S_0 shaken with 500 rpm at 30°C and pH 9.5 for 30 min; 250 mg CPAC in 50 mL S_1 with 450 rpm at 30°C for 10 min.

As shown in Table 3.6, the flocculation led to 40% and 62% reduction of TS and TSS, respectively, but the decrease of TDS was limited (only 18%). Subsequently, the *RE* values reached 31% and 81% for TS and TSS using CPAC adsorption. Thus *TRE*s of the combined process were calculated to be 58% and 93% for TS and TSS. Notably, the combined adsorption/flocculation process provided higher removal of TS and TSS. However, *RE* of TDS was low for both flocculation and adsorption. Lee *et al.* reported that certain amounts of metal ions were observed in wastewater after flocculation using inorganic flocculants [176]. As a result, the removal of dissolved matter, such as salts in ionic form, was limited by flocculation with $FeSO_4$ and adsorption with CPAC.

Besides, this speculation was further verified by TGA of both TS and TDS and the TGA method is shown in Section S.3.3. The TGA curves of the TS and TDS obtained from S_0, S_1 and S_2 are reported in Fig. 3.11.

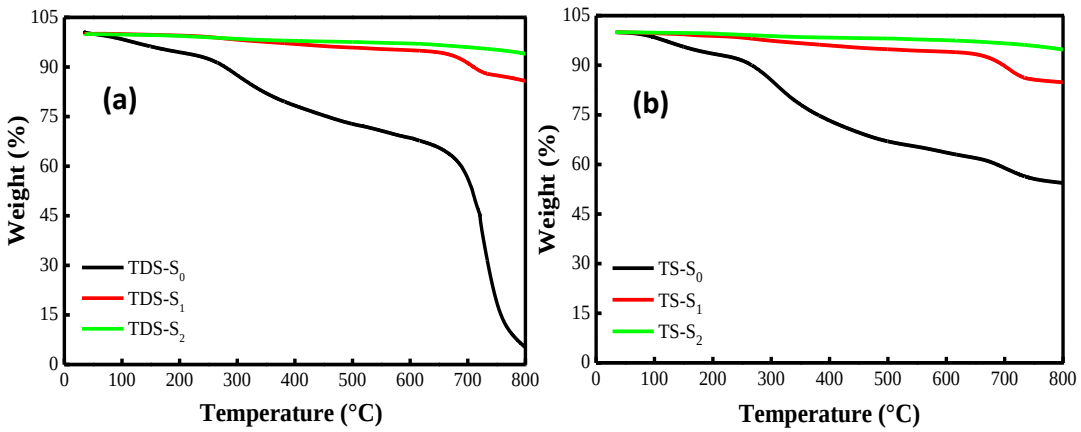

Fig. 3.11 TGA curves of TS (a) and TDS (b) obtained from S_0, S_1, and S_2

As shown in Fig. 3.11, the weight loss of TS and TDS from S_0 and S_1 was evident from 50°C to 800°C. In particular, rapid weight loss occurred between 100°C and 300°C with a peak at about 250°C. This weight loss can be attributed to the decomposition of the carboxylic groups of organic compounds present in the samples [196]. A continuous and clear loss, extending from 300°C to 650°C, was then observed. The degradation of lignin and other, more complex, aromatic structures occurs under such conditions [197]. Significant weight loss was observed from 650°C to 800°C. It has been suggested that most organic compounds of lignocellulosic origin begin to decompose at temperatures above

650°C [137]. Moreover, the weight loss in TDS from S_0 was higher than that found in TS from S_0. This could be explained by assuming that the dissolved matter in CW is reasonably small matters, making it easier to thermally decompose it.

Indeed, S_0 showed more significant weight loss than S_1, indicating that the flocculation process removed a large amount of TS (Fig. 3.11b). In contrast to S_2, higher weight loss was observed between 650°C and 800°C in S_1, indicating that there is some TS and TDS after flocculation that the adsorption process can remove. Overall, the flocculation as a pre-treatment is to remove a large amount of TSS and a little amount of TDS, and the adsorption as post-treatment is to further remove the left TSS, TDS, and dissolved organics. Therefore, the combined flocculation/adsorption process exhibited a superior performance for CW.

3.3.6 Regeneration of activated carbon using microwave irradiation

The adsorption performance of exhausted ACs was recovered at 800°C with MW heating due to the thermal decomposition of organic matter on carbons [137, 198]. Therefore, the temperature was set at 800°C in this study to regenerate the spent CPAC via MW heating. Fig. 3.12 depicted the *REs* of UV_{254} by adsorption of S_1 onto CPAC regenerated (reg.) over five cycles with MW.

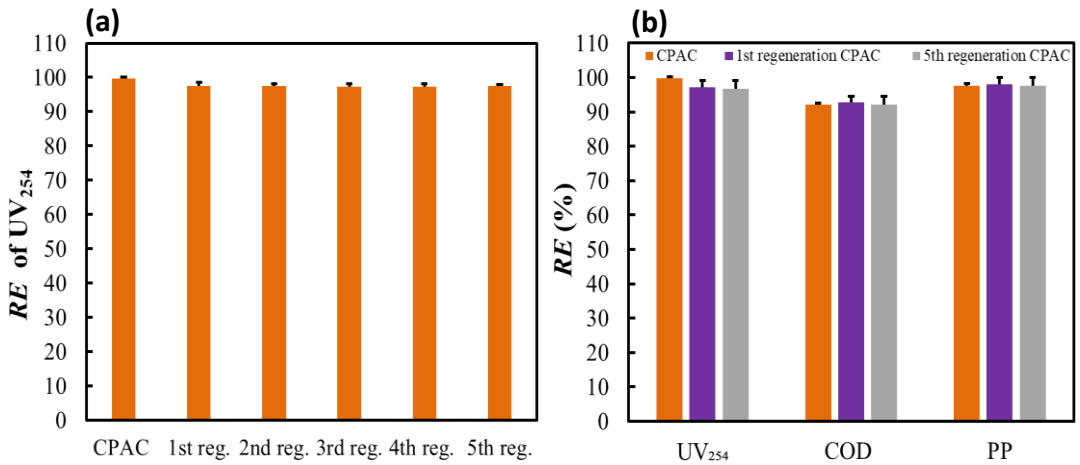

Fig. 3.12 Comparison of removal efficiencies among using the pristine and MW-regenerated CPAC (a) UV_{254}; (b) UV_{254}, COD and PP

(MW-regeneration conditions: 1.5 g of CPAC samples in crucibles heated with 10 NL h^{-1} N_2 flow at 800°C for 3 min; Adsorption conditions: 250 mg of CPAC in 50 mL S_1 shaken with 450 rpm at 30°C for 10 min)

As shown in Fig. 3.12a, the *RE*s of UV_{254} remained stable over the five-cycle operation and were still *ca.* 97% in the last cycle. Similarly, the *RE* values of COD and PP after 1st and 5th regeneration also further confirmed the results (Fig. 3.12b). Moreover, these results were further verified by TEM (as shown in Fig. S3.3), and BET analysis (Table 3.5 and Fig. 3.13).

The N_2 adsorption-desorption isotherms of the fifth MW-regenerated CPAC are quite similar to the original sample, as depicted in Fig. 3.13. Compared with the porosity properties of pristine CPAC (Table 3.5), 5th regeneration CPAC sample was efficiently recovered, which S_{BET}, V_{micro}, V_{meso} and D_p are 1810.6 m^2 g^{-1}, 1.76 cm^3 g^{-1}, 1.57 cm^3 g^{-1}, and 4.17 nm, respectively. The results indicated that the porous structure was not appreciably disrupted by MW regeneration. The pore size of ACs determines the accessibility of the adsorbate molecule, and total pore volume is responsible for the total number of adsorption sites [199]. Thus, the adsorption performance of CPAC after the fifth cycles of adsorption and MW-regeneration maintained equally due to analogous textural properties [190].

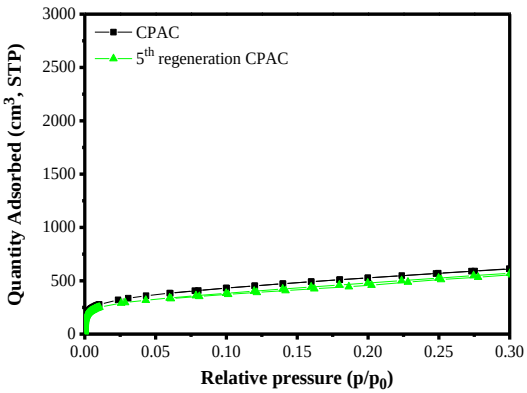

Fig. 3.13 N_2 adsorption-desorption isotherms of pristine CPAC and CPAC after five MW-regeneration cycles

Moreover, TGA of CPAC, 1st and 5th regeneration of CPAC samples were depicted in Fig. S3.4. The regeneration process recovered properties of spent carbons are further confirmed. The TGA results indicate that MW irradiation is an efficient and feasible regeneration method.

Supplementary Data

S.3.1 The linear correlations between UV_{254} and COD, UV_{254} and PP

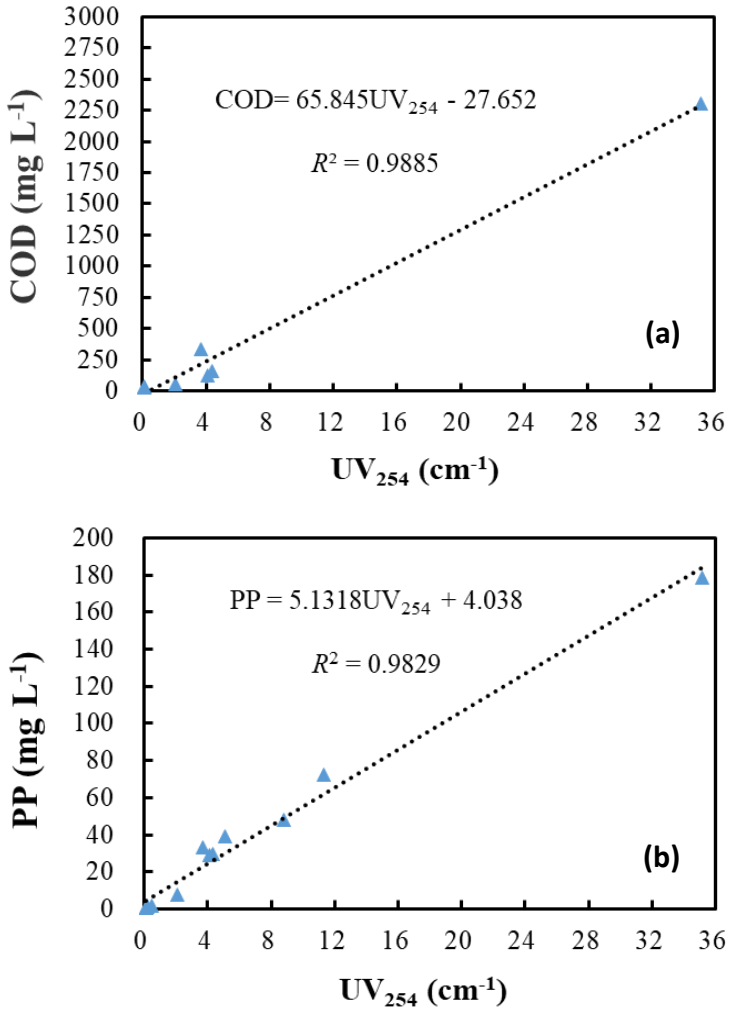

Fig. S3.1 The linear correlations between UV_{254} and COD (a); UV_{254} and PP (b)

S.3.2 Transmission electron microscope images

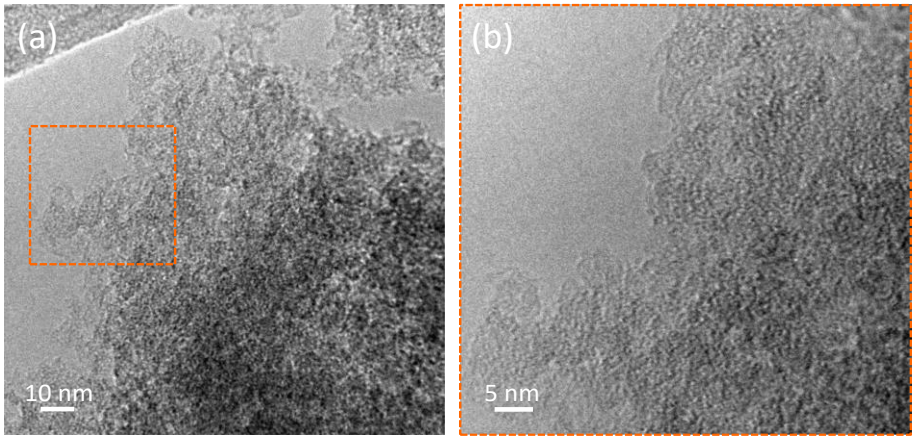

Fig. S3.2 TEM image of pristine CPAC (a); detail of the region in the square (b) Instrumental magnification 150000× and 300000×, respectively

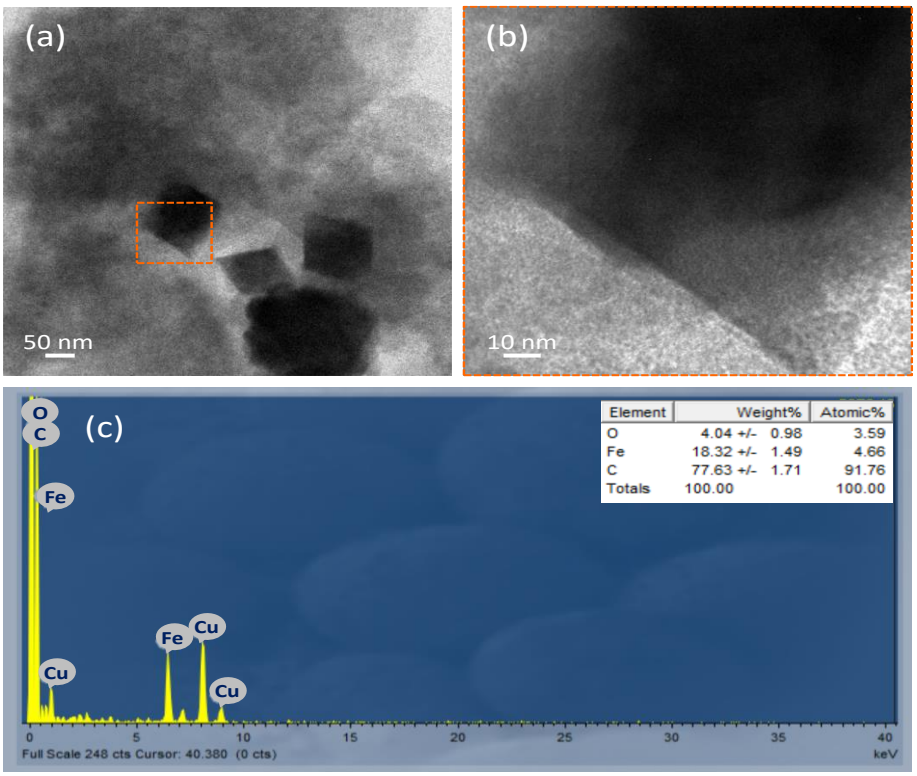

Fig. S3.3 TEM image of 5th MW-regenerated CPAC (a); detail showing the region in the square (b) Instrumental magnification 25000× and 150000×, respectively; EDS spectrum and relative abundance of iron (c)

S.3.3 Thermogravimetric analysis

TGA of dried samples of TS and TDS obtained from S_0, S_1, and S_2 was conducted using A TGA 4000 thermogravimetric analyzer (Perkin Elmer), so that the variation in chemical composition of TS and TDS can be observed from S_0, S_1, S_2 through the comparison between thermal behavior of the TS and TDS, reflecting the various removal objects with flocculation or adsorption. 30 mg of dried TS and TDS samples were used, and the temperature was raised from 50°C to 800°C at a heating rate of 10°C min^{-1} under flowing Argon 5.0 (80 mL min^{-1}).

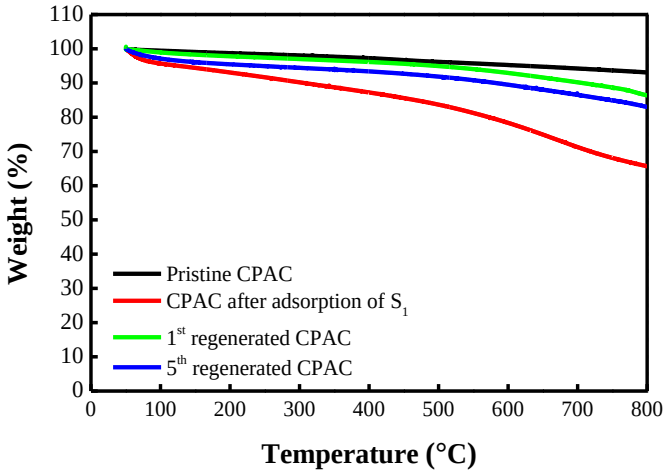

Fig. S3.4 TGA of CPAC samples of pristine, after adsorption of S_1, 1st regenerated and 5th regenerated

References

[165] De Torres-Socías, E., Fernández-Calderero, I., Oller, I., Trinidad-Lozano, M. J., Yuste, F. J., Malato, S. Cork boiling wastewater treatment at pilot plant scale: comparison of solar photo-Fenton and ozone (O_3, O_3/H_2O_2). Toxicity and biodegradability assessment. Chemical Engineering Journal, 234 (2013) 232-239.

[166] Wu, Z., Yuste-Córdoba, F. J., Cintas, P., Wu, Z., Boffa, L., Mantegna, S., Cravotto, G. Effects of ultrasonic and hydrodynamic cavitation on the treatment of cork wastewater by flocculation and Fenton processes. Ultrasonics Sonochemistry, 40 (2018) 3-8.

[167] Ge, X., Wu, Z., Cravotto, G., Manzoli, M., Cintas, P., Wu, Z. Cork wastewater purification in a cooperative flocculation/adsorption process with microwave-regenerated activated carbon. Journal of Hazardous Materials, 360(2018) 412-419.

[168]Aroso, I. M., Araújo, A. R., Pires, R. A., Reis, R. L. Cork: current technological developments and future perspectives for this natural, renewable, and sustainable material. ACS Sustainable Chemistry & Engineering, 5(2017) 11130-11146.

[169] Santos, A., Bernardo, M., Vespeira, C., Cantinho, P., Minhalma, M. Cork industry wastewater characterization: assessment of the biodegradability, reuse and of the relationship between BOD, COD and tannins with TOC. Journal of Water Reuse and Desalination, 2(2012) 33-39.

[170] Benitez, F. J., Acero, J. L., Garcia, J., Leal, A. I. Purification of cork processing wastewaters by ozone, by activated sludge, and by their two sequential applications. Water Research, 37(2003) 4081-4090.

[171] Benítez, F. J., Acero, J. L., Leal, A. I., Real, F. J. Ozone and membrane filtration based strategies for the treatment of cork processing wastewaters. Journal of Hazardous Materials, 152(2008) 373-380.

[172] A. Scott, Wastewater alchemy. Chemical Engineering News (November), 2017, 30–34.

[173] Bernardo, M., Santos, A., Cantinho, P., Minhalma, M. Cork industry wastewater partition by ultra/nanofiltration: a biodegradation and valorisation study. Water Research, 45(2011) 904-912.

[174] Peres, J. A., de Heredia, J. B., Domınguez, J. R. Integrated Fenton's reagent-coagulation/flocculation process for the treatment of cork processing wastewaters. Journal of Hazardous Materials, 107(2004) 115-121.

[175] Minhalma, M., De Pinho, M. N. Flocculation/flotation/ultrafiltration integrated process for the treatment of cork processing wastewaters. Environmental Science & Technology, 35(2001) 4916-4921.
[176] Teixeira, A. R. S., Santos, J. L. C., Crespo, J. G. Sustainable membrane-based process for valorisation of cork boiling wastewaters. Separation and Purification Technology, 66(2009) 35-44.
[177] Vázquez, I., Rodriguez-Iglesias, J., Maranon, E., Castrillon, L., Alvarez, M. Removal of residual phenols from coke wastewater by adsorption. Journal of Hazardous Materials, 147(2007) 395-400.
[178] Zhang, M.H., Zhao L., Bai, Q. X., Zhang, F.Y., Adsorption of organic pollutants from coking wastewater by activated coke. Colloids and Surfaces A: Physicochemical and Engineering Aspects, 362(2010) 140-146.
[179] Beltrán de Heredia, J., Domínguez, J. R., López, R. Treatment of Cork Process Wastewater by a Successive Chemical–Physical Method. Journal of Agricultural and Food Chemistry, 52(14) 4501-4507.
[180] Lee, C. S., Robinson, J., Chong, M. F. A review on application of flocculants in wastewater treatment. Process Safety and Environmental Protection, 92(2014) 489-508.
[181] Teh, C. Y., Wu, T. Y., Juan, J. C. Potential use of rice starch in coagulation–flocculation process of agro-industrial wastewater: treatment performance and flocs characterization. Ecological Engineering, 71(2014) 509-519.
[182] Peng, X., Hu, F., Zhang, T., Qiu, F., Dai, H. Amine-functionalized magnetic bamboo-based activated carbon adsorptive removal of ciprofloxacin and norfloxacin: A batch and fixed-bed column study. Bioresource Technology, 249(2018) 924-934.
[183] Beltrán, F. J., García-Araya, J. F., Álvarez, P. M. Wine distillery wastewater degradation. 1. Oxidative treatment using ozone and its effect on the wastewater biodegradability. Journal of Agricultural and Food Chemistry, 47(1999) 3911-3918.
[184] Ahmaruzzaman, M. Adsorption of phenolic compounds on low-cost adsorbents: a review. Advances in colloid and interface science, 143(2008) 48-67. [185] D. Wu, Y.J. Wang, S.J. Hou, J.C. Chen, X.K. Xing, G.F. Chen, Physico-chemical method for treatment food industry wastewater: A review. Chinese Food Industrial Technology, 35 (2014) 364-367.
[186] Foo, K. Y., Hameed, B. H. Microwave-assisted regeneration of activated carbon. Bioresource Technology, 119(2012) 234-240.
[187] Cicco, N., Lanorte, M. T., Paraggio, M., Viggiano, M., Lattanzio, V. A reproducible, rapid and inexpensive Folin–Ciocalteu micro-method in

determining phenolics of plant methanol extracts. Microchemical Journal, 91(2009) 107-110.
[188] Tang, D., Zheng, Z., Lin, K., Luan, J., Zhang, J. Adsorption of p-nitrophenol from aqueous solutions onto activated carbon fiber. Journal of Hazardous Materials, 143(2007) 49-56.
[189] Arslanoglu, F. N., Kar, F., Arslan, N. Adsorption of dark coloured compounds from peach pulp by using powdered-activated carbon. Journal of Food Engineering, 71(2005) 156-163.
[190] Dias, J. M., Alvim-Ferraz, M. C., Almeida, M. F., Rivera-Utrilla, J., Sánchez-Polo, M. Waste materials for activated carbon preparation and its use in aqueous-phase treatment: a review. Journal of Environmental Management, 85(2007) 833-846.
[191] Hameed, B. H., Salman, J. M., Ahmad, A. L. Adsorption isotherm and kinetic modeling of 2, 4-D pesticide on activated carbon derived from date stones. Journal of Hazardous Materials, 163(2009) 121-126.
[192] Liu, Q. S., Wang, P., Zhao, S. S., Zhang, W. Treatment of an industrial chemical waste-water using a granular activated carbon adsorption-microwave regeneration process. Journal of Chemical Technology & Biotechnology, 87(2012) 1004-1009.
[193] Ania, C. O., Parra, J. B., Menéndez, J. A., Pis, J. J. Effect of microwave and conventional regeneration on the microporous and mesoporous network and on the adsorptive capacity of activated carbons. Microporous and Mesoporous Materials, 85(2005) 7-15.
[194] Tan, I. A. W., Ahmad, A. L., Hameed, B. H. Adsorption of basic dye using activated carbon prepared from oil palm shell: batch and fixed bed studies. Desalination, 225(2008) 13-28.
[195] Shen, Y. H. Removal of phenol from water by adsorption–flocculation using organobentonite. Water Research, 36(2002) 1107-1114.
[196] Teh, C. Y., Wu, T. Y., Juan, J. C. Potential use of rice starch in coagulation–flocculation process of agro-industrial wastewater: treatment performance and flocs characterization. Ecological engineering, 71(2014) 509-519.
[197] Brebu, M., Vasile, C. Thermal degradation of lignin—a review. Cellulose Chemistry & Technology, 44(2010) 353-363.
[198] San Miguel, G., Lambert, S. D., Graham, N. J. D. The regeneration of field-spent granular-activated carbons. Water Research, 35(2001) 2740-2748.
[199] Sattler, K. D. (Ed.). Carbon nanomaterials sourcebook: nanoparticles, nanocapsules, nanofibers, nanoporous structures, and nanocomposites, CRC Press, 2(2016).

Chapter 4: Adsorptive Recovery of Iopamidol and Reuse of Activated Carbon

Abstract

In this study, the adsorptive recovery of valuable Iopamidol (IOP) and the reuse of the adsorbent AC after elution with alcohol were accomplished. Of the adsorbents selected, CPAC displayed the best adsorption performance toward IOP. The batch investigation on the adsorption kinetics, isotherm, activation energy, and thermodynamics parameters supported the occurrence of physisorption process. The adsorption mechanism was determined using the intra-particle diffusion model. A Boyd plot revealed that IOP adsorption onto CPAC was mainly governed by external mass transport where particle diffusion was the rate limiting step. In a semi-continuous flow system, IOP was well adsorbed on the CPAC-packed column and IOP was efficiently eluted and recovered using methanol. Moreover, the spent CPAC was efficiently regenerated and reused in five adsorption/desorption cycles. The characterization of CPAC samples by SEM, DRIFTS, and TGA shows that IOP is absorbed onto CPAC. After desorption with methanol in the flow system, the surface properties of CPAC were almost fully recovered. Thus, it is proposed that π-π interactions, donor-acceptor complex, Van der Waals forces and hydrogen bonding interactions govern the adsorption of IOP. The polarity of solvents and hydrogen bonding interactions between IOP and alcohols influence the desorption process. A lot of benefits, such as simple operations and low treatment costs, can be achieved from adsorption/desorption processes.

4.1 Introduction

Iodinated contrast agents (ICAs) are diagnostic drugs containing iodine that are used to visualize blood vessels and organs in medical imaging [200]. ICAs are commonly used worldwide in the medical field, which has been reported that the annual worldwide consumption is approximately 3500 tons [201, 202]. Normally, ICAs exhibit high biochemical stability; and high doses are injected in clinical exams [203], which are rapidly excreted with one day, mainly in the non-metabolized form [204]. ICAs include: (1) ionic ICA compounds, such as Diatrizoate, containing a free carboxylic moiety; (2) non-ionic compounds, containing IOP, Iopromide and Iomeprol that are amide derivatives [205].

Non-ionic dimers are favored because of their low osmolality, but it owned considerably higher price [206], for example, the average price of IOP is 1791 USD g^{-1} (Sigma-Aldrich, product number 1344702). However, the inertness and metabolic stability of ICA mean that it may represent a long-term potential risk for organisms [207, 208]. Suitable and economical technologies should be developed to effectively treat these compounds to minimize potential risks and meet wastewater discharge standards.

In detail, ICA compounds are highly hydrophilic and display high aqueous solubility meaning that they are difficult to eliminate from wastewaters. IOP is currently classified as an emerging pollutant, which indicates a new chemical pollutant without a regulatory status that impact on the environment and human health is still poorly understood [204]. Its basic physicochemical properties are shown in Table 4.1. Moreover, it is difficult to completely eliminate ICA by conventional treatment processes [204]. IOP concentrations in wastewater have been reported from μg to mg scale, with particular high content in industrial reaction liquor [201, 209, 210]. IOP has therefore been chosen as the model compound in this study, and IOP (99%) was kindly supplied by Bracco Spa, Italy.

Table 4.1 The properties of IOP [210]

CAS number	Chemical structure	Solubility (mg dm^{-3})	log K_{ow}	pKa	Molecular dimensions (nm×nm×nm)
60166-93-0	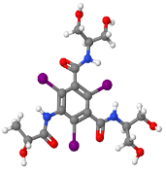	>200000	-2.42	10.7	1.5 (length)×1.5 (width)×0.6 (thickness)

Adapted with permission from reference 210, Copyright © 2014 Elsevier B.V.

A range of technologies, such as ultrasound [205], adsorption [204, 211], biological [212], ozonation [205], electrochemical [213], and hybrid technologies [205, 208], have been investigated for removing ICAs from wastewaters. From an economic viewpoint, the adsorption is a practical and simple method as compared with biodegradable and AOPs. In previous studies [204, 211, 213], ACs adsorption has been utilized for the removal of the lower concentration of IOP and efficiently achieved the decontamination of IOP-polluted wastewater. However, the purpose of traditional adsorption processes is to move pollutants from the wastewater

onto the adsorbents [214]. Therefore, the recovery of valuable substances and adsorbent regeneration are both important in wastewater treatment [215].

The present work reports the adsorptive removal of IOP from aqueous solutions by CPAC and the desorption of IOP using various organic solvents. The adsorption kinetics, isotherm, thermodynamics properties and adsorption mechanism have also been studied in batch mode. Moreover, the *AE* of PACs and GAC, as well as the *DE* with solvents have been compared. Adsorption/desorption cycles were carried out up to five times. The CPAC samples were characterized before and after adsorption/desorption using FESEM, DRIFTS, porosity properties (BET analysis), XPS, and TGA. The pristine and recovered IOP were both identified by NMR and examined using DRIFTS. Our procedure can get rid of secondary pollution and cut post-treatment costs thanks to the compensation from highly valuable compounds recovery.

4.2 Methodology

4.2.1 Adsorption/desorption in batch mode

The adsorption of IOP in batch mode was performed in 50 mL glass tubes that were shaken with 450 rpm at 25°C. CPAC was mixed with 10-50 mL IOP solutions for adsorption kinetics and isotherm studies. Initial IOP concentrations ranged from 1 to 10 mM (corresponding to 777-7771 mg L^{-1}), and those solutions were absorbed onto CPAC (2-4 g L^{-1}). Each experiment was duplicated under identical conditions. After shaking, CPAC was filtered and the IOP concentration in the filtrates was analysed by UV-Vis at 242 nm. The adsorption amount (q_t, mg g^{-1}), which is termed as the adsorption capacity (q_e, mg g^{-1}) at the equilibrium state, was calculated by equation (3), and the *AE* was calculated by equation (4):

$$q_t = \frac{(C_0 - C_t) \times V}{M} \quad (3)$$

$$AE(\%) = \frac{C_0 - C_t}{C_0} \times 100\% \quad (4)$$

where C_0 and C_t (mg L^{-1}) are the initial concentrations and concentration at given time, respectively; V (mL) is the solution volume and M (g) is the mass of dried CPAC used.

IOP-loaded CPAC was prepared according to follows: 1.5 g of CPAC was added to 100 mL of a 10 mM IOP solution and the mixture was stirred at 450 rpm at 25°C for 60 min. After adsorption, the IOP-loaded CPAC was filtered and oven dried at 65°C. For desorption in batch mode, methanol (MeOH 99.9%, Sigma-Aldrich), ethanol (EtOH, 96.0-97.2%, Sigma-Aldrich), and acetonitrile (ACN, 99.9%, Sigma-Aldrich) were chosen as eluents to recover IOP loaded CPAC according to follows: 2.5-80 mg of dried IOP-loaded CPAC were mixed with 2-10 mL of solvent and shaken with 450 rpm at 25°C for 10 min. After desorption, the filtrates were analysed by UV-Vis spectrophotometer. Each adsorption/desorption experiment was performed and duplicated. Error bars are calculated based on 2 replicates. If error bars not visible in Figures, they are smaller than the symbols representing the average data values.

4.2.2 Adsorption/desorption in semi-continuous flow mode

The adsorption of aqueous IOP was performed in semi-continuous flow mode using a glass column (15 × 0.62 cm I.D.) that was packed with 0.75 g of CPAC, which corresponded to a 5 cm bed height and 1.5 cm^3 of volume. A specified amount, 10 mM of IOP solution was passed through the CPAC column at a 0.75 mL min^{-1} flow rate with the help of vacuum pump (VP 18R vacuum pump, Lab Tech, USA). The IOP solution from the outlet was collected using either 5 or 10 mL of interval volume. Fig. 4.1 shows the schematic of the semi-continuous flow setup for the adsorption/desorption of IOP solution.

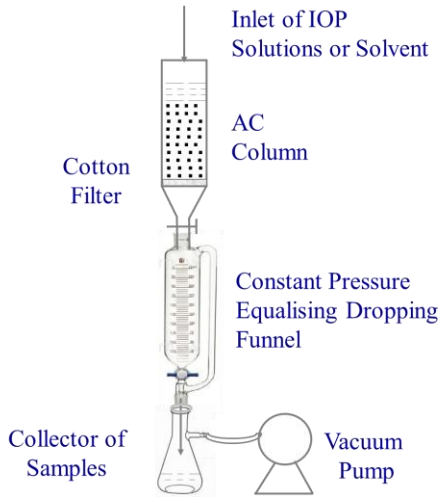

Fig. 4.1 Scheme of semi-continuous flow setup for adsorption/desorption

The amount of IOP loaded was calculated by integrating the IOP adsorbed vs. the throughput volume (equation (5)):

$$q_{\text{IOP - loaded}} = \int_0^{V_i} \frac{(C_i - C_t)dV_i}{M} \quad (5)$$

where $q_{\text{IOP-loaded}}$ (mg g^{-1}) is the IOP amount loaded onto CPAC, V_i is the effluent volume, C_i and C_t (mg L^{-1}) are the initial and effluent concentrations, respectively, and M (mg) is the amount of CPAC in the column.

Regarding to IOP desorption, MeOH or EtOH was added to the IOP-loaded columns from the top, and the eluent was then allowed to flow out at a rate of 1.0 mL min^{-1} with the help of a vacuum pump. The eluent was collected using 2.5 or 5.0 mL of interval volume and analysed after dilution with deionized water. The efficiency of IOP desorption was calculated as equation (6):

$$DE(\%) = \frac{q_e}{q_{\text{IOP - loaded}}} \times 100\% = \frac{\int_0^{V_d} C_d dV_d}{q_{\text{IOP - loaded}}} \times 100\% \quad (6)$$

where DE (%) is the efficiency of IOP desorption, q_e (mg g^{-1}) is the amount of IOP desorbed, $q_{\text{IOP-loaded}}$ (mg g^{-1}) is the IOP amount absorbed onto the CPAC in the column, C_d (mg L^{-1}) is the IOP concentration in the eluent and V_d is the volume of eluent (mL).

4.3 Results and discussion

4.3.1 Iopamidol adsorption in batch mode

Adsorption kinetics and equilibrium isotherms were studied, and thermodynamics parameters were calculated in order to gain a deeper insight into the adsorption process. On one hand, adsorption kinetics describes the adsorption rate, the equilibrium time of adsorption, and effective factors [20]. On the other hand, the adsorption isotherm is basically important to describe how adsorbates interact with adsorbents until that the adsorption process reached an equilibrium state [216]. In adsorption process, thermodynamics parameters are the actual indicators for practical applications [217].

4.3.1.1 Adsorption kinetics

Adsorption kinetics was recorded at 25°C, 40°C and 55°C. Adsorption kinetics fitted to pseudo-second-order kinetics curves, and the pseudo-second-order kinetics plots are presented in Figs. 4.2a and 4.2b, respectively.

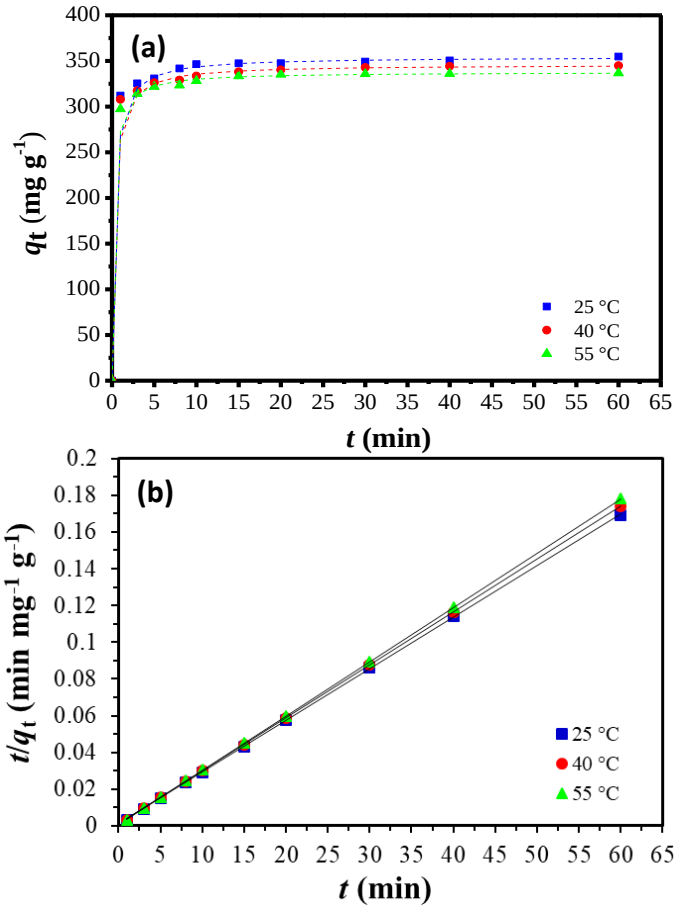

Fig. 4.2 (a) Adsorption kinetics fitting to pseudo second-order kinetics curves; (b) Pseudo second-order kinetics plots for IOP adsorption onto CPAC

(Adsorption conditions: 20 mg of CPAC in 10 mL of 1 mM IOP solution shaken with 450 rpm at 25°C, 40°C and 55°C for 1-60 min)

As shown in Fig. 4.2a, q_t of CPAC for IOP increases with time and reaches equilibrium after 10 min. It indicates that the adsorption of IOP takes place in a short time. Analogously, q_t slightly decreases with increasing temperature, which suggests that IOP adsorption onto CPAC is an exothermic process, as the

interactions between the active sites of the adsorbent and the adsorbates are weakened at higher temperatures [218].

The following pseudo-first-order and pseudo-second-order kinetics models, as well as the Elovich equation were used to evaluate the adsorption kinetics:

Pseudo-first-order: $\ln (q_e - q_t) = -k_1 t + \ln q_e$ (7)

Pseudo-second-order: $\frac{t}{q_t} = \frac{1}{k_2 q_e^2} + \frac{t}{q_e}$ (8)

Elovich equation: $q_t = (\frac{1}{b}) \ln(ab) + (\frac{1}{b}) \ln t$ (9)

The adsorption kinetics parameters of IOP onto CPAC are listed in Table 4.2.

Table 4.2 Adsorption kinetics parameters of IOP onto CPAC

Temperature	Parameters			
		Pseudo-first-order		
	$q_{e,\ exp}$ (mg g^{-1})	$q_{e,\ cal}$ (mg g^{-1})	k_1 (min^{-1})	R^2
25°C	354.8	24.96	0.0352	0.7691
40°C	344.9	31.38	0.0248	0.7798
55°C	336.7	36.05	0.0159	0.6009
		Pseudo-second-order		
	$q_{e,\ exp}$ (mg g^{-1})	$q_{e,\ cal}$ (mg g^{-1})	k_2 (g mg^{-1} min^{-1})	R^2
25°C	354.8	354.6	0.00870	0.9999
40°C	344.9	346.0	0.00930	0.9999
55°C	336.7	337.8	0.0125	1.0000
		Elovich equation		
	$q_{e,\ exp}$ (mg g^{-1})	a (mg g^{-1}min^{-1})	b (g mg^{-1})	R^2
25°C	354.8	1.90×10^{14}	0.09670	0.9238
40°C	344.9	7.16×10^{14}	0.1033	0.9694
55°C	336.7	1.81×10^{15}	0.1082	0.9321

Note: $q_{e,\ exp}$ is the equilibrium adsorption capacity of IOP adsorption onto CPAC (experimental data); $q_{e,\ cal}$ is the equilibrium adsorption capacity of IOP adsorption onto CPAC calculated from pseudo first and second order models. k_1 and k_2 is the rate constant of first-order and second-order model, respectively. a is the initial sorption rate and b is related to the extent of surface coverage and activation energy for chemisorption.

As illustrated in Table 4.2, it was observed that the pseudo-second-order model gave a considerably better fitting comparison with the two other models at all temperatures. Moreover, experimental and calculated q_e values were found to be in good agreement. Similar kinetics have also been reported for the adsorption of IOP onto AC in the previous study [204]. Moreover, the pseudo-second-order rate constants k_2 increased with increases in temperature from 25°C to 55°C (Fig. 4.2b and Table 4.2). It proposes that the adsorption of IOP onto CPAC follows a physisorption mechanism [219].

4.3.1.2 Adsorption equilibrium

When optimizing the design of an adsorption system, it is important to establish the most appropriate correlations for the equilibrium curves [220]. The adsorption isotherm experimental data collected at different IOP concentrations and various temperatures were fitted with Langmuir, Freundlich, Temkin, and Elovich models. These equations are listed as follows:

Langmuir isotherm: $$\frac{C_e}{q_e} = \frac{1}{q_m} C_e + \frac{1}{q_m K_L} \quad (10)$$

Freundlich isotherm: $$\ln q_e = \frac{1}{n} \ln C_e + \ln K_F \quad (11)$$

Temkin isotherm: $$q_e = B_T \ln K_T + B_T \ln C_e \quad (12)$$

Elovich isotherm: $$\frac{\ln q_e}{C_e} = \ln K_E q_m - \frac{q_e}{q_m} \quad (13)$$

where q_m (mg g^{-1}) is the maximum amount of IOP per unit weight onto CPAC to form a complete monolayer on the surface, and K_L (L mg^{-1}) is Langmuir constant related to the affinity of the binding sites; K_F (mg g^{-1} (L $mg^{-1})^{1/n}$) is Freundlich constant related to sorption capacity and n is sorption intensity of the adsorbent; B_T (J mol^{-1}) is the Temkin constant related to heat of sorption and K_T (L g^{-1}) is the equilibrium binding constant corresponding to the maximum binding energy. K_E (L g^{-1}) is the Elovich equilibrium constant.

The equilibrium adsorption isotherms and the fitted Langmuir adsorption isotherm for IOP onto CPAC at various temperatures are separately depicted in Figs. 4.3a and 4.3b.

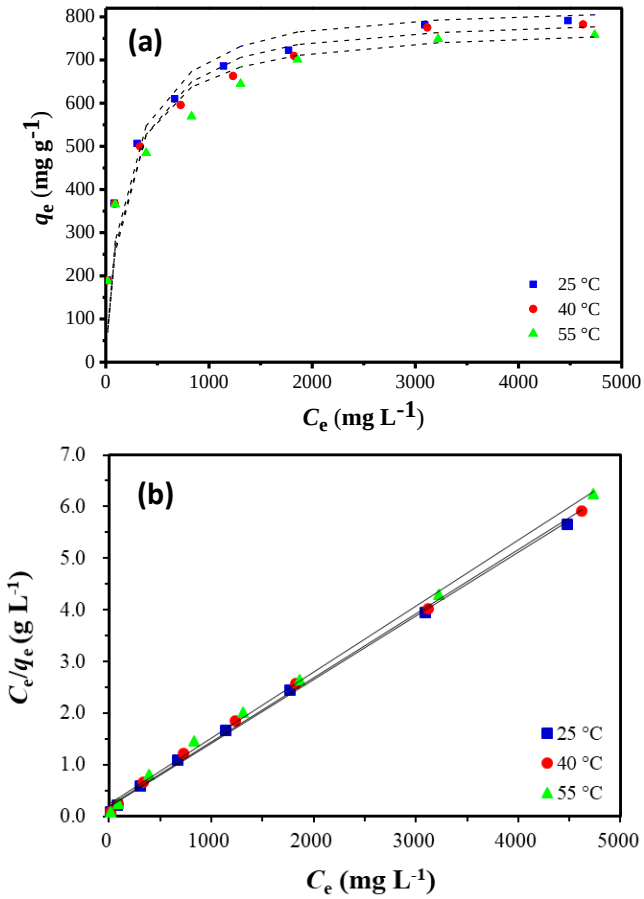

Fig. 4.3 (a) Equilibrium adsorption isotherms fitting to Langmuir curves; (b) Langmuir isotherm plots for IOP adsorption onto CPAC

(Adsorption conditions: 40 mg of CPAC in 10 mL of 1-10 mM IOP solutions shaken with 450 rpm at 25°C, 40°C and 55°C for 10 min)

As shown in Fig. 4.3a, q_e exhibits a steep increase with increasing initial concentration of IOP in the range of low concentrations, and then increases slightly, showing the almost horizontal plateaus in the high IOP concentration range. The L-type curves belong to the type I of adsorption isotherm (Fig. 1.3), suggesting that the adsorption of IOP onto CPAC is monolayer [9, 213], as

mentioned in Section 1.1.2. Moreover, the slight decrease of q_e with increasing temperature suggests an exothermic process.

All the correlation coefficient (R^2 values) and the constants obtained for the isotherms models are summarized in Table 4.3. The highest values of $R^2 > 0.99$ was found when fitting the Langmuir model (Table 4.3 and Fig. 4.3b). The monolayer q_e of CPAC toward IOP, as calculated from the Langmuir isotherms, were 813.0, 806.5 and 783.7 mg g^{-1} at 25°C, 40°C and 55°C, respectively. As seen from Table 4.3 and Fig. 4.3a, the q_e values predicted from the Langmuir model agreed well with the experimental values. It demonstrates that Langmuir model is the most suitable for a description of the sorption equilibrium of IOP onto CPAC.

Table 4.3 Isotherm model parameters for the adsorption of IOP onto CPAC

Model	Parameters	Temperature		
		25°C	40°C	55°C
Langmuir isotherm	q_m (mg g^{-1})	813.0	806.5	783.7
	K_L(L mg^{-1})	0.0065	0.0057	0.0052
	R_L	0.01941-0.1656	0.02207-0.1842	0.02354-0.1942
	R^2	0.9984	0.9976	0.9972
Freundlich isotherm	K_F (mg g^{-1} (L $mg^{-1})^{1/n}$)	111.2	106.5	105.2
	n	4.011	4.023	4.045
	R^2	0.9549	0.9624	0.9644
Temkin isotherm	B_T (J mol^{-1})	111.16	109.44	106.14
	K_T (L g^{-1})	0.3473	0.3283	0.3207
	R^2	0.9957	0.9968	0.9916
Elovich isotherm	q_m (mg g^{-1})	149.3	147.1	142.9
	K_E (L g^{-1})	0.3288	0.3157	0.2950
	R^2	0.9868	0.9922	0.9863

The Langmuir constant K_L represents the interaction extent between IOP and the CPAC surface. The lower K_L values, 0.0052-0.0065 L mg^{-1} in Table 4.3, indicate that the interaction between IOP and CPAC surface is very weak.

The separation factor (R_L) indicates the affinity between adsorbate and adsorbent. The calculated R_L value describes the isotherm type: unfavorable (R_L>1), linear (R_L=1), favorable (0<R_L<1), or irreversible (R_L= 0). As shown in Table 4.3, the calculated R_L values are between 0 and 1 for the various initial concentrations, which demonstrates that the adsorption of IOP onto CPAC is favored. However, the R_L values decreased as the initial concentration increased from 1.0 to 10.0 mM, as seen in Fig. 4.4, indicating that the adsorption was more favorable at higher concentrations.

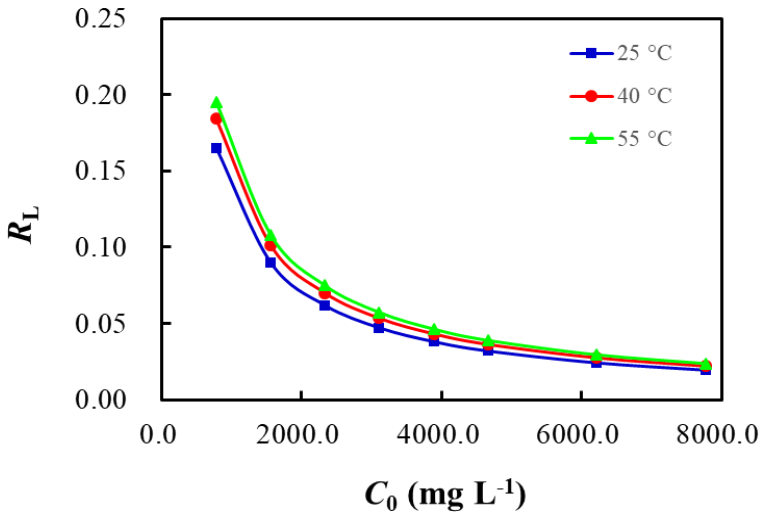

Fig. 4.4 Effect of IOP initial concentration on separation factor R_L
(Experimental conditions: 1-10 mM, corresponding 777-7771 mg L^{-1})

4.3.1.3 Adsorption thermodynamics

According to the laws of thermodynamics, entropy change is the driving force in an isolated system in which energy cannot be gained or lost [221]. The following parameters characterize the adsorption thermodynamics: ΔH^0, ΔS^0, ΔG^0, and E_a [216, 221-223], by the following equations (14)-(17):

$$\ln K_c = \frac{\Delta S^0}{R} - \frac{\Delta H^0}{RT} \qquad (14)$$

$$\Delta G^0 = -RT \ln K_c \qquad (15)$$

$$\ln k_2 = \ln A - \frac{E_a}{RT} \quad (16)$$

in which K_c is the thermodynamic equilibrium constant without units, T is the absolute temperature in kelvins, and R is the gas constant with a value of 8.314 J·mol^{-1} K^{-1}; k_2 is the rate constant of the pseudo second-order model (g mg^{-1} min^{-1}), A is the Arrhenius factor.

The calculated parameters for the adsorption of IOP onto CPAC are listed in Table 4.4.

Table 4.4 Thermodynamics parameters for IOP adsorption onto CPAC

T (°C)	ΔG^0 (kJ mol^{-1})	ΔH^0 (kJ mol^{-1})	ΔS^0 (J mol^{-1}·K^{-1})	E_a (kJ mol^{-1})
25	-2.18			
40	-1.99	-5.37	-10.7	9.63
55	-1.86			

Adsorption Conditions: 20 mg CPAC in 5 mM, 10 mL IOP volume shaken with 450 rpm at 25°C, 40°C, and 55°C for 10 min.

The negative ΔG^0 values at temperatures of 25 °C-55 °C indicate that the process is feasible, that adsorption occurs spontaneously and that IOP has a high preference for CPAC (Table 4.4). Meanwhile, ΔG^0 values were found to decrease with increasing temperature. The negative ΔH^0 suggests that adsorption is exothermic. This is also supported by the fact that IOP adsorption onto CPAC decreased with increasing temperature (Fig. 4.2a and Fig. 4.3a). Moreover, herein ΔH^0 value is less than 40 kJ mol^{-1}, implying that IOP adsorption is mainly a physisorption process [224]. The adsorption type (physical or chemical) can also be demonstrated by the magnitude of E_a [24]. In this study, the low value of E_a (9.63 kJ mol^{-1}) indicates that IOP adsorption onto CPAC is a rapid and reversible physical process.

4.3.2 Comparison with various activated carbons

Different types of ACs, such as CPAC, WPAC, PPAC, and PGAC, were used to probe their adsorption performance toward IOP solutions. The adsorption

capacity (q_t) and *AE* values of CPAC, WPAC, PPAC and PGAC from 1 to 1440 min are shown in Fig. 4.5.

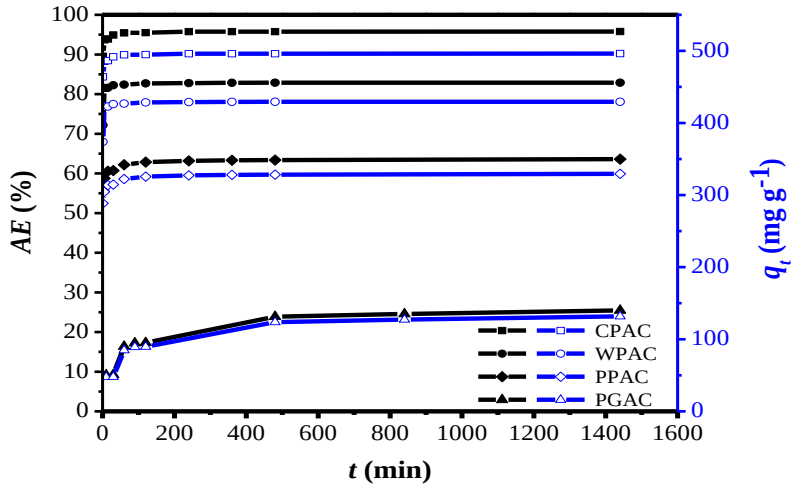

Fig. 4.5 *AE* and q_t obtained using different ACs for IOP adsorption
(Adsorption conditions: 1.5 g of ACs in 100 mL of 10 mM IOP solutions stirred with 450 rpm at 25°C for 0-1440 min)

As shown in Fig. 4.5, CPAC showed the best adsorption performance under the same experimental conditions. The superior adsorption performance of CPAC is related to the textural properties (Table 3.5). The linear correlations between q_e and S_{BET}, V_{micro}, V_{meso} were analysed in Section S.4.1, respectively. As seen in Fig. S4.1, q_e values of IOP onto CPAC, WPAC, PPAC, and PGAC show a certain correlation with S_{BET} (R^2=0.9253), and q_e value increases as the increasing S_{BET}, V_{micro}, V_{meso}. Moreover, the *AE* increased rapidly with the first minutes of the adsorption process for all AC materials, and the equilibrium was achieved in 10 min for all PACs (CPAC, WPAC and PPAC), whereas 8 h was required to reach the equilibrium for PGAC. This clearly demonstrates that diffusion into powder particles is much faster than in granules [225].

So far, only few studies about the removal of IOP by ACs were reported [204, 210, 211, 226, 227]. In Table 4.5, commercial and preparation of ACs for IOP removal were compared. It can be seen that CPAC demonstrates a larger monolayer adsorption capacity of 813.0 mg g^{-1} (Table 4.3).

Table 4.5 Comparison of adsorption capacities among various ACs for IOP

Adsorbent	Adsorption condition	Monolayer adsorption capacity ($mg\ g^{-1}$)
commercial material CP supplied by Quimitejo, Portugal	6 mg CP, VP, S2 or S3 in 9 and 30 mL 20-150 mg L^{-1} IOP solutions stirred with 700 rpm for 24 h at 30°C	135.5 [204]
commercial material VP supplied by Quimitejo, Portugal		147.0 [204]
sisal-derived activated carbon by KOH activation (sisal : KOH of 1:1, S2 and 1 : 0.5, S3)		105.3 and 112.4 [204]
industrial pretreated cork activated carbon by steam (S) and KOH (H) activation at 800°C (S800 and H800)	6 mg S800 or H800 in 9 mL, 12 mg L^{-1} IOP solution stirred with 700 rpm for 24 h at 30°C	136.9 and 174.4 [210]
commercial material NS supplied by Norit, Salmon & Cia, Portugal	6 mg NS, SC800 or SH800 in 9 mL, 80 mg L^{-1} IOP solution stirred with 700 rpm for 24 h at 30°C	472 [211]
sucrose-derived (S) activated carbon by K_2CO_3 (C) and KOH (H) activation of hydrochar at 800°C (SC800 and SH800)		150.9 and 1049.6 [211]
commercial material CPAC supplied ACEF S.P.A., Italy	40 mg of CPAC in 10 mL of 1-10 mM IOP solutions shaken with 450 rpm at 25°C, 40°C for 10 min	813.0 in this study

4.3.3 Desorption of Iopamidol in batch mode

The huge amount of spent ACs obtained after adsorption could cause secondary pollution without its regeneration. Due to high hydrophilicity of IOP, alcohol was selected to be eluent. As with EtOH, MeOH is relatively easier to be recycled with considerable less energy. In order to optimize the *DE*, the effect of the ratio of the mass of IOP-loaded CPAC and MeOH volume (*RMV*) was investigated in batch mode, and the results are shown in Fig. 4.6.

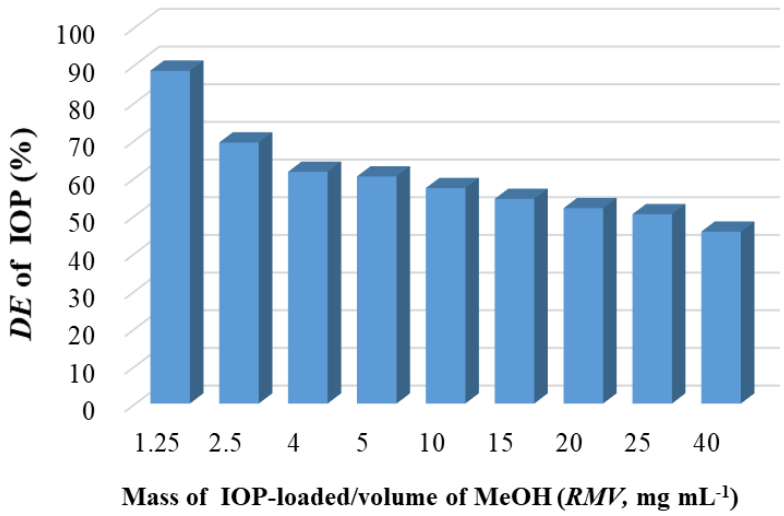

Fig. 4.6. *DE* values of IOP in MeOH as a function of *RMV*

(Desorption conditions: 2.5−80 mg of IOP-loaded CPAC (496.1 mg IOP/g CPAC) in 2 mL MeOH shaken with 450 rpm at 25°C for 10 min)

As shown in Fig. 4.6, the *DE* values of IOP in MeOH progressively decreased with increasing *RMV.* While *RMV* is 1.25, the highest *DE* value of IOP can reach 88.3%. It indicates that MeOH is good eluent for IOP desorption and higher amounts of MeOH lead to higher IOP desorption. Besides, the effect of IOP content on CPAC ($q_{IOP\text{-}loaded}$) significantly on *DE* values was shown in Fig. 4.7*.* All other things being equal, *DE* decreases with increasing IOP content on CPAC, as shown in Fig. 4.7. An acceptable correlation coefficient is obtained (R^2= 0.9497) when $q_{IOP\text{-}loaded}$ is plotted vs. *DE*. Therefore, the amount of solvent and IOP content on carbon are both important for desorption.

For economic and environmental, higher amounts of solvent used for desorption is not beneficial. In order to enhance the *DE* value, the multistep desorption was performed at an *RMV* of 5.0. As a result, the second step enhanced *DE* by about 20%. The results also are the basis of the desorption in the flow mode. It would be confirmed by the complete desorption with fewer amount solvents in a flow system.

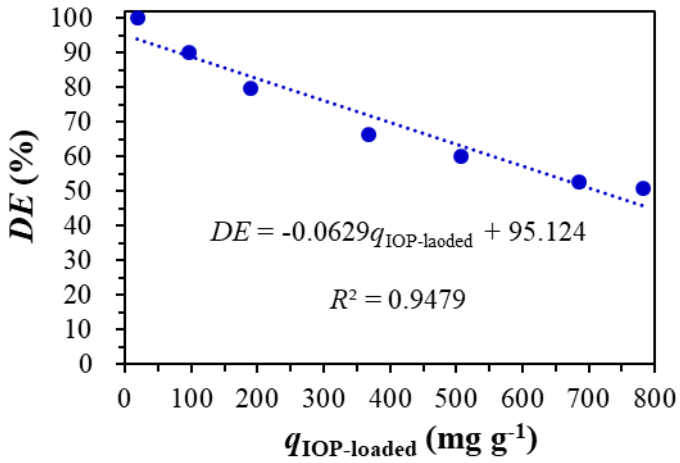

Fig. 4.7. Correlation plot of $q_{IOP\text{-}loaded}$ and *DE* values

(Adsorption conditions: 40 mg of CPAC in 10 mL of 1-10 mM IOP solutions shaken with 450 rpm at 25°C for 10 min; Desorption conditions: 40 mg of IOP-loaded CPAC (18.9-781.4 mg IOP/g CPAC) in 8 mL MeOH shaken with 450 rpm at 25°C for 10 min)

4.3.4 Adsorption/desorption of Iopamidol in semi-continuous flow mode

Fig. 4.8 shows the breakthrough curves of five consecutive cycles of IOP adsorption/desorption process onto CPAC.

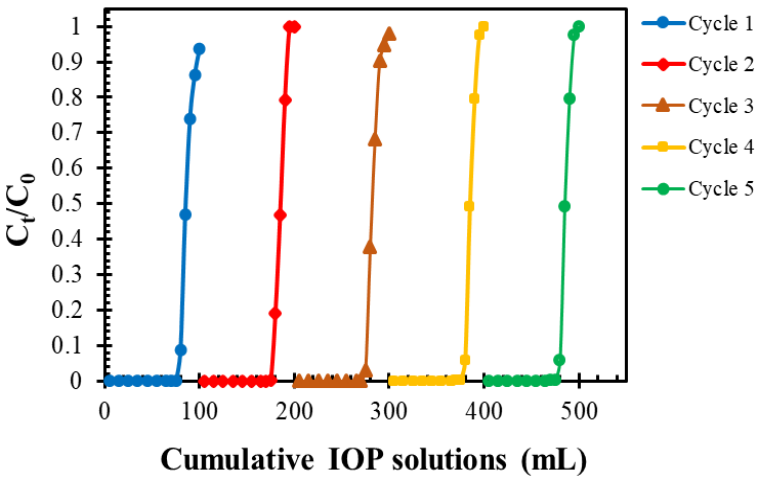

Fig. 4.8. The breakthrough curves of adsorption/desorption process of IOP on CPAC for five cycles (Adsorption conditions: 5×100 mL of 10 mM IOP solution passed through the column at 0.75 mL min^{-1} flow rate (Periodical sampling: 10 mL aliquots); Desorption conditions: 40 mL MeOH eluted the column at 1 mL min^{-1} of flow rate (Periodical sampling: 5 or 10 mL aliquots)

The amount of IOP absorbed was approximately 776.9 mg g^{-1} in each cycle and the total *RE* reached 100% as 75.0 mL of IOP solution passed through the CPAC column. It is in coincidence with the breakthrough point at C_t/C_0= 0.05 [216]. When 100.0 mL of IOP solution was passed through the column, CPAC was able to retain a maximum adsorption capacity of 864.7 mg g^{-1}, while C_t/C_0 reached 0.93-0.99 in five cycles. The elution of 100 mL of 10.0 mM IOP solution in 0.75 g of CPAC in the column indicated that the adsorption reaches a saturation state. In addition, the whole adsorption/desorption process can be repeated for five cycles. q_e is higher in flow mode than that (496.1 mg g^{-1}) in batch mode (as shown in Fig. 4.5) and the previous studies (Table 4.5). In the case of desorption with MeOH, the *DE* in flow mode is superior compared to batch treatments. In each cycle, the desorption amount of IOP was close to CPAC-loaded IOP. It further demonstrates that IOP loaded by the monolayer adsorption can be easily eluted with MeOH to attain simultaneous regeneration of CPAC and recovery of IOP. Furthermore, the NMR and DRIFT spectroscopy for recovered IOP and pristine IOP are identical, which indicates that the compound is not modified during the adsorption/desorption processes (see Fig. S4.2 and Fig. S4.3).

4.3.5 Comparison of characterization among pristine, spent and regenerated activated carbons

4.3.5.1 Morphology and textural properties

FESEM images clearly show the morphologic changes occurred at the surface of the adsorbent before and after adsorption [188, 228], as well as before and after desorption. The FESEM images of pristine, IOP-loaded and regenerated CPACs with MeOH elution in batch and flow modes are given in Fig. 4.9.

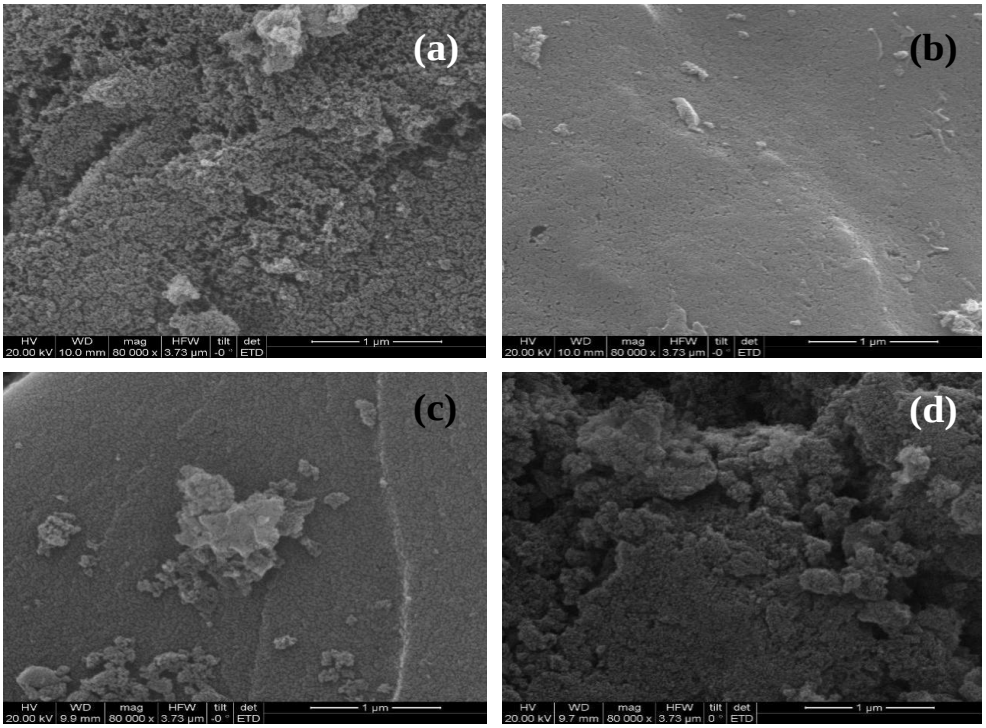

Fig. 4.9 FESEM images of pristine CPAC (a); IOP-loaded CAPC (b); CPAC after desorption in batch (c) and flow mode (d) (Instrumental magnification 80000×)

As shown in Fig. 4.9a, the surface morphology of pristine CPAC appears to be rough and quite uniformly grainy, with a wider distribution of pores. After adsorption, the CPAC surface became smooth, the grains appeared to be poorly defined and intra-particle porosity was significantly lower (Fig. 4.9b). Upon desorption in batch mode, the CPAC surface seems to be relatively bumpy and grains partially reappeared (Fig. 4.9c). These features indicate that IOP was not completely recovered, and that a fraction of the loaded molecules remained adsorbed on the CPAC surface. A comparison with Fig. 4.9a shows that, after desorption in the flow mode, the surface of the regenerated CPAC became similar to that of the pristine sample, as numerous grains and intra-particle porosity were restored, as shown in Fig. 4.9d.

The textural properties of AC determine their performance in removing organic compounds from the liquid phase [204]. The larger micropores and mesopores volume of ACs causes the high *AE* of IOP [213]. BET surface areas and

the porosity of the IOP-loaded CPAC and CPAC samples after desorption in batch and flow modes, are compared in Table 4.6. Data for the pristine CPAC sample are also reported for the sake of comparison.

Table 4.6 Textural properties of CPAC samples

Samples	S_{BET} ($m^2 g^{-1}$)	V_{micro} ($cm^3 g^{-1}$)	V_{meso} ($cm^3 g^{-1}$)	D_P (nm)
Pristine CPAC	1952	1.76	1.57	3.95
IOP-loaded CAPC in batch	313	0.41	0.45	5.89
CPAC after desorption in batch	1392	1.20	0.97	3.63
IOP-loaded CPAC in flow*	211	0.20	0.20	5.23
CPAC after desorption in flow*	1659	1.50	1.30	3.90

*"in-flow" CPAC samples were collected after five cycles of adsorption/desorption.

The data in Table 4.6 indicates that the BET surface area and pore volume for IOP-loaded CPAC samples significantly decreased, compared to pristine CPAC material [167]. Furthermore, the mesoporous diameter of IOP-loaded samples is shifted toward larger pores because micropores are more easily occupied by IOP. IOP is a voluminous molecule (Table 4.1), and its dimensions mainly allow it to access CPAC pores with an average diameter of at least 3.95 nm [167]. Importantly, the textural properties of CPAC were almost recovered by desorption in flow mode, compared to the pristine CPAC.

4.3.5.2 Nature of surface functional groups

Oxygen-containing functional groups, including hydroxyl, carboxyl, carbonyl and lactone groups usually exist on the surface of ACs [136, 230]. These groups can be identified by the DRIFTS. The DRIFT spectra of pristine, IOP-loaded and regenerated CPAC in batch and flow mode are compared in Fig. S4.4. For the sake of clarity, the absorption bands of surface functional groups assigned in the DRIFT spectra are listed in Table 4.7. Additionally, the nature of these functional groups of pristine CPAC was further confirmed by high-resolution XPS spectra, as shown in Fig. S4.5.

Table 4.7 Functional groups on CPAC samples, according to DRIFT spectra

Wavenumber (cm^{-1})	Functional groups	CPAC	IOP-loaded CPAC	CPAC eluted in batch	CPAC eluted in flow
3565	ν(O-H)	√	-	√	√
3300	ν(O-H)/ν(N-H)	-	√	-	-
3060/2940/2870	ν(C-H)	√	√	√	√
2369/2317	ν(C-N)		√	-	-
1700	-COOH/-COOR, ν(C=O)	√	-	√	√
1600	-COOR, ν(C-O), ν(C=C)	√	-	√	√
1050	ν(C-O)	-	√	-	-
880/817/760	out-of-plane bending ν(C-H)	√	√	√	√

Note: √ (present); - (not present).

As seen in Fig. S4.4 and Table 4.7, both the intensity and shape of absorption at 1600, 1700 cm^{-1} of the stretching of C=O belonging to different functional groups change upon IOP adsorption, which indicates that these groups are strongly perturbed by IOP interaction. At the same time, new bands were detected in IOP-loaded CPAC, at 1050, 2317, 2369, 3300 cm^{-1}, and these were assigned to the C-O, C-N and O-H/N-H stretching modes of the IOP molecule, respectively. The observation is consistent of the study by Bellich et al, confirming that IOP was effectively adsorbed onto CPAC [231]. On the basis of this study, we can propose that the C=O of different functional groups on the CPAC surface are the sites that interact with the IOP molecule. The spectra of CPAC samples after desorption in both batch and flow modes have similar overall profiles to those of pristine CPAC, while the three CPAC forms bear identical functional groups.

Moreover, TGA measurements of pristine, IOP-loaded and regenerated CPACs were carried out, as shown in Fig. S4.6. 42.2% of weight loss of IOP-loaded CPAC indicates that IOP was efficiently adsorbed onto CPAC. In contrast, 25.2 % and 20.6 % of weight losses of CPAC samples after desorption in batch and flow mode were observed, respectively. Such weight losses are comparable to that of

pristine CPAC. It indicates that IOP loaded onto CPAC was eluted with MeOH in batch and flow modes.

4.3.6 Adsorption and desorption mechanisms of Iopamidol

4.3.6.1 Adsorption mechanism

As the above kinetic models were not able to identify the diffusion mechanism, intra-particle diffusion model is based on the theory proposed by Weber and Morris [229], which was applied using equation (17):

$$q_t = K_{id} t^{1/2} + C_i \qquad (17)$$

where K_{id} (mg g^{-1} $min^{-1/2}$) is the intra-particle diffusion rate constant, and the value of the intercept C_i gives an indication of the boundary layer thickness.

The curve-fitting plots obtained for the intra-particle diffusion model are reported in Fig. 4.10.

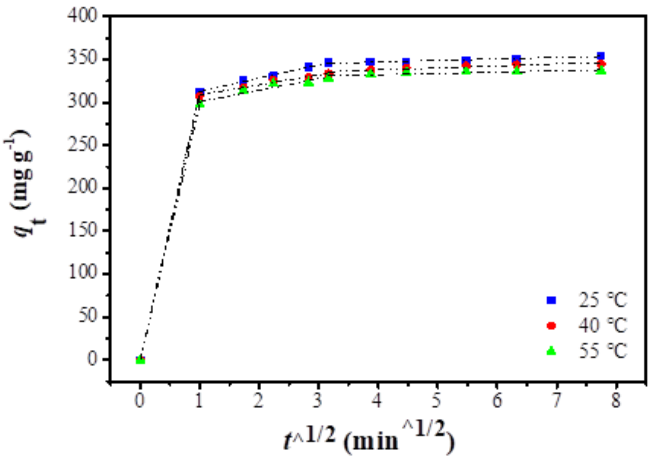

Fig. 4.10 Intra-particle diffusion equation fit of the adsorption kinetics

As shown in Fig. 4.10, the curves were not linear over the whole time range at 25°C, 40°C and 55°C and the plots did not pass through the origin, suggesting that some other mechanisms along with intra-particle diffusion are also involved. The first stage is the fastest, which describes IOP diffusion in the solution to the external CPAC surface [232]. The second region corresponds to a gradual adsorption stage that is governed by the intra-particle diffusion of IOP molecules

into the larger micropores and mesopores [233, 234]. The third region represents the final equilibrium at which intra-particle diffusion starts to slow down [216]. The curve trend may therefore be explained by external/film diffusion, which gives rise to the first portion, and by internal/intra-particle diffusion, which is responsible for the two further linear portion [233, 235].

The Boyd model was used to further examine whether IOP adsorption onto CPAC is controlled by external diffusion or internal diffusion. The Boyd model follows equation (18):

$$B_t = -0.4977 - \ln(1-F) = -0.4977 - \ln(1-q_t/q_0) \quad (18)$$

where B_t is a mathematical function of F, and F represents the fraction of solute adsorbed at any time (t).

Boyd plots for adsorption of IOP onto CPAC at 25°C, 40°C, and 55°C are shown in Fig. 4.11.

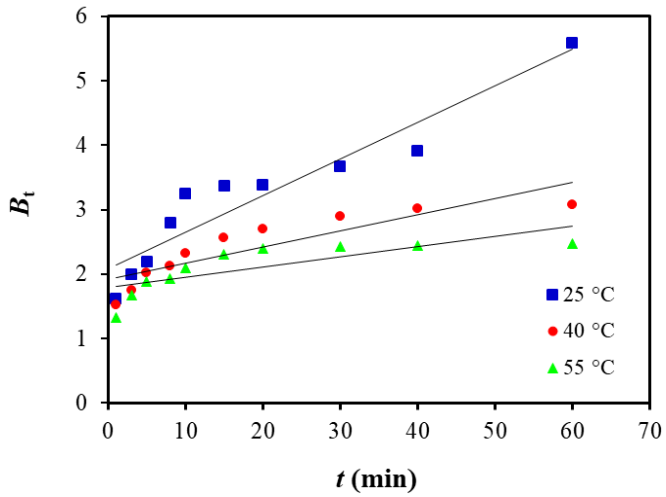

Fig. 4.11 Boyd plots for adsorption of IOP onto CPAC at 25°C, 40°C and 55°C

Particle diffusion determines the adsorption rate when the role of external transport is more important than that of internal transport [236]. It was observed that the linear lines do not pass through the origin and that the points were a little scattered (Fig. 4.11), which demonstrates that IOP adsorption onto CPAC was mainly governed by external mass transport where particle diffusion was the rate limiting step [237].

Adsorption kinetics studies confirm that the faster initial adsorption rate is due to the CPAC mesoporous network, which favors the diffusion of the molecule toward defined adsorption sites. Moreover, the Langmuir model suggests that monolayer adsorption was formed at the external surface of the AC material. The IOP molecule was mainly absorbed onto the exterior surface and into the large micropores and mesopores of CPAC. The Boyd model confirmed that IOP adsorption onto CPAC was mainly governed by external mass transport, for which particle diffusion was the rate-limiting step. Considering IOP structure, the graphene-like structures and other functional groups on CPAC surface, the different following interactions have been proposed: (1) dispersive interactions between π electrons of the aromatic ring and π electrons of the graphene planes of the carbon surface; (2) donor-acceptor complex involving the IOP molecule and carbon surface functional groups; (3) Van der Waals forces that occur between polar groups on IOP and polar surfaces of CPAC; (4) hydrogen bonding interactions between the IOP molecule and carbon surface functional groups. Therefore, IOP adsorption is governed by non-electrostatic interactions, such as donor-acceptor interactions between the surface carbonyl groups (electron donors) and the aromatic rings of IOP (electron acceptor) and hydrogen bonds interactions between the O-H, N-H of IOP molecule and the C=O on the carbon surface.

4.3.6.2 Desorption mechanism

The solubility of the compounds in the solvent and their affinity to AC surfaces are important factors in determining the *DE* values [238]. Owing to the high polarity and hydrophilicity, thus the polar solvents were chosen to elute IOP from CPAC. *DE* values of IOP that were obtained using MeOH, EtOH, and ACN in batch modes are presented in Fig. 4.12.

As shown in Fig. 4.12, *DE* values obtained with MeOH and EtOH were higher than that with ACN. The dielectric constant indicates polarity of solvents. The dielectric constant values of EtOH, MeOH, and ACN are 24.6, 32.7, 37.5 at 20°C [239], respectively, it is fact that ACN has higher polarity. Obviously, lower polarity among polar solvents is favorable for eluting IOP. In addition, other interactions, such as hydrogen bonds, also influence the *DE* except for the polarity. Solubility of solvents in various solvents was studied in terms of Hansen solubility parameters [239, 240], which are defined as:

$\delta_t = \delta_d + \delta_p + \delta_h$.....(19)

Where δ_t is the total solubility parameter (unit $MPa^{0.5}$), and the subscripts d, p, h refer to the dispersive, polar contributions and the contribution arising from hydrogen-bond interactions between adsorbents and solvents, respectively.

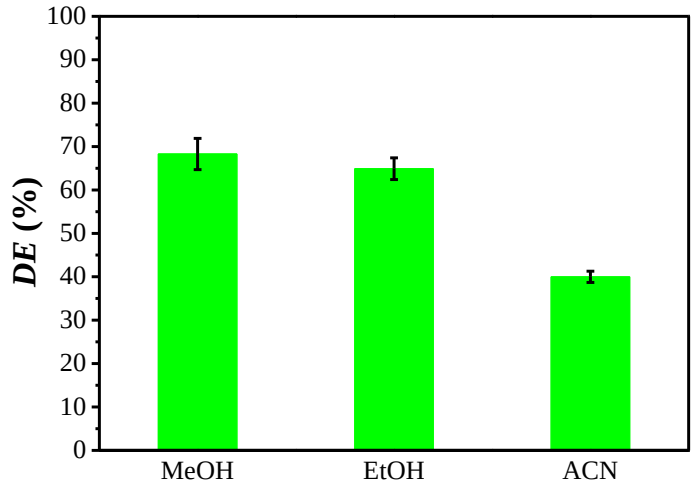

Fig.4. 12 Desorption of IOP with MeOH, EtOH, and ACN in batch modes
(Desorption conditions: 10 mg of IOP-loaded CPAC (496.1 mg IOP/g CPAC) in 4 mL MeOH, EtOH, and ACN; the mixture was shaken for 10 min at 450 rpm at 25°C)

The hydrogen bonding solubility parameters (δ_h, unit $MPa^{0.5}$) of MeOH, EtOH, and ACN in sequences are 22.3, 19.4, 6.1 [239, 240]. Thus MeOH and EtOH can form stronger hydrogen bonds with IOP, thus enhancing the *DE* values. Therefore, MeOH and EtOH are both suitable solvents for eluting IOP from CPAC. Therefore, it is concluded that the polarity of solvents and hydrogen bonding interactions between IOP and alcohols influence the desorption process.

Supplementary Data

S.4.1 The linear correlations between adsorption capacity and specific surface area, micropore and mesopore volumes

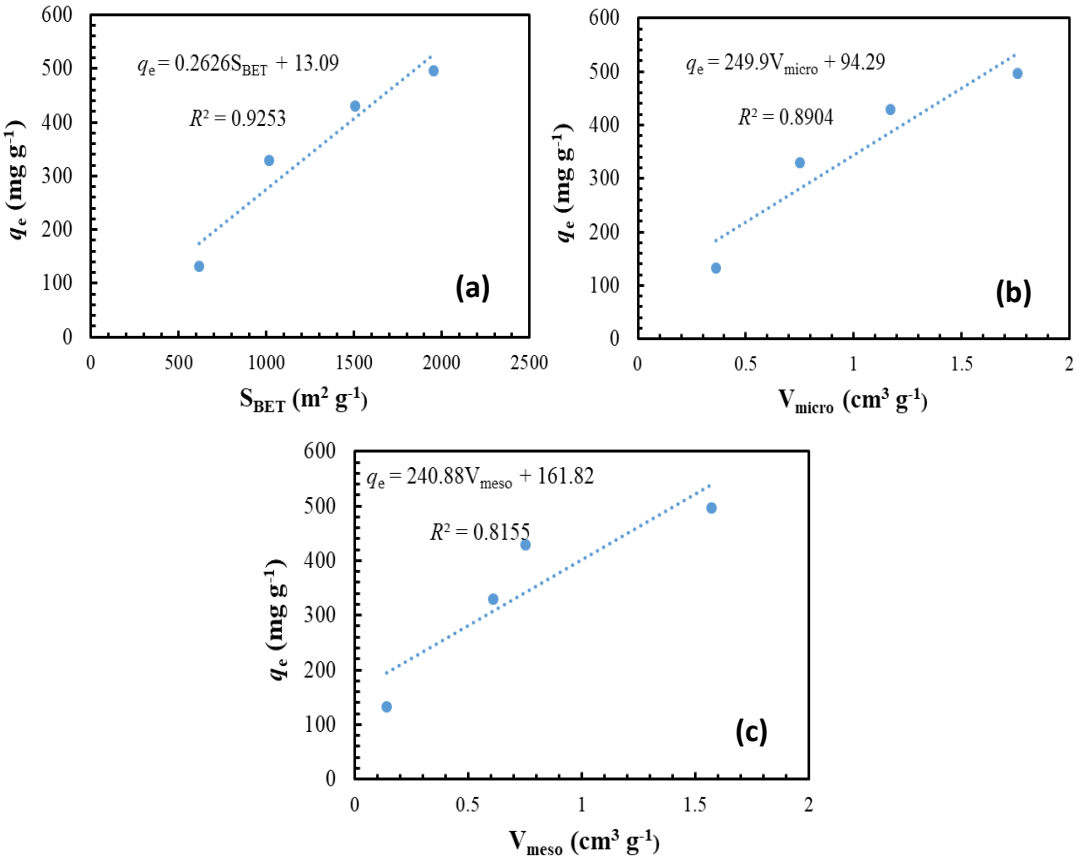

Fig. S4.1 The linear correlations between (a) S_{BET} and q_e of IOP adsorbed on ACs; (b) V_{micro} and q_e of IOP adsorbed on ACs; (c) v_{meso} and q_e of IOP adsorbed on ACs

S.4.2 Comparison of the NMR and DRIFT spectroscopy of the pristine Iopamidol (IOP) and the recovered IOP

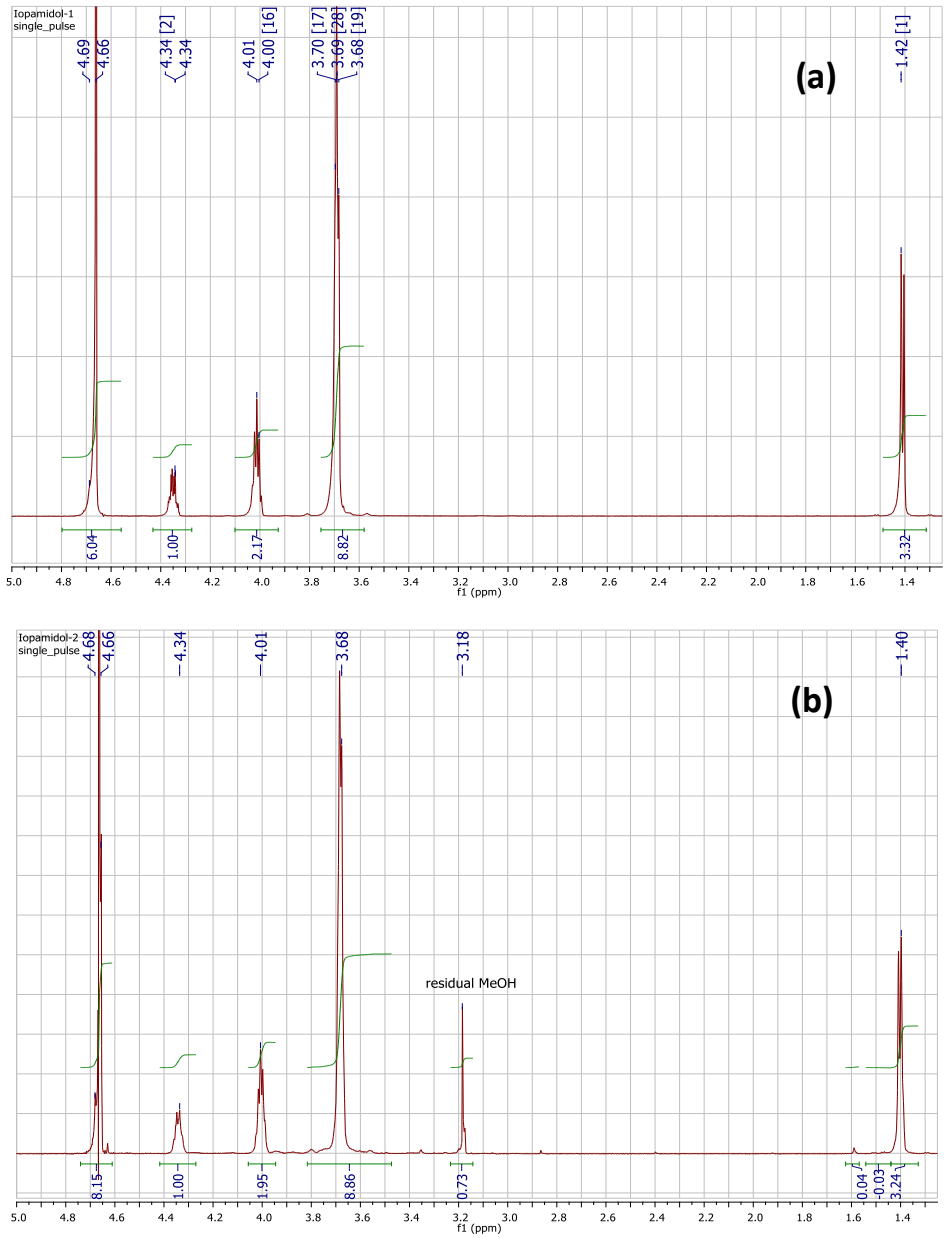

Fig. S4.2 NMR for the pristine IOP (a) and recovered IOP (b)

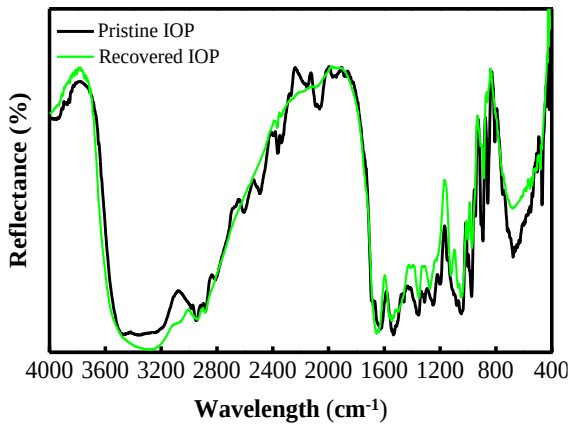

Fig. S4.3 DRIFT spectra of the pristine IOP and the recovered IOP

S.4.3 DIRFT spectra of pristine, spent and regenerated activated carbons

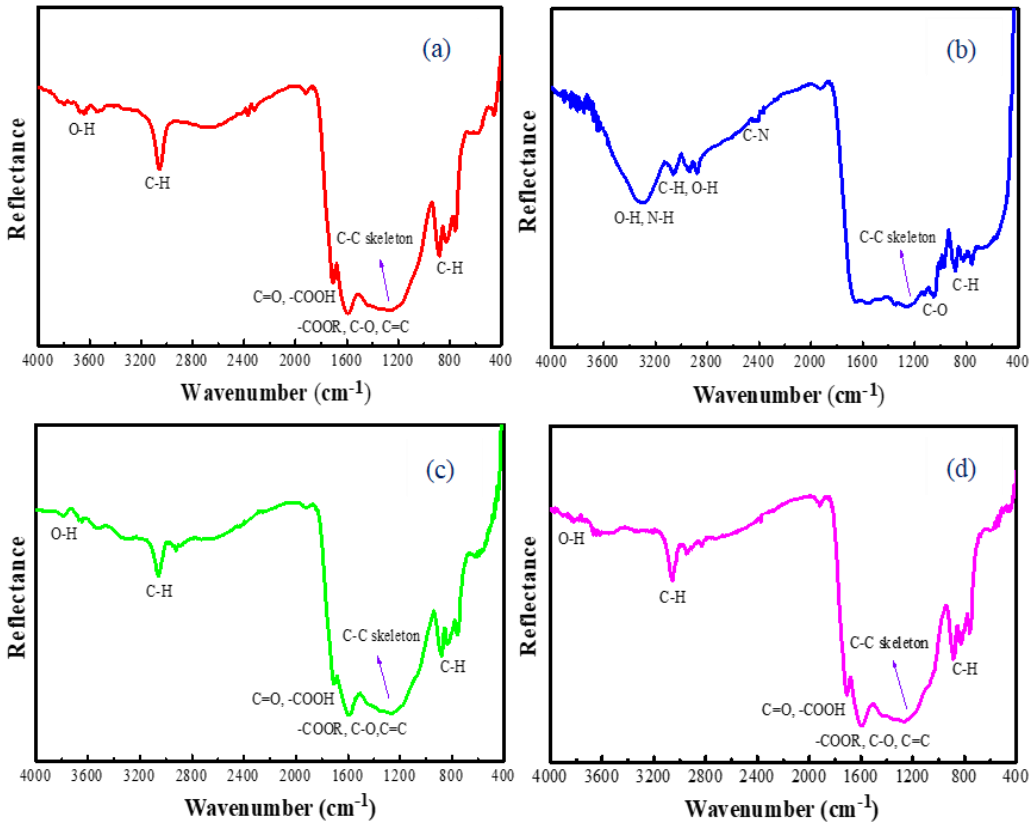

Fig. S4.4 DRIFT spectra (a) Pristine CPAC; (b) IOP-loaded CPAC; (c) CPAC after desorption in batch mode; (d) CPAC after desorption in flow mode

S.4.4 XPS spectra of coconut powder activated carbon

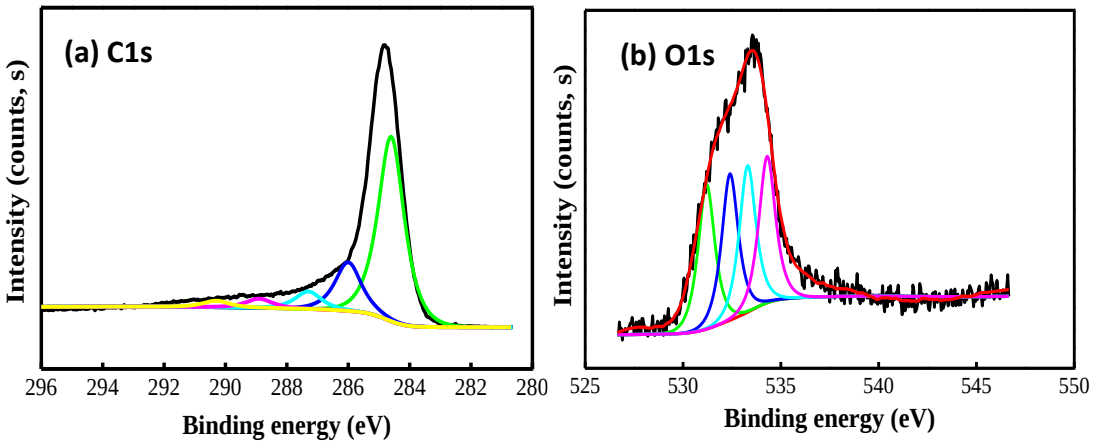

Fig. S4.5 High-resolution XPS spectra of C1s (a); O1s (b)

S.4.5TGA analysis of pristine, spent and regenerated activated carbons

In general, the pyrolysis products of IOP under 50°C to 800°C include carbon monoxide (CO), carbon dioxide (CO_2), hydrogen iodide (HX), nitrogen oxides (NOx), other pyrolysis products typical of burning organic material.

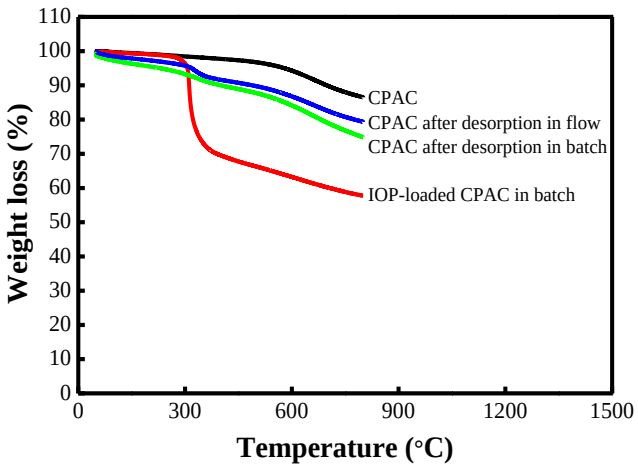

Fig. S4.6 TGA curves of pristine, spent and regenerated activated carbons

References

[200] Busetti, F., Linge, K. L., Rodriguez, C., Heitz, A. Occurrence of iodinated X-ray contrast media in indirect potable reuse systems. Journal of Environmental Science and Health Part A, 45(2010) 542-548.

[201] Pérez, S., Barceló, D. Fate and occurrence of X-ray contrast media in the environment. Analytical and Bioanalytical Chemistry, 387(2007) 1235-1246.

[202] Jeong, J., Jung, J., Cooper, W. J., Song, W. Degradation mechanisms and kinetic studies for the treatment of X-ray contrast media compounds by advanced oxidation/reduction processes. Water Research, 44(2010) 4391-4398.

[203] Radjenovic, J., Flexer, V., Donose, B. C., Sedlak, D. L., Keller, J. Removal of the X-ray contrast media diatrizoate by electrochemical reduction and oxidation. Environmental science & technology, 47(2013) 13686-13694.

[204] Mestre, A. S.; Machuqueiro, M.; Silva, M.; Freire, R.; Fonseca, I. M.; Santos, I. M.; Calhorda, M. J.; Carvalho, A. P. Influence of activated carbons porous structure on Iopamidol adsorption. Carbon, 77 (2014) 607-615.

[205] Ning, B., Graham, N. J., Lickiss, P. D. Degradation of X-ray contrast media compounds by combined ozone and ultrasound. Water Environment Research, 79(2007) 2427-2436.

[206] Thomson, K. R., Varma, D. K. Safe use of radiographic contrast media. Australian Prescriber, 33(2010) 19-22.

[207] Busetti, F., Linge, K. L., Blythe, J. W., Heitz, A. Rapid analysis of iodinated X-ray contrast media in secondary and tertiary treated wastewater by direct injection liquid chromatography-tandem mass spectrometry. Journal of Chromatography A, 1213(2008) 200-208.

[208] Huber, M. M., Canonica, S., Park, G. Y., Von Gunten, U. Oxidation of pharmaceuticals during ozonation and advanced oxidation processes. Environmental science & technology, 37(2003) 1016-1024.

[209] McArdell, C. S., Kovalova, L., Eugster, J., Hagenbuch, M., Wittmer, A., Siergrist, H. Elimination of pharmaceuticals from hospital wastewater in a pilot membrane bioreactor with PAC or ozone post-treatment. In Conference proceeding: SETAC Europe, 20 th Annual meeting, Spain, May, 2010, 23-27.

[210] Mestre, A. S.; Pires, R. A.; Aroso, I.; Fernandes, E. M.; Pinto, M. L.; Reis, R. L.; Andrade, M. A.; Pires, J.; Silva, S. P.; Carvalho, A. P. Activated carbons prepared from industrial pre-treated cork: sustainable adsorbents for pharmaceutical compounds removal. Chemical Engineering Journal 253(2014) 408-417.

[211] Mestre, A. S., Tyszko, E., Andrade, M. A., Galhetas, M., Freire, C., Carvalho, A. P. Sustainable activated carbons prepared from a sucrose-derived hydrochar: remarkable adsorbents for pharmaceutical compounds. RSC Advances, 5(2015) 19696-19707.

[212] Redeker, M., Wick, A., Meermann, B., Ternes, T. A. Removal of the iodinated X-ray contrast medium diatrizoate by anaerobic transformation. Environmental Science & Technology, 48(2014) 10145-10154.

[213] Bocos, E., Oturan, N., Sanromán, M. Á., Oturan, M. A. Elimination of radiocontrast agent diatrizoic acid from water by electrochemical advanced oxidation: kinetics study, mechanism and mineralization pathway. Journal of Electroanalytical Chemistry, 772(2016) 1-8.

[214] Mansour, F., Al-Hindi, M., Yahfoufi, R., Ayoub, G. M., Ahmad, M. N. The use of activated carbon for the removal of pharmaceuticals from aqueous solutions: a review. Reviews in Environmental Science and Bio/Technology, 17(2018) 109-145.

[215] García, V., Häyrynen, P., Landaburu-Aguirre, J., Pirilä, M., Keiski, R. L., Urtiaga, A. Purification techniques for the recovery of valuable compounds from acid mine drainage and cyanide tailings: application of green engineering principles. Journal of Chemical Technology & Biotechnology, 89(2014) 803-813.

[216] Tan, I. A. W., Ahmad, A. L., Hameed, B. H. Adsorption of basic dye on high-surface-area activated carbon prepared from coconut husk: Equilibrium, kinetic and thermodynamic studies. Journal of Hazardous Materials, 154(2008) 337-346.

[217] Djordjevic, D.; Stojkovic, D.; Djordjevic, N., Smelcerovic, M. Thermodynamics of reactive dye adsorption from aqueous solution on the ashes from city heating station. Ecological Chemistry and Engineering S, 18(2011) 527-536.

[218] Hameed, B. H. Equilibrium and kinetics studies of 2, 4, 6-trichlorophenol adsorption onto activated clay. Colloids and Surfaces A: Physicochemical and Engineering Aspects, 307(2007) 45-52.

[219] Özcan, A., Öncü, E. M., Özcan, A. S. Kinetics, isotherm and thermodynamic studies of adsorption of Acid Blue 193 from aqueous solutions onto natural sepiolite. Colloids and Surfaces A: Physicochemical and Engineering Aspects, 277(2006) 90-97.

[220] Hameed, B. H.; Tan, I. A. W.; Ahmad, A. L. Adsorption isotherm, kinetic modeling and mechanism of 2, 4, 6-trichlorophenol on coconut husk-based activated carbon. Chemical Engineering Journal, 144(2008) 235-244.

[221] Namasivayam, C., Ranganathan, K. Waste Fe (III)/Cr (III) hydroxide as adsorbent for the removal of Cr (VI) from aqueous solution and chromium plating industry wastewater. Environmental Pollution, 82(1993) 255-261.

[222] Liu, Y. (2009). Is the free energy change of adsorption correctly calculated? Journal of Chemical & Engineering Data, 54(2009) 1981-1985.
[223] Wu, C. H. Adsorption of reactive dye onto carbon nanotubes: equilibrium, kinetics and thermodynamics. Journal of Hazardous Materials, 144(2007) 93-100.
[224] Chen, G. C., Shan, X. Q., Zhou, Y. Q., Shen, X. E., Huang, H. L., Khan, S. U. Adsorption kinetics, isotherms and thermodynamics of atrazine on surface oxidized multiwalled carbon nanotubes. Journal of Hazardous Materials, 169(2009) 912-918.
[225] Tancredi, N., Medero, N., Möller, F., Píriz, J., Plada, C., Cordero, T. Phenol adsorption onto powdered and granular activated carbon, prepared from Eucalyptus wood. Journal of Colloid and Interface Science, 279(2004) 357-363.
[226] Carvalho, A. P., Galhetas, M., Andrade, M. A., Batista, M. K., Mestre, A. S. Synthesis of biomass-derived activated carbons for liquid phase application. Boletín del Grupo Español del Carbón, 2016, 13-18.
[227] Mestre, A. S., Galhetas, M., Andrade, M. A. Micropore size distribution of activated carbons: a key factor for a deeper understanding of the adsorption mechanism of pharmaceuticals. Boletín del Grupo Español del Carbón, 2016, 22-27.
[228] Ahmad, R., Kumar, R. Adsorptive removal of congo red dye from aqueous solution using bael shell carbon. Applied Surface Science, 257(2010) 1628-1633.
[229] Arulkumar, M., Sathishkumar, P., Palvannan, T. Optimization of Orange G dye adsorption by activated carbon of Thespesia populnea pods using response surface methodology. Journal of Hazardous Materials, 186(2011) 827-834.
[230] Zhang, D., Yin, J., Zhao, J., Zhu, H., Wang, C. Adsorption and removal of tetracycline from water by petroleum coke-derived highly porous activated carbon. Journal of Environmental Chemical Engineering, 3(2015) 1504-1512.
[231] Bellich, B.; Di Fonzo S.; Tavagnacco, L.; Paolantoni, M.; Masciovecchio, C.; Bertolotti, F.; Giannini, G.; De Zorzi, R.; Geremia, S.; Maiocchi, A.; Uggeri, F.; Masciocchi, N.; Cesaro, A. Myelography iodinated contrast media. 2. Conformational versatility of Iopamidol in the solid state. Molecular Pharmaceutics, 14(2017) 468-477.
[232] Chen, S., Yue, Q., Gao, B., Li, Q., Xu, X., Fu, K. Adsorption of hexavalent chromium from aqueous solution by modified corn stalk: a fixed-bed column study. Bioresource Technology, 113(2012) 114-120.

[233] Cheung, W. H., Szeto, Y. S., McKay, G. Intraparticle diffusion processes during acid dye adsorption onto chitosan. Bioresource Technology, 98(2007) 2897-2904.
[234] Ahmad, M. A., Alrozi, R. Removal of malachite green dye from aqueous solution using rambutan peel-based activated carbon: Equilibrium, kinetic and thermodynamic studies. Chemical Engineering Journal, 171(2011) 510-516.
[235] Goswami, A., Raul, P. K., Purkait, M. K. Arsenic adsorption using copper (II) oxide nanoparticles. Chemical Engineering Research and Design, 90(2012) 1387-1396.
[236] Sotelo, J. L., Ovejero, G., Rodríguez, A., Álvarez, S., García, J. Analysis and modeling of fixed bed column operations on flumequine removal onto activated carbon: pH influence and desorption studies. Chemical Engineering Journal, 228 (2013) 102-113.
[237] Zamora, F., Sabio, E., Román, S., González-García, C. M., Ledesma, B. Modelling the adsorption of p-Nitrophenol by the Boyd method in conjunction with the finite element method. Adsorption Science & Technology, 28(2010) 671-687.
[238] Kwon, D. S.; Tak, S. Y.; Lee, J. E.; Kim, M. K.; Lee, Y. H.; Han, D. W.; Kang, S.; Zoh, K. Desorption of micropollutant from spent carbon filters used for water purifier. Environmental Science and Pollution Research, 24(2017) 17606-17615.
[239] Hansen, C. M. Hansen solubility parameters. CRC Press Boca Raton, 2007.
[240] Subrahmanyam, R., Gurikov, P., Dieringer, P., Sun, M., Smirnova, I. On the road to biopolymer aerogels—Dealing with the solvent. Gels, 1(2015) 291-313.

Chapter 5: Feasibility and Mechanism of Desorption of Phenols from Activated Carbons

Abstract

The desorption efficiency (*DE*) of phenols, including *p*-nitrophenol, *p*-chlorophenol, *p*-hydroxybenzoic acid, phenol and hydroquinone, from various ACs has been investigated with a variety of solvents to gain insight into the feasibility and mechanism of phenols desorption. US, MW and flow mode have been used to facilitate phenols desorption. Typically, 100 mg phenols-loaded ACs in 10 mL solvent was shaken with 450 rpm at 25°C for 60 min and then the phenols concentration in the filtrates was analyzed by UV/Vis spectrophotometer. It was found that basicity, polarity and hydrogen bonding of solvents synergistically affected phenols desorption. The preferred solvents (Lewis basic solvents, acetic acid and alcohols) gave highly efficient elution. Increasing the alkaline or/and hydrogen bonding interactions, by adding ammonia or urea, enhanced the desorption in most solvents. Moreover, although US and MW heating slightly improved desorption, complete desorption was easily achieved in flow mode. It is demonstrated herein that phenols adsorption on the ACs is a reversible physical process, therefore, proving the feasibility of phenols desorption with proper solvents. Comparisons of DRIFT spectra and the porosity properties of pristine, loaded and eluted ACs were also performed to verify the results. It can therefore be stated that our procedure can be used to dispose of secondary pollution while cutting post-treatment costs thanks to the recovery of valuable compounds and ACs recycling.

5.1 Introduction

Phenolic compounds have been extensively produced and used the world over, resulting in a large amount of phenolic discharge and their widespread occurrence in the environment. While they are typical organic pollutants, phenols have also attracted specific attention due to their high hydrophilicity, toxicity and persistence [184, 241-243]. Moreover, phenols have been frequently used as model compounds for the development of wastewater-treatment technology. A wide variety of technologies, such as membrane separation [244], solvent extraction [245], adsorption [108, 152, 246-248], biodegradation [249], AOPs [152, 250, 251] have been applied to remove phenols from wastewaters. Of all the

methods, adsorption appears to be the most suitable process as it can provide high removal efficiency, furnishes no harmful by-products, can potentially reuse adsorbents, and is an easy-to-operate and scalable process. Activated carbons (ACs) have been commonly used as adsorbents for the removal of organic pollutants (phenols, aromatics, pharmaceuticals and pesticides, etc.) from highly polluted wastewaters [136, 191, 252], because of their well-developed porous structure, which is made up of hydrophobic graphene layers and hydrophilic surface functional groups [253]. A variety of ACs that are derived from renewable biomass, such as coconut shells, wood sawdust and peat, have increasingly attracted interest from the wastewater-treatment field in recent decades [48-50, 184].

In general, classical adsorption processes are only focused on moving pollutants from the wastewater onto the adsorbents, meaning that the post-treatment of pollutant-loaded adsorbents must be considered and performed [248, 254]. Otherwise, secondary pollution becomes extremely problematic. The feasibility of adsorption processes, overall, depends on treatment efficiency and costs, in fact, both adsorbent regeneration and adsorbate recovery are critical to success [255]. Although the adsorptive removal of phenols onto ACs is easily achieved [108, 152, 246-248], the desorption of phenols is still an attractive challenge. As already mentioned in Section 1.1.2 and Section 1.4, physical adsorption, involving Van der Waals forces and/or weak charge-transfer complexes in adsorption sites, is reversible [243]. Irreversible adsorption can be caused by: (1) chemisorption, i.e., the bonding of an adsorbate with specific functional groups onto the active sites of ACs; (2) the oxidative polymerization of phenols onto the carbon surface via oxidative coupling reactions [243, 256]. As mentioned in Section 1.4, various desorption techniques including solvent elution, related aqueous thermal, MW-assisted and US desorption [118-125] have been applied for the regeneration of spent carbons. Compared to the pyrolytic method, solvent elution requires relatively lower energy consumption and avoids the loss of carbons, while enabling adsorbate recovery [118, 129, 126]. In theory, the desorption of adsorbates depends on the accessibility of the solvent to the micropores, solubility and adsorbate-carbon surface interactions [243].

This study aims to achieve high *DE* and gain a better understanding of the desorption mechanism involved. Phenols were eluted from ACs with various solvents under SK, US and MW. Moreover, the effects of different ACs, AC mass

and a variety of phenols have been investigated. A comparative analysis of the relationship between the adsorption and desorption efficiencies of *p*-nitrophenol (PNP), *p*-chlorophenol (PCP), *p*-hydroxybenzoic acid (PHBA), phenol (PH) and hydroquinone (HQ) has been performed. The adsorption/desorption process of PNP in semi-continuous flow has also been studied to demonstrate the feasibility of the desorption, which was also verified by a comparison of DRIFT spectroscopy and porosity properties in the pristine, loaded and eluted ACs.

5.2 Experiment section

5.2.1 Chemicals

In this study, the physicochemical properties of phenols, PNP (99%, Alfa Aesar), PCP (98%, Merck), PHBA (98%, Merck), PH (99%, Sigma Aldrich) and HQ (99%, Sigma Aldrich), are listed in Table 5.1.

Table 5.1 Physicochemical properties of phenols

Parameters	PNP	PCP	PHBA	PH	HQ
Chemical structure	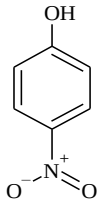	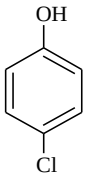	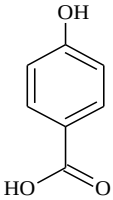	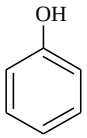	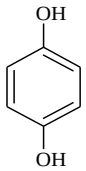
Formula weight (FW, g mol^{-1})	139.1	128.6	138.1	94.11	110.1
Density (ρ, g cm^{-3})	1.490	1.224	1.460	1.071	1.330
Melting point (°C)	113.8	42.7	214.5	40.9	172.3
Boiling point (°C)	279	220	nd	181.8	287
UV, λ_{max} (nm)	400	280	246.7	270	288.5
Octanol/water partition coefficient (log K_{OW})	1.91	2.39	1.58	1.46	0.59
Water solubility at 25°C (WS, g L^{-1})	15.6	24.0	5.0	83.0	72.0
Dissociation constants (pKa)	7.15	9.41	4.54	9.99	10.85
Dipole moment (μ, D)	5.05	2.15	2.73	1.61	1.40
Polarity/polarizability (α, Å^3)	13.74	13.09	15.81	11.15	10.75

Note: Data referred from Pubchem (https://pubchem.ncbi.nlm.nih.gov/).

Sodium hydroxide (NaOH, 98.0%) and urea (99.5%) were obtained from Alfa Aesar, and ammonia solution (NH_3 (aq), 30.0%) was provided by Carlo Erba. Other organic solvents, ethylene glycol (EG, 98.0%), ethanol (EtOH, 96.0-97.2%), methanol (MeOH, 99.9%), *n*-butanol (*n*-BuOH, 99.5%), *n*-propanol (*n*-PrOH, 99.0%), acetic acid (HOAc, 99.0%), methyl ethyl ketone (MEK, 99.0%), dimethyl ketone (DMK, 99.0%), acetonitrile (ACN, 99.9%), gamma-valerolactone (GVL, 98.0%), *N,N*-dimethylformamide (DMF, 99.8%), tetrahydrofuran (THF, 99.9%), dimethylsulfoxide (DMSO, 99.9%) and diethyl ether (Et_2O, 99.0%), were purchased from Sigma Aldrich. All chemicals were used as received.

5.2.2 Set up

The information of experimental setups (Heating magnetic stirrer for stirring desorption; Liquid phase parallel synthesizer for shaking adsorption and desorption) used in this part referred to Table 3.1 and Fig. 3.1. In particular, Single reaction chamber microwave synthesis system (SynthWave, Milestone Srl, Italy) and Ultrasonic bath (Sonic digital MG BASIC, Weber Ultrasonics AG, Germany) were used for desorption process and the setup images are attached in Fig. 5.1.

Fig. 5.1 Setups images: Single reaction chamber microwave synthesis system (left, 2.45 GHz, 1500 W); Ultrasonic bath (right, 40-120 kHz, 200 W)

5.2.3 Adsorption of phenols in batch mode

To prepare sufficiently phenol-loaded ACs for desorption studies, 3.5 g of the dried ACs was added to 500 mL of aqueous solutions containing 1 g L^{-1} selected phenolic compound, and then the mixture was stirred at 450 rpm, using a magnetic stirrer (AREX VELP Scientifica, Italy), at 25°C for 60 min. Subsequently, the loaded ACs were filtered and oven-dried at 103°C for 24 h. The phenol concentration in the aqueous solutions was analysed using a UV-Vis

spectrophotometer. The amount of phenols loaded q_e (mg g^{-1}) and *AE* (%) are calculated as equations (3) and (4).

5.2.4 Desorption of phenols in batch mode

To understand the influence of the critical factors on the desorption of phenols, typical runs were performed. 100 mg ACs loaded with a phenolic compound were immersed in 10 mL of various solvents and then shaken in a Liquid Phase Parallel Synthesizer (Heidolph Synthesis 1, Italy) at 450 rpm and 25°C for 60 min. In this study, the effect of numerous solvents, ACs and phenolic compounds on *DE* was investigated. Moreover, the effects of the AC-mass-to-EtOH-volume ratio (*RMV*, 25-500 mg 10 mL^{-1}), US and MW heating were also investigated. US was performed under the following conditions: frequency, 40-120 kHz; power, 100-180 W; sonication time, 1-60 min in an ultrasonic bath (Sonic digital MG BASIC, Weber Ultrasonics AG, Germany). MW heating was conducted at 25°C-55°C in a single reaction chamber microwave synthesis system (SynthWave, Milestone Srl, Italy). *DE* values of phenols are calculated as equation (20):

$$DE(\%) = \frac{C_d \times V_d}{M_a \times q_e} \times 100\% \qquad (20)$$

where C_d is the phenols concentration after desorption (mg L^{-1}), V_d is the volume of solvent (mL), M_a is the mass of phenols-loaded ACs (mg), q_e is the amount of phenols loaded on ACs (mg phenols/g ACs).

5.2.5 Adsorption/desorption of *p*-nitrophenol in flow mode

0.35 g CPAC was packed into a glass column (15 × 0.62 cm I.D.), corresponding to a 2 cm bed height and a 0.7 cm^3 volume. A scheme of the flow device for the adsorption/desorption processes has been depicted in Fig. 4.1. A 1 g L^{-1} PNP solution passed through the CPAC-column at a flowrate of 0.75 mL min^{-1} with a vacuum pump. The PNP solution from the outlet was periodically collected in either 5 or 10 mL aliquots. After adsorption, the loaded CPAC-column was eluted with EtOH at a flowrate of 1 mL min^{-1} and the eluents were periodically collected in either 2.5 or 5 mL aliquots. The PNP concentration in the aqueous solutions was analysed using a UV-Vis spectrometer. All experiments are duplicated and errors

were shown by the difference between the higher measured value and the average value. If the errors are not visible in Figures, they are smaller than the symbols representing the average values.

5.3 Results and discussion

5.3.1 Adsorption of phenols on activated carbons

Both of ACs physiochemical characteristics and phenols properties could affect the adsorption performance. Thus, the pH_{PZC} values and FTIR spectra of ACs were analysed and depicted in Section S2 and S3. Table 5.2 lists q_e of various ACs and *AE* values of PNP. Table 5.3 lists q_e of WPAC and *AE* values of various phenols.

Table 5.2 Adsorption performances of PNP onto ACs

Adsorption performance	CPAC	WPAC	PPAC	PGAC	CGAC
q_e (mg PNP/g ACs)	142.0	141.3	140.8	125.1	138.5
AE (%)	99.4%	98.9%	98.6%	87.6%	97.0%

Table 5.3 Adsorption performances of phenols onto WPAC

Adsorption performance	PNP	PCP	PHBA	PH	HQ
q_e (mg phenols/gWPAC)	141.3	130.2	135.4	128.9	96.4
AE (%)	98.9%	91.1%	99.9%	90.2%	67.5%

As listed in Table 5.2, most ACs exhibited efficient adsorption performance toward PNP, except for PGAC. The results were verified by the porosity properties of the ACs (see in Table 3.5), as shown in the Supporting Information. The poor adsorption performance of PGAC is attributed to the low BET surface area and pore volumes.

Except for HQ, most model phenols were efficiently adsorbed onto WPAC, as shown in Table 5.3. The q_e values of WPAC for various phenols run in the following order: PNP > PHBA > PCP > PH > HQ. The functional groups -NO_2, -COOH and -Cl in PNP, PHBA and PCP are electron-withdrawing groups, and thus reduce the overall electron density in the π-system of the ring [108]. As a result, the interactions of PNP, PHBA, PCP and the functional groups on the ACs are enhanced, promoting the adsorption. However, hydroxyl (-OH) is an electron donor group, that can

augment the electron density of the aromatic rings of PH and HQ, thereby reducing adsorption [108, 256].

5.3.2 Desorption in batch mode

5.3.2.1 Effect of solvents on the desorption of PNP

The physicochemical properties of the solvents, such as acidity and basicity, polarity, hydrogen bonding, etc., considerably affect phenols desorption [120]. A variety of aqueous and non-aqueous solvents were used to explore the DE of PNP from CPAC in this study. The results were compared and are illustrated in Fig. 5.2.

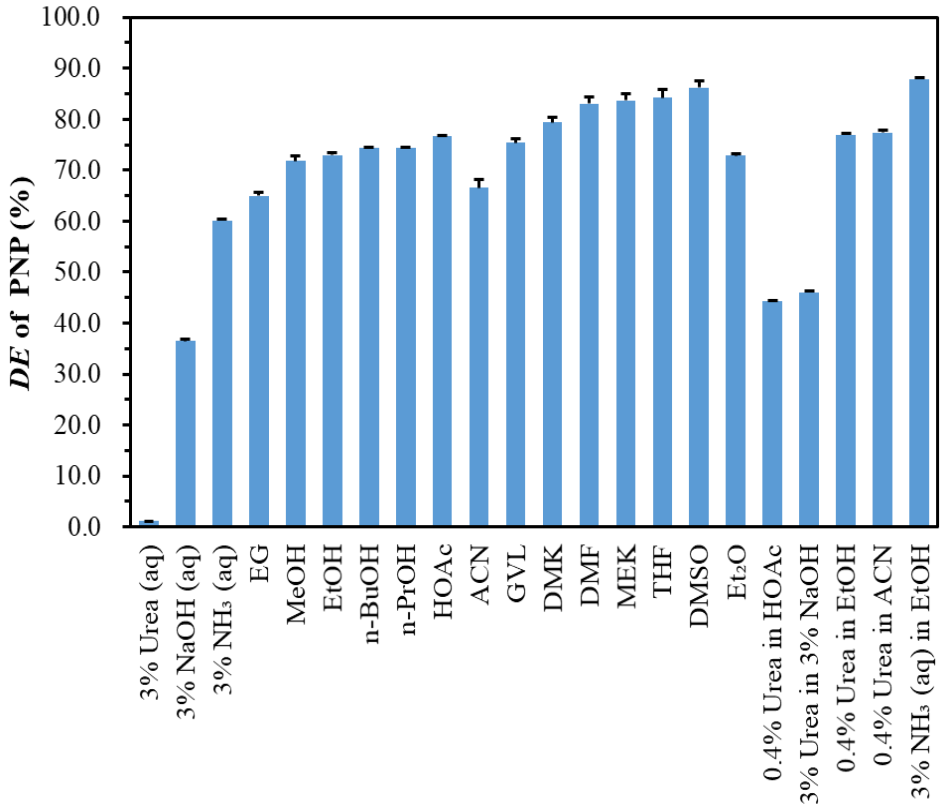

Fig. 5.2 *DE* values of PNP with various solvents

(Desorption conditions: 100 mg of PNP-loaded CPAC (142.0 mg PNP/g CPAC) immersed in 10 mL of solvents and shaken with 450 rpm at 25°C for 60 min)

As shown in Fig. 5.2, *DE* values of 36.4% and 60.1% were obtained with 3% NaOH (aq) and 3% NH_3 (aq), and were generally attributed to acid-base

neutralization in basic aqueous solutions. Phenolic salts that formed in the basic solutions may have facilitated the desorption of PNP from ACs [248, 256]. It was previously reported that *DE* values of 24.8% and 36.0% for PNP from ACs had been achieved via elution with 0.1 M and 0.3 M NaOH, respectively [257, 258]. In this study, the *DE* value of PNP was much higher by elution with 3% NH_3 (aq) than that with 3% NaOH (aq). It indicates that the hydrogen bonds formed between ammonia with hydroxyl- and nitro- moieties of PNP enhances the desorption.

To verify the role of hydrogen bonding, the aqueous urea solution was used to elute PNP from CPAC, as urea exhibits strong hydrogen-bonding interactions in aqueous solution. However, a *DE* of only 1.2% was achieved with 3% urea (aq) under neutral conditions, indicating that the hydrogen-bonding interactions between adsorbates and eluents do not work alone and are not the dominant factor in elution. However, the role of hydrogen bonds in desorption has regularly been proven using co-solvents, as discussed below. For instance, the *DE* value of PNP from CPAC increased from 36.4%, with 3% NaOH, to 46.1%, with 3% urea in 3% NaOH.

Higher *DE* values for PNP were observed in non-aqueous solvents than in basic aqueous solutions. The *DE* values of PNP with the various solvents are ordered as follows: 3% urea (aq) < 3% NaOH (aq) < 3% NH_3 (aq) < EG < ACN < MeOH < Et_2O < EtOH < *n*-BuOH < *n*-PrOH < GVL < HOAc < DMK < DMF < MEK < THF < DMSO. In non-aqueous solvents, Lewis base solvents exhibit better elution efficiency than acid and neutral solvents, while the hydrogen bonding interactions of alcohols and HOAc facilitate desorption [237, 259].

Moreover, the *DE* values with several co-solvents were compared and are depicted in Fig. 5.2. Except for 0.4% urea in HOAc, most co-solvents displayed higher *DE* values than the single solvents. For example, the *DE* value of PNP increased from 66.5%, with ACN, to 77.4%, with 0.4% urea in ACN. The *DE* value of PNP increased from 73.0%, with EtOH, to 87.9%, with 3% NH_3 (aq) in EtOH. This indicates that the basicity, polarity and hydrogen bonds of co-solvents synergistically enhance the desorption of PNP. However, *DE* values decreased from 76.7%, with HOAc, to 44.3%, with 0.4% urea in HOAc. The interaction between HOAc and urea probably diminishes the desorption. The desorption mechanism is discussed in details in the Section 5.3.3.

5.3.2.2 Effect of AC mass on PNP desorption

As mentioned above, EtOH has been demonstrated to be a superior solvent for the desorption of PNP from ACs, which is consistent with a previous study [261]. Furthermore, the effect of ACs mass (25-500 mg) in 10 mL EtOH, i.e., the ratio of loaded-PNP CPAC mass to EtOH volume (*RMV*), on PNP desorption was examined. The results are shown in Fig. 5.3.

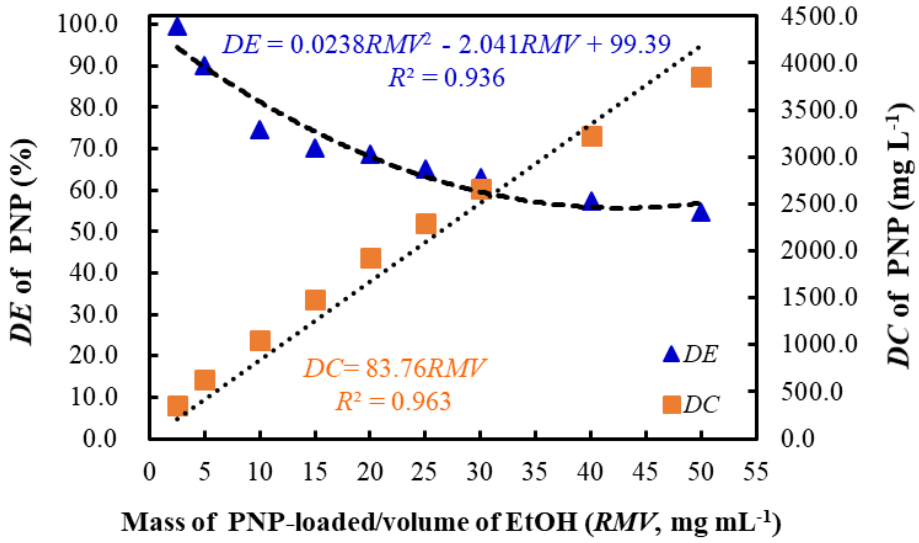

Fig. 5.3 Effect of mass of PNP-loaded CPAC with EtOH

(Desorption conditions: 25-500 mg of PNP-loaded CPAC (142.0 mg PNP/g CPAC) immersed in 10 mL of EtOH and shaken with 450 rpm at 25°C for 60 min)

As shown in Fig. 5.3, the efficient desorption of PNP from CPAC was achieved with EtOH. Also, the *DE* decreased polynomially as the mass of PNP-loaded CPAC increased in 10 mL of EtOH, indicating that lower amounts of PNP-loaded CPAC favor the desorption of PNP in a certain volume of EtOH. The dissolved concentration of PNP in the filtrates increased linearly with the mass of PNP-loaded CPAC. A cross-point between the above two curves was observed at 30 mg mL^{-1} of *RMV* (300 mg PNP-loaded CPAC with 10 mL EtOH), demonstrating that an *RMV* of over 30 mg mL^{-1} made the desorption difficult.

In the best case, 99.8% *DE* was achieved with 25 mg of PNP-loaded CPAC in 10 mL EtOH. Obviously, the complete desorption of phenols can be accomplished

with EtOH via successive cycles of elution in a flow system. The porosity properties of the recovered and pristine CPACs were compared to confirm the recovery efficiency. As a result, the S_{BET} surface area values of the recovered and pristine CPACs were determined to be 1794.7 and 1951.3 $m^2\ g^{-1}$, the V_{micro} 1.60 and 1.76 $cm^3\ g^{-1}$, the V_{meso} 1.36 and 1.57 $cm^3\ g^{-1}$, and the D_p 3.94 and 3.95 nm, respectively.

5.3.2.3 PNP Desorption from various ACs

The loading amounts of PNP onto one gram of the various ACs used were in the range of 125.1-142.0 mg, as listed in Table 5.2. 100 mg of PNP-loaded ACs was shaken in 10 mL of the selected solvents, including 3% NH_3 (aq), EtOH, HOAc and a co-solvent (3% NH_3 (aq) in EtOH). The results are shown in Fig. 5.4.

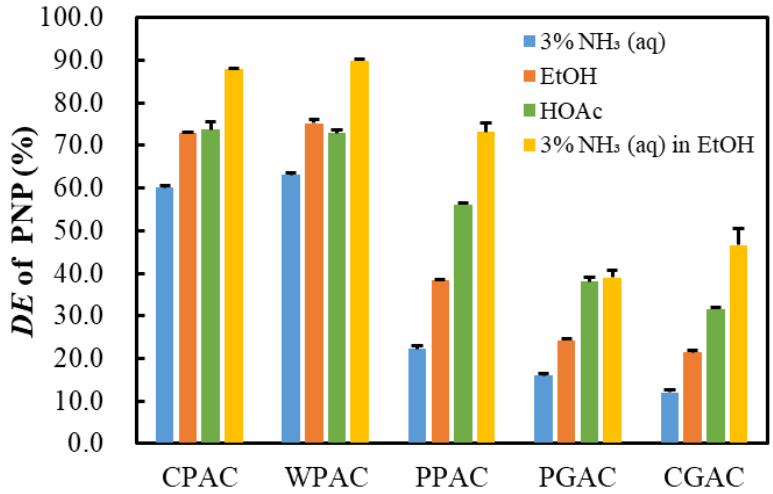

Fig. 5.4 Comparison of desorption of PNP among various loaded ACs

(Adsorption conditions: 3.5 g of ACs in 500 mL, 1 g L^{-1} of PNP stirred with 450 rpm at 25°C for 60 min; Desorption conditions: 100 mg PNP-loaded ACs in 10 mL various solvents shaken with 450 rpm at 25°C for 60 min)

With acidic CPAC and WPAC (Section S2) in Supplementary Data, on the one hand, the higher *AE* values for PNP were observed (Table 5.2), while on the other, much higher *DE* values for PNP were also found with all the selected solvents, especially with the basic co-solvent (3% NH_3 (aq) in EtOH), as shown in Figure 3. In general, the porosity and surface chemical properties of ACs dominate the adsorption/desorption efficiencies. In Table 3.5, for example, the average pore

diameters of CPAC (3.95 nm), WPAC (3.28 nm) and PPAC (3.46 nm) are higher than those of PGAC (2.47 nm) and CGAC (1.90 nm), allowing the adsorbate and solvent easy access to the pores [184, 243].

The special surface chemistry of basic PPAC (Section S2), i.e., the adsorbate-carbon surface interactions, results in the lower *DE* value. The existence of pyrone- and chromene-type structures have been suggested to account for the basic nature of the carbon surface [80, 261, 262], which is likely the key factor in promoting irreversible adsorption [263]. More abundant basic groups exist on the surface of basic PPAC, PGAC, and CGAC (Section S2), resulting in the lower DE values. The hypothesis was further proven by the fact that HOAc is a more efficient eluent than EtOH for basic PPAC, PGAC, and CGAC (Figure 5.4). Therefore, it is recommended that acidic ACs (CPAC and WPAC) are used as the adsorbents so that phenols can be easily loaded and eluted.

5.3.2.4 Desorption of various phenols

To distinguish the desorption behavior of various phenols, the *DE* values of PNP, PCP, PHBA, PH, and HQ from WPACs with EtOH were determined under SK and US conditions. The results were compared to those of standing (ST) conditions and are shown in Fig. 5.5.

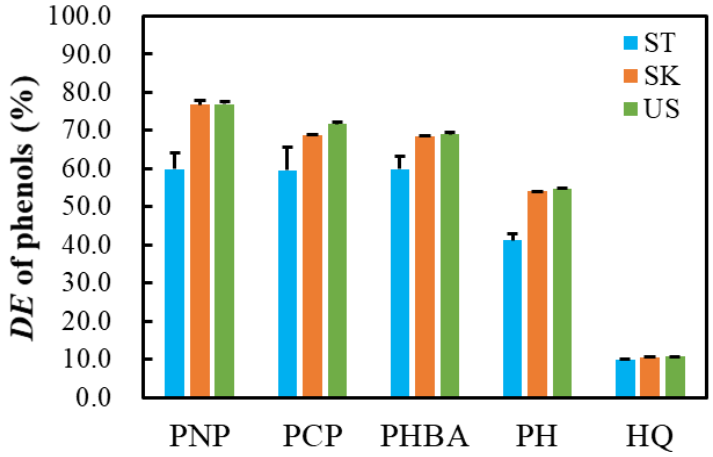

Fig. 5.5 *DE* values of various phenols from loaded WPAC

(Desorption conditions: 100 mg phenols-loaded WPAC (96.4-141.3 mg phenols/g WPAC) immersed in 10 mL EtOH and stood or shaken with 450 rpm at 25°C for 15 min; US with 10 mL EtOH for 15 min at 40 kHz, 100 W and 25°C)

As depicted in Fig. 5.5, the various phenols presented different *DE* values due to the effect of their substituted groups in combination with the desorption modes (ST, SK and US). The values are arranged in order of decreasing *DE* values: PNP > PCP > PHBA > PH > HQ. It has been reported that it is relatively difficult to desorb phenols that contain electron-donating groups (PH and HQ) from ACs with EtOH [259]. By contrast, phenols with electron-withdrawing groups (PNP, PCP and PHBA) achieved higher *DE* values.

Except for the desorption of HQ, SK can dramatically enhance the desorption of phenols, compared to desorption under ST conditions; the *DE* value increased by 6.9% to 31.0% with the various phenols. This indicates that the mass transfer of phenols between the adsorbents and solvents plays a critical role in the elution of phenols. It therefore stands to reason that sonication was used to further improve the *DE* of phenols with EtOH. However, the *DE* values of all phenols were only increased slightly by sonication (0.2-1.4% in Fig. 5.5). Although sonication has frequently been reported to significantly improve the surface diffusivity of adsorbates, decrease overall activation energy and accelerate desorption[122, 152], it cannot affect the equilibrium concentration of phenols during desorption. Even at the desorption time of 1 min, the *DE* value of PNP increased only by 1.8%, compared to SK, when US was used. This implies that the equilibrium state of adsorption/desorption was reached in a very short time in EtOH under SK.

5.3.2.5 Effects of sonication and microwave heating

US and MW have been widely used as common enabling technologies to intensify desorption processes [122, 125, 152]. Sonication is not only a facile means to improve *DE*, but also to clean adsorbent surfaces [122, 152]. MW-assisted chemistry is based on the efficient dielectric heating of materials, which promotes the migration of desorbed molecules from the pores of the adsorbents [125]. Moreover, the mechanical structure of adsorbents can be maintained during MW heating. In this study, the desorption of PNP with various solvents was further studied under US and MW heating and the results are shown in Fig. 5.6 and Fig. 5.7.

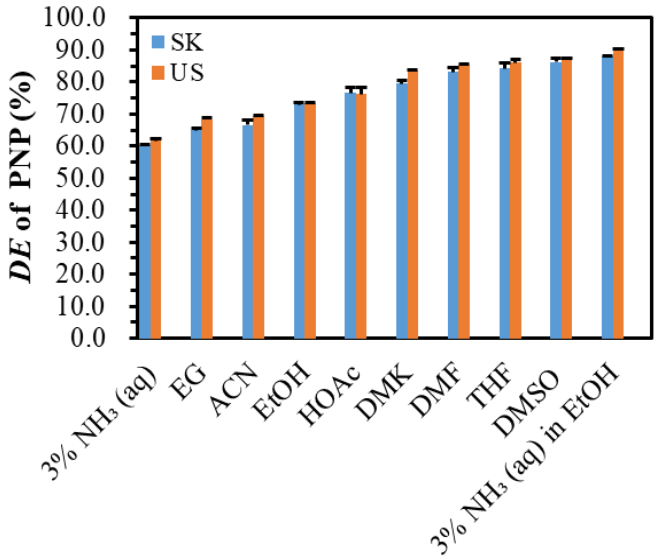

Fig. 5.6 Effects of sonication on *DE* of PNP

(Desorption conditions: 100 mg PNP-loaded CPAC (142.0 mg phenols/g CPAC) immersed in 10 mL selected solvents and shaken with 450 rpm at 25°C for 60 min; Sonication with US (40 kHz and 100 W) at 25°C for 15 min)

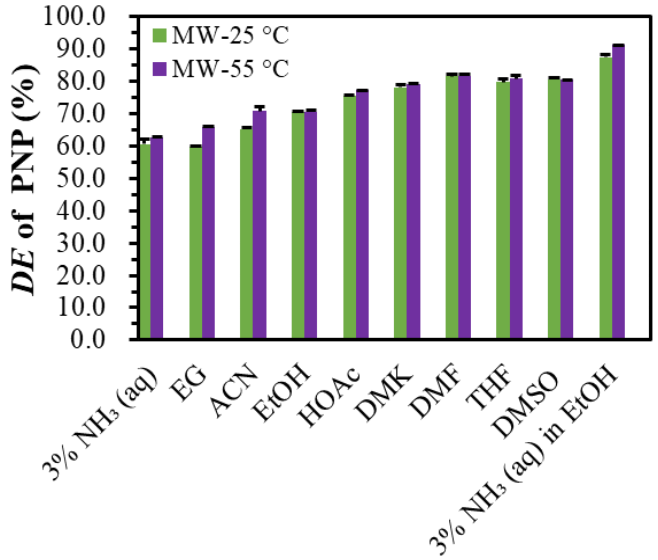

Fig. 5.7 Effects of MW heating on *DE* of PNP

(Desorption conditions: 100 mg PNP-loaded CPAC (142.0 mg phenols/g CPAC) immersed in 10 mL solvents and shaken with 450 rpm at 25°C for 60 min; heating with MW (2.5 GHz and maximal power 1500 W for 15 min)

Fig. 5.6 presents the *DE* values of PNP in various solvents under SK and US. The *DE* values increased slightly under sonication in all solvents, compared with the SK mode. Similarly to the desorption of various phenols with EtOH, sonication enhanced the desorption of phenols very slightly (Figure 5.5). As for the effect of MW heating, Fig. 5.7 shows that the *DE* values of PNP with different solvents were marginally increased between 25°C and 55°C when using MW heating. Overall, the equilibrium state of adsorption/desorption with proper eluents can be achieved in a short time using SK, meaning that additional assistance, such as US and MW heating, is not necessary.

5.3.3 Desorption mechanism

Solvents are classified into three categories: polar protic solvents (PPS); polar aprotic solvents (PAS) and non-polar solvents (NPS). In general, PPS has high dielectric constants and high polarity. The polarity of the PPS stems from the bond dipole of the O-H bond. NH_3 (aq), alcohols (MeOH, EtOH, *n*-PrOH, *n*-buOH), HOAc, and EG in this study all are PPS. PAS lacks an acidic hydrogen, consequently, they are not hydrogen bond donors. These solvents generally have intermediate dielectric constants and polarity. In the present study, DMK, ACN, MEK, GVL, DMF, THF, and DMSO in this study belong to PAS; Only Et_2O is an NPS.

In order to illustrate the desorption mechanism, the correlation between the properties of PNP and *DE* values in different solvents was evaluated (see Fig. 5.8 and Fig 5.9). The dependence of *AE* and *DE* values of phenols on their properties are reported in Table 5.4.

5.3.3.1 Effect of dielectric constant of PPS

Generally, the dielectric constant of the solvent roughly indicates the polarity of that solvent [264]. The lower *DE* values of PNP with 3% NH_3 (aq) or EG are shown in Fig. 5.1. These values are probably caused by the high polarity of 3% NH_3 (aq) and the high viscosity of EG. Except for 3% NH_3 (aq) and EG, a linear correction between the dielectric constants of PPS and the *DE* values of PNP was well established, as shown in Fig. 5.8. Obviously, lower dielectric constants, favor the desorption of PNP. Additionally, hydrogen bonding interactions support the desorption of PPS phenols [184].

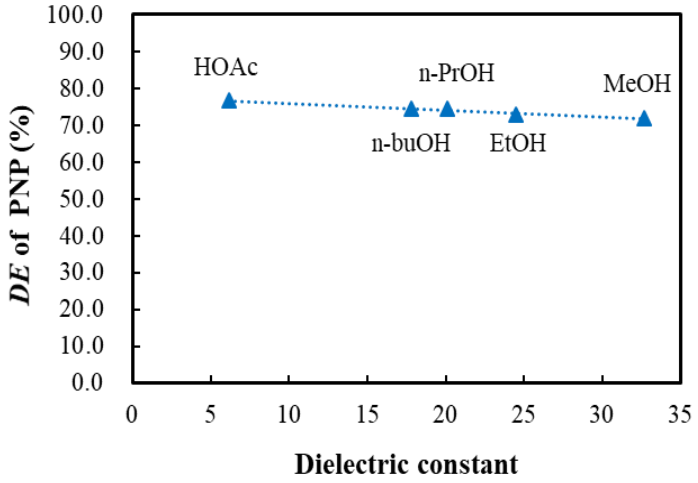

Fig. 5.8 Dependence of *DE* values of PNP on dielectric constant of PPS

(Desorption conditions: 100 mg of PNP loaded CPAC (142.0 mg PNP/g CPAC) immersed with 10 mL of PPS and shaken with 450 rpm at 25°C for 60 min)

5.3.3.2 Effect of donor number of PAS

Both anions and aprotic solvents act as Lewis bases [265], and donor number is a quantitative measure of Lewis basicity [266]. Fig. 5.9 illustrates the correlation between the donor number and *DE* values of PAS.

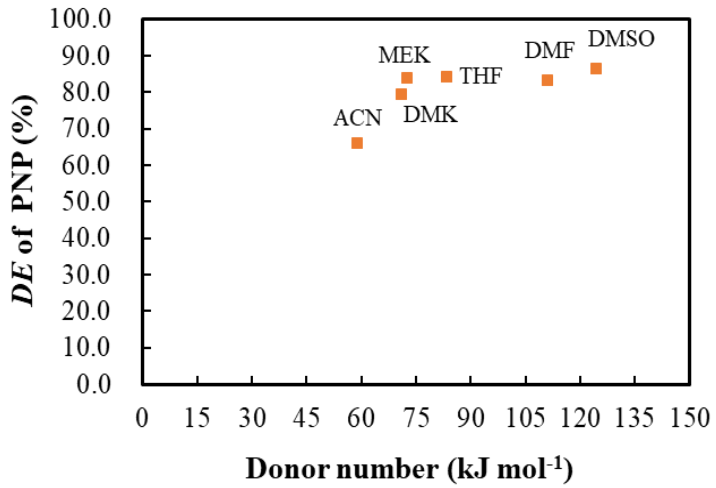

Fig. 5.9 Dependence of *DE* values of PNP on donor number of PAS

(Desorption conditions: 100 mg of PNP loaded CPAC (142.0 mg PNP/g CPAC) immersed with 10 mL of PAS and shaken with 450 rpm at 25°C for 60 min)

As seen in Fig. 5.9, the *DE* values of PNP increase with the donor number values of PAS. Obviously, Lewis base solvents act as electron-donating solvents and therefore give higher PNP desorption. The polarity of Lewis base solvents probably plays a minor role, similar to the role of basic solvents in the desorption of phenols [258].

5.3.3.3 Effect of phenols properties on adsorption and desorption

The main physicochemical parameters of phenols such as log Kow, α, pKa, WS, μ, FW have been considered as effective factors and listed in Table 5.1. The dependence of phenols *AE* by WPAC and *DE* with EtOH on the physicochemical parameters of phenols are compared and summarized in Table 5.4.

Table 5.4 The dependence of *AE* and *DE* values of phenols on their properties

***AE* vs Parameters**	R^2	***DE* vs Parameters**	R^2
AE=15.11log K_{ow}+60.54	0.8314	DE=36.14log K_{ow}-6.849	0.8682
AE=5.720α+9.5445	0.7841	DE=12.22α-112.2	0.7414
AE=7.268μ+64.15	0.6674	DE=16.518μ+1.456	0.7139
AE=-3.090pK_a+110.3	0.5212	DE=-6.868pK_a+102.5	0.6067
AE=-3.090WS+93.83	0.2371	DE=-0.4247WS+67.03	0.3531
AE=0.2534FW+55.86	0.1401	DE=-0.7212FW-35.40	0.2389

As listed in Table 5.4, a variety of properties of phenols synergistically affect *AE* and *DE* values, not only one factor. The lower R^2 values demonstrate the above statement. Two relatively important factors, log K_{ow} and α of phenols, as the polarity parameters, play critical roles for both adsorption and desorption through comparison of regression coefficients R^2. Thus, the relationship between the *AE* values of phenols onto WPAC and their *DE* values with EtOH were established and is shown in Fig. 5.10.

As shown in Figure 5.10, a superior correlation between *AE* and *DE* values was obtained at a high regression coefficient of R^2 (0.9688). Moreover, the *DE* values increase with their *AE* values, indicating that the phenols adsorption is easier, the elution with ethanol will be easier; both the adsorption and desorption of phenols are similarly dominated by physicochemical properties.

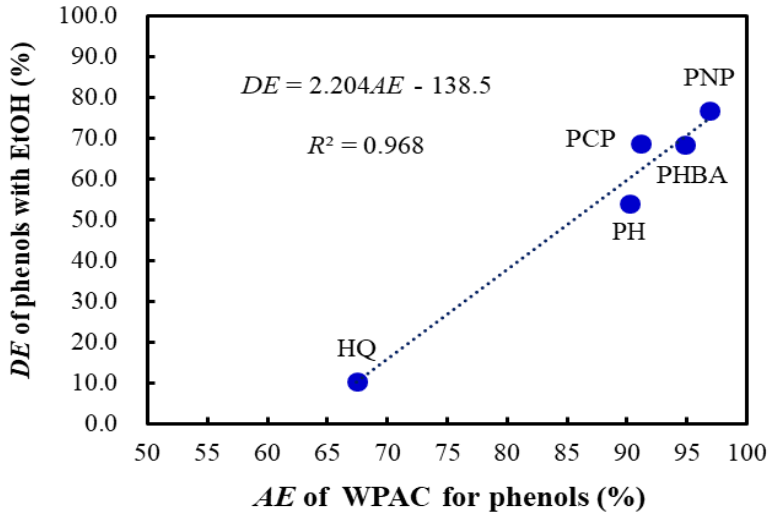

Fig. 5.10 The relationship between *AE* and *DE* values of phenols

(Adsorption conditions: 3.5 g WPAC in 500 mL, 1000 mg L^{-1} of PNP stirred for 60 min at 450 rpm; Desorption conditions: 100 mg phenols loaded WPAC immersed in 10 mL EtOH with SK for 60 min at 450 rpm)

5.3.3.4 Comparison of DRIFT Spectra among Pristine, Loaded and Eluted ACs.

The adsorption and desorption mechanisms of phenols can be further explained by DRIFT spectra analysis of pristine, various phenols-loaded and eluted WPAC. The DRIFTS spectra of WPAC samples are compared and showed in Fig. 5.11.

As show in Fig. 5.11a-5.11e, oxygen functional groups such as phenolic (-OH), carbonyl groups (-C=O-), carboxylic acid (-COOH), ethanoate (-COOR), and ether (-C-O-C-) are observed in pristine WPAC sample. A broad absorption peak at 3430 cm^{-1} corresponds to overlap of O-H and N-H peaks [267]. The carboxylic acid band at 1700 cm^{-1} was found and attributed to the C=O vibration [268]. The absorption from 1230-1250 cm^{-1} is the C-O bond in an ethanoate [269]. In addition, the absorption in 3068 cm^{-1} is due to methyl stretching vibrations (C-H) [270]. Moreover, the absorption around 1600 cm^{-1} is ascribed to the overlap of the polyaromatic C=C stretching bands of the highly conjugated carbonyl and/or quinone groups [271]. The peak generated at 500 cm^{-1} is due to out plane bending O-H, C-C [272].

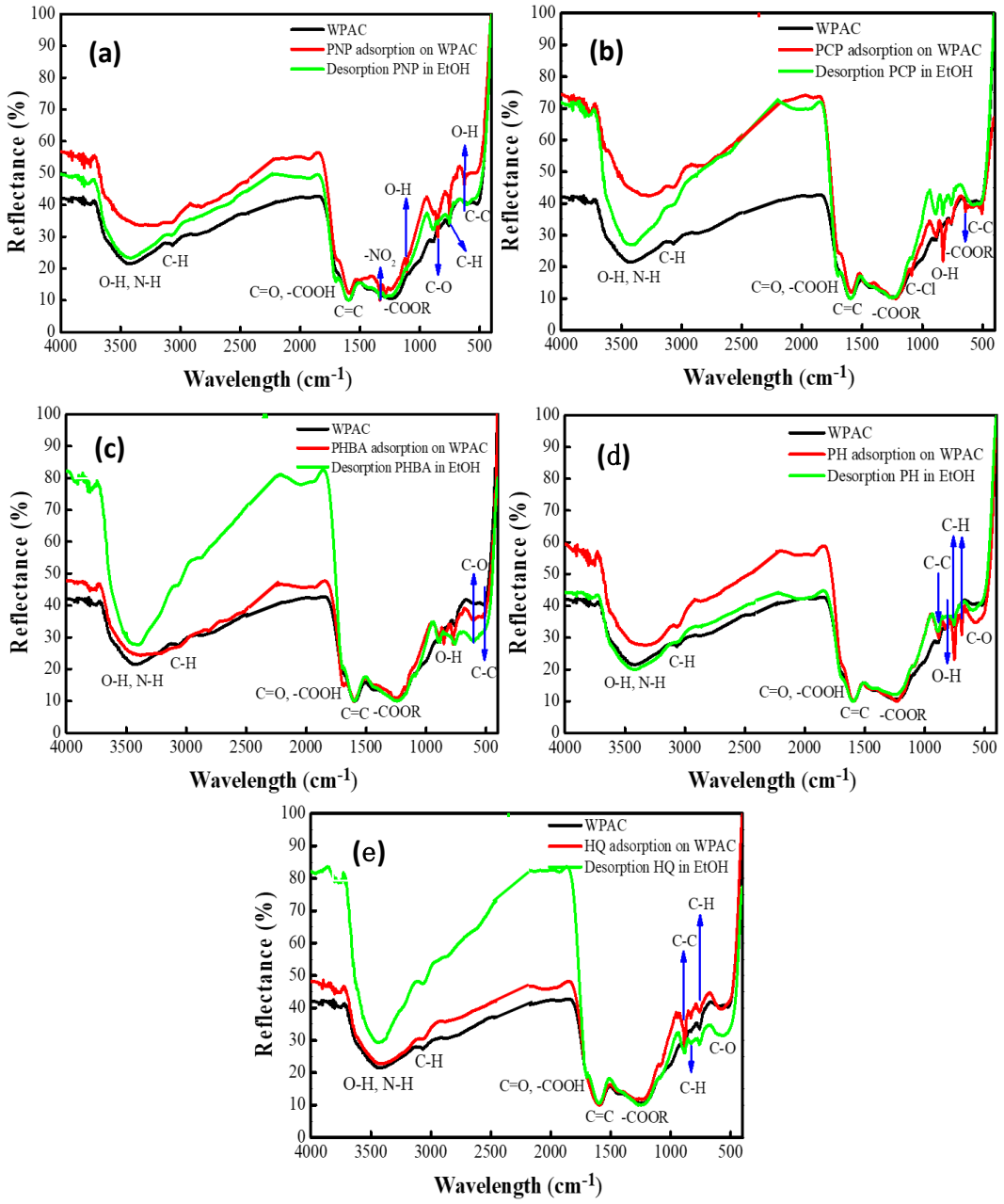

Fig. 5.11 Comparison of DRIFT spectra among WPAC samples after adsorption and desorption of various phenols

Moreover, the absorption bands of the various phenols that were loaded onto WPAC are listed in Table 5.5. The peaks that occurred in the phenols-loaded WPACs disappear after desorption with EtOH (Fig. 5.11). It is worth noting that the

band at 3430 cm^{-1} on WPAC shifts to the right after the adsorption of phenols, except for HQ [273], and that the peak shifts back to 3430 cm^{-1} after the desorption of phenols with EtOH (Fig. 5.11), indicating efficient phenol adsorption/desorption.

Table 5.5Adsorption bands of various phenols on WPAC

Adsorbates	Adsorption bands	Assignments	References
PNP in Fig. 5.11a	1508 cm^{-1}	N=O stretching	[273]
	1330 cm^{-1}	symmetric stretching of -NO_2 in benzene ring	[274]
	1100/620 cm^{-1}	H-bonded -O-H stretch of the phenolic group	[275]
	750 cm^{-1}	mono-substituted rings	
PCP in Fig. 5.11b	820 cm^{-1}	-OH stretch	[276]
	1088 cm^{-1}	C-Cl bond	[277]
PHBA Fig. 5.11c	1700 cm^{-1}	–COOH	[278]
PH in Fig. 5.11d	820/ 690, 750 cm^{-1}	-OH stretch/mono-substituted rings	[274]
HQ in Fig. 5.11e	887 / 820 cm^{-1}	C-C / O-H stretching vibration	[276]

5.3.4 Adsorption/desorption in flow mode

The adsorption/desorption of PNP was carried out in semi-continuous flow mode with CPAC, according to Fig. 4.1 [279]. The breakthrough curves of the three consecutive cycles of adsorption/desorption are depicted in Fig. 5.12.

Based on the breakthrough curves in Fig. 5.12, the q_e was approximately 320.8 mg g^{-1} in each cycle and the total *AE* reached 100% as 115 mL of PNP solution passed through the CPAC-column. By contrast, the q_e of PNP only reached 142.0 mg g^{-1} in batch mode (Table 5.3), as expected the flow mode provided better adsorption performance than the batch mode. Furthermore, the loaded CPAC was completely regenerated using 30 mL of EtOH and the adsorption/desorption process was efficiently recycled three times in flow mode. The additional advantage of the flow mode is that it greatly minimizes the consumption of solvents and remarkably reduces overall costs [259].

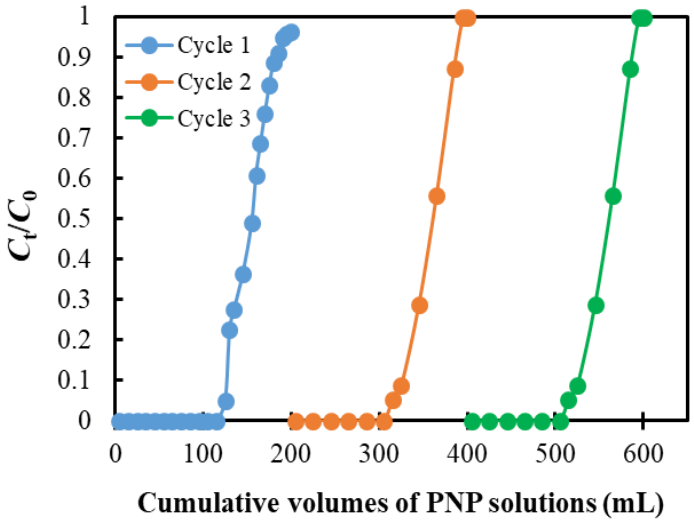

Fig. 5.12 Breakthrough curves of adsorption/desorption of PNP via CPAC-packed column for three cycles

(Adsorption conditions: 3 × 100 mL of 1 g L^{-1} PNP solution passed through the column at 0.75 mL min^{-1} flow rate (Periodical sampling: 10 or 20 mL aliquots); Desorption conditions: 30 mL of EtOH eluted the column at 1 mL min^{-1} flow rate (Periodical sampling: 2.5 or 5 mL aliquots))

Supplementary Data

S.5.1 Porosity properties of activate carbons

As listed in Table 3.5, the higher S_{BET}, larger V_{micro} and V_{meso} of PACs (CPAC, WPAC and PPAC), as well as D_p were observed than that of CGAC and PGAC. Thus, these textural properties lead to the different adsorption performance for aqueous *p*-nitrophenol (PNP) solutions, as shown in Table 5.2. Moreover, the selected WPAC sample also presented the efficient adsorption performance for phenols except for hydroquinone (HQ), as listed in Table 5.3. Additionally, the pore structures and D_p of ACs also could affect the desorption of phenols including PNP, *p*-chlorophenol (PCP), *p*-hydroxybenzoic acid (PHBA), phenol (PH) and HQ.

S.5.2 The pH_{PZC} values of activate carbons

The pH_{PZC} values of CPAC, WPAC, PPAC, PGAC and CGAC were measured to be 5.8, 4.9, 7.9, 10, and 8.2, respectively, which suggests the acidic type (L) carbons of CPAC and WPAC, as well as basic type (H) carbons of PPAC, PGAC and CGAC [263]. The chemistry properties of ACs will affect the adsorption and desorption efficiencies.

S.5.3 Fourier transform infrared spectra of activate carbons

As we depicted in Section 1.3.1, the existence of surface oxygen containing functional groups such as carboxyl, lactone, phenol, carboxylic anhydride has been postulated as constituting the source of surface acidity [62, 78]. Whereas the basic properties of ACs is associated with the presence of oxygen containing groups, i.e., pyrone, chromene and carbonyl structures, at the edge of carbon crystallite; and oxygen free Lewis basic site on the graphene layers [62, 79, 80].

As shown in Fig. S5.1, FTIR reveals the same functional groups of O-H, C-O, C=C, C-C, C-H on CPAC, WPAC, PPAC, PGAC and CGAC from spectrometer analysis. A broad absorption peak at 3430 cm^{-1} corresponding to overlapping of O-H peak [254]. Twin peaks at about 2920 and 2850 cm^{-1} are found because of symmetrical

and asymmetrical stretching of aliphatic C-H [280]. The 2360 cm^{-1} band is due to atmospheric CO_2 [281]. 1585-1640 cm^{-1} is attributed to C=O stretching of double bonds in cyclic and acyclic compounds [280]. The bands at 1080 cm^{-1} is assigned to C–OH stretching of phenolic [282]. The broad band in the domain of 870–750 cm^{-1} was attributed to off-plane vibrations of C–H bonds in aromatic systems [283]. The surface chemistry of carbons has been indicated to have a significant effect on the uptake of small molecules of organic compounds [284].

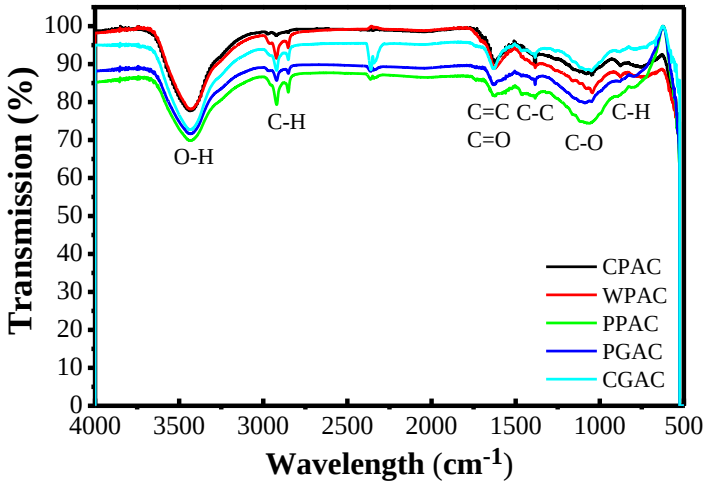

Fig. S5.1 FTIR analysis of original carbons used in this study

References

[241] Ahmaruzzaman, M., Sharma, D. K. Adsorption of phenols from wastewater. Journal of Colloid and Interface Science, 287(2005) 14-24.

[242] Michałowicz, J., Duda, W. Phenols--Sources and Toxicity. Polish Journal of Environmental Studies, 16(2007) 347-362.

[243] Rappoport, Z. The chemistry of phenols. John Wiley & Sons, 2004.

[244] Luan, J., Plaisier, A. Study on treatment of wastewater containing nitrophenol compounds by liquid membrane process. Journal of Membrane Science, 229(2004) 235-239.

[245] Mahugo Santana, C., Sosa Ferrera, Z., Esther Torres Padrón, M., Juan Santana Rodríguez, J. Methodologies for the extraction of phenolic compounds from environmental samples: new approaches. Molecules, 14(2009) 298-320.

[246] Haydar, S., Ferro-Garcıa, M. A., Rivera-Utrilla, J., Joly, J. P. Adsorption of p-nitrophenol on an activated carbon with different oxidations. Carbon, 41(2003) 387-395.

[247] Villegas, L. G. C., Mashhadi, N., Chen, M., Mukherjee, D., Taylor, K. E., Biswas, N. A short review of techniques for phenol removal from wastewater. Current Pollution Reports, 2(2016) 157-167.

[248] Özkaya, B. Adsorption and desorption of phenol on activated carbon and a comparison of isotherm models. Journal of Hazardous Materials, 129(2006) 158-163.

[249] Peng, S. S., Ling, N. S., Rohana, A. Kinetics of biodegradation of phenol and p-nitrophenol by acclimated activated sludge. Journal of Physical Science, 29 (2018) 107-113.

[250] Ghime, D., Ghosh, P. Kinetic Model for the oxidative degradation of aqueous p-nitrophenol by fenton's reagent. Journal of Scientific & Industrial Research, 77(2018) 208-212.

[251] Zhao, D., Cheng, J., Hoffmann, M. R. Kinetics of microwave-enhanced oxidation of phenol by hydrogen peroxide. Frontiers of Environmental Science & Engineering in China, 5(2011) 57-64.

[252] Garcia-Araya, J. F., Beltran, F. J., Alvarez, P., Masa, F. J. Activated carbon adsorption of some phenolic compounds present in agroindustrial wastewater. Adsorption, 9(2003) 107-115.

[253] Seredych, M., Hulicova-Jurcakova, D., Lu, G. Q., Bandosz, T. J. Surface functional groups of carbons and the effects of their chemical character, density and accessibility to ions on electrochemical performance. Carbon, 46(2008), 1475-1488.

[254] De la Luz-Asunción, M., Sánchez-Mendieta, V., Martínez-Hernández, A. L., Castaño, V. M., Velasco-Santos, C. Adsorption of phenol from aqueous solutions by carbon nanomaterials of one and two dimensions: kinetic and equilibrium studies. Journal of Nanomaterials, 16(2015) 422-435.

[255] Kulkarni, S., Kaware, J. Regeneration and recovery in adsorption-a review. International Journal of Innovative Science, Engineering & Technology, 1(2014) 61-64.

[256] Laszlo, K., Szűcs, A. Surface characterization of polyethyleneterephthalate (PET) based activated carbon and the effect of pH on its adsorption capacity from aqueous phenol and 2, 3, 4-trichlorophenol solutions. Carbon, 39(2001) 1945-1953.

[257] Ahmaruzzaman, M., Gayatri, S. L. Batch adsorption of 4-nitrophenol by acid activated jute stick char: equilibrium, kinetic and thermodynamic studies. Chemical Engineering Journal, 158(2010) 173-180.

[258] Ahmaruzzaman, M., Gayatri, S. L. Activated neem leaf: a novel adsorbent for the removal of phenol, 4-nitrophenol, and 4-chlorophenol from aqueous solutions. Journal of Chemical & Engineering Data, 56(2011) 3004-3016.

[259] Tamon, H., Saito, T., Kishimura, M., Okazaki, M., Toei, R. Solvent regeneration of spent activated carbon in wastewater treatment. Journal of Chemical Engineering of Japan, 23(1990) 426-432.

[260] Tanthapanichakoon, W., Ariyadejwanich, P., Japthong, P., Nakagawa, K., Mukai, S. R., Tamon, H. Adsorption–desorption characteristics of phenol and reactive dyes from aqueous solution on mesoporous activated carbon prepared from waste tires. Water Research, 39(2005) 1347-1353.

[261] Boehm, H. P. Voll, M. Basic surface oxides on carbon. 1. adsorption of acids. Carbon, 8(1970) 227-240.

[262] Papirer, E., Li, S., Donnet, J. B. Contribution to the study of basic surface groups on carbons. Carbon, 25(1987) 243-247.

[263] Tessmer, C. H., Vidic, R. D., Uranowski, L. J. Impact of oxygen-containing surface functional groups on activated carbon adsorption of phenols. Environmental Science & Technology, 31(1997) 1872-1878.

[264] Sonkar, P. A., Suryavanshi, P. S., Sutar, S. H., Shukla, S. T. Effect of solvent properties on equivalent conductivity of electrolytes. Journal of Chemical and Pharmaceutical Research, 4(2012) 1978-1982.

[265] Sharratt, P. N. (Ed.). Handbook of batch process design. Springer Science & Business Media, 1997.

[266] Jakubczyk, M., Adamczyk-Woźniak, A., Sporzyński, A., Rybachenko V.I. (Ed.). Acceptor number of organoboron molecules quantitative determination of Lewis acidity. Molecular Receptors, East Publisher House, Donetsk, 2011, 53-68.

[267] Moyo, M., Mutare, E., Chigondo, F., Nyamunda, B. C. Removal of phenol from aqueous solution by adsorption on yeast, Saccharomyces cerevisiae. International Journal of Research and Reviews in Applied Sciences, 11(2012) 486-94.
[268] Mattson, J. S., Mark Jr, H. B. Infrared internal reflectance spectroscopic determination of surface functional groups on carbon. Journal of Colloid and Interface Science, 31(1969) 131-144.
[269] Sabantina, L., Rodríguez-Cano, M., Klöcker, M., García-Mateos, F., Ternero-Hidalgo, J., Mamun, A., Cordero, T. Fixing PAN nanofiber mats during stabilization for carbonization and creating novel metal/carbon composites. Polymers, 10(2018) 735-746.
[270] Raj, A., Raju, K., Varghese, H. T., Granadeiro, C. M., Nogueira, H. I., Panicker, C. Y. IR, Raman and SERS spectra of 2-(methoxycarbonylmethylsulfanyl)-3, 5-dinitrobenzene carboxylic acid. Journal of the Brazilian Chemical Society, 20(2009) 549-559.
[271] Manzoli, M. Boosting the Characterization of Heterogeneous Catalysts for H_2O_2 Direct Synthesis by Infrared Spectroscopy. Catalysts, 9(2019) 30-64.
[272] Kumar, S. Vibrational study of aspartic acids. AKGEC International Journal of Technology, 7 (2016) 60-64.
[273] Ahmaruzzaman, M., Gayatri, S. L. Activated tea waste as a potential low-cost adsorbent for the removal of p-nitrophenol from wastewater. Journal of Chemical & Engineering Data, 55(2010) 4614-4623.
[274] Sugumaran, P., Susan, V. P., Ravichandran, P., Seshadri, S. Production and characterization of activated carbon from banana empty fruit bunch and Delonix regia fruit pod. Journal of Sustainable Energy & Environment, 3(2012) 125-132.
[275] Pavia, D. L., Lampman, G. M., Kriz, G. S., Vyvyan, J. A. Introduction to spectroscopy. Cengage Learning, 2008.
[276] Calvini, P., Gorassini, A. FTIR–deconvolution spectra of paper documents. Restaurator, 23(2002) 48-66.
[277] Bardakçi, B. FTIR-ATR spectroscopic characterization of monochlorophenols and effects of symmetry on vibrational frequencies. Cankaya University Journal of Arts and Sciences, 1(2007) 13-19.
[278] Cherbański, R., Molga, E. Intensification of desorption processes by use of microwaves—an overview of possible applications and industrial perspectives. Chemical Engineering and Processing: Process Intensification, 48(2009) 48-58.
[279] Ge, X., Wu, Z., Manzoli, M., Jicsinszky, L., Wu, Z., Nosyrev, A. E., Cravotto, G.. Adsorptive recovery of Iopamidol from aqueous solution and parallel reuse of

activated carbon: batch and flow study. Industrial & Engineering Chemistry Research, 58(2019) 7284-7295.

[280] Krumins, J., Klavins, M., Seglins, V., Kaup, E. Comparative study of peat composition by using FT-IR spectroscopy. Material Science and Applied Chemistry, 26 (2012) 106-114.

[281] Kebukawa, Y., Nakashima, S., Otsuka, T., Nakamura-messenger, K., Zolensky, M. E. Rapid contamination during storage of carbonaceous chondrites prepared for micro FTIR measurements. Meteoritics & Planetary Science, 4 (2009) 545-557.

[282] Vargas, A. M., Cazetta, A. L., Garcia, C. A., Moraes, J. C., Nogami, E. M., Lenzi, E., Lenzi, W. F.Costa, Almeida, V. C. Preparation and characterization of activated carbon from a new raw lignocellulosic material: Flamboyant (Delonix regia) pods. Journal of Environmental Management, 92(2011) 178-184.

[283] Petuhov, O., Lupascu, T., Behunová, D., Povar, I., Mitina, T., Rusu, M. Microbiological Properties of Microwave-Activated Carbons Impregnated with Enoxil and Nanoparticles of Ag and Se. Journal of Carbon Research, 5(2019) 31-43.

[284] Prahas, D., Kartika, Y., Indraswati, N., Ismadji, S. Activated carbon from jackfruit peel waste by H_3PO_4 chemical activation: pore structure and surface chemistry characterization. Chemical Engineering Journal, 140(2008) 32-42.

Chapter 6: Modification of Activated Carbons for Adsorption of Antibiotics from Aqueous Solutions

Abstract

In general, the modification of adsorbent increases its affinity, selectivity and capacity for certain contaminants. Especially, the adsorption mechanism can be further explained by surface modification. WPAC was then effectively modified by the oxidation with H_2O_2 under SK, US or MW heating to enhance the adsorption performance toward marbofloxacin (MAR) as an antibiotic model. The results showed that the oxidation enhanced the adsorption performance. As compared with oxidation using SK, US or MW heating significantly accelerated the oxidation. Moreover, the modified samples under MW heating exhibited the highest adsorption performance.

Moreover, various type of ACs including CPAC, WPAC, PPAC, PGAC and CGAC with MW calcination modification all greatly enhanced adsorption performance for MAR. The results indicate that the physicochemical properties of ACs were modified under appropriate oxidation or MW calcination. Therefore, the consumption of adsorbents and treatment costs can be significantly reduced to reach the similar adsorption performance.

6.1 Introduction

Antibiotics have been widely used for several decades in both human and animals for treatment of microbial infections, and also as feed additives for promotion of the growth of livestock animals [285-288]. Antibiotics of global production may move to the environment after usage and as residues in sewage [286, 288, 289]. A serious problem was evidenced in veterinary, in particular in cows, where the milk from treated animals is polluted by antibiotics [290, 291]. Although the amount of these pharmaceuticals in the environment is low, its continuous input over recent years may be a long-term potential risk in aquatic environment [292] and in general for the growth of the antibiotic resistance phenomenon.

Adsorption is considered a very effective method for the removal of various antibiotics in the range of concentration from a few to several hundred μg mL^{-1} in aqueous solutions or wastewaters [288, 293-295]. It is well known that the surface

physiochemical properties of carbon materials significantly affect the adsorption performance [98, 296]. Recently, much attention has been paid in the modification of ACs to improve its affinity toward pollutants [98]. Carbon-oxygen surface groups are the most important surface groups which influence the surface characteristics or physicochemical properties such as the wettability, polarity, acidity, and chemical reactivity [6]. A variety of functional groups interact with the adsorbents [93, 297-299] and affect the adsorptive performance of activated carbons [98, 300-303]. As compared with pristine ACs, the changes in the surface oxygen-containing groups have been observed by oxidation such as HNO_3 and H_2O_2 [100, 304, 305], and MW calcination [98, 136].

Different types of veterinary antibiotics including MAR, sulfamonomethoxine (SMMX), ceftiofur hydrochloride (CEF), oxytetracycline (OXY), and dihydrostreptomycin sulphate (DS) all have been detected in water or wastewater [306]. MAR is a synthetic, broad-spectrum bactericidal fluoroquinolone antibiotic and used for infections of the respiratory system and mammary glands, as well as with urinary tract infections. SMMX is a long-acting sulfonamide antibiotic and frequently used for prevention or treatment of diseases. CEF is a β-lactam antimicrobial and occasionally used for the intramammary treatment of mastitis. OXY is a tetracycline antibiotic and used for treatment of infections which caused by a variety of Gram positive and G. negative microorganisms. DS is a semisynthetic aminoglycoside antibiotic and used in the treatment of tuberculosis. The physicochemical properties of MAR, SMMX, CEF, OXY and DS are compared and listed in Table 6.1.

The modification of ACs aims to further verify the effect of the MW-calcination and oxidation with H_2O_2 under SK, US, and MW heating on the q_e of ACs and *REs* of antibiotics in aqueous solutions. To achieve this goal, the adsorption of selected antibiotics (MAR, SMMX, CER, OXY and DS) on the pristine WPAC are respectively studied to compare their *REs* so that an antibiotic can reasonably selected to be the model compound (MAR). Importantly, various commercial ACs including CPAC, WPAC, PPAC, PGAC, and CGAC were modified under MW calcination for the adsorption removal of MAR.

Table 6.1 The physicochemical properties of selected veterinary antibiotics

Antibiotics	Molecular Formula	Molecular Weight (g mol^{-1})	Structure	Solubility (mg mL^{-1})	pKa	logK_{ow}
MAR	$C_{17}H_{19}FN_4O_4$	362.4	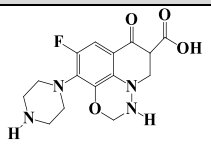	< 1	5.38	0.51
SMMX	$C_{11}H_{12}N_4O_3S$	280.31	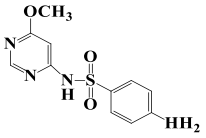	10	6.33	0.7
CEF	$C_{19}H_{18}ClN_4O_7S_3$	560	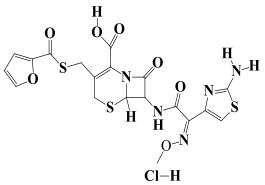	0.105	2.83	1.22
OXY	$C_{22}H_{24}N_2O_9$	460.4	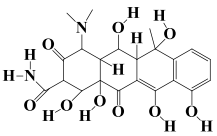	6.9	3.27	-4.5
DS	$C_{21}H_{43}N_7O_{16}S$	681.7	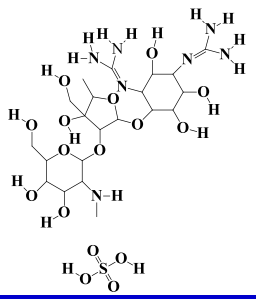	50	12.11	-7.3

6.2 Experimental

6.2.1 Chemicals

Antibiotics MAR (Marbocyl 10%, Vetoquinol), SMMX (Daimeton 40, IZO Srl), CER (Ceva Santé Animale), OXY (Oxtra MV 10, Huvepharma) and DS (Association of Procaine Penicillin and Dihydroestreptomycin in a ratio of 1:1.25, Repen,

Fatro) were used in this study. H_2O_2 (35%, w/w), NaOH (98%), HCl (36%, w/w) were all analytical grade are purchased from Alfa Aesar. 1% HCl and 1% NaOH solutions are used for pH adjustment. Deionized water (conductivity $\leq$ 2.0 µS cm^{-1}) was used to prepare all solutions and purification.

6.2.2 Set up

The information of experimental setups (Liquid phase parallel synthesizer for adsorption and modification; MicroSynth and SynthWave for modification) used in this part are referred to Table 3.1 and Fig. 5.1. Moreover, an ultrasonic horn reactor (Hainertec, HNG-20500-SP, Suzhou, China) was used for modification and the image of this setup is shown in Fig. 6.1.

Fig. 6.1 Ultrasonic horn reactor for modification (20 kHz, 0-500 W)

6.2.3 Oxidation of wood powder activated carbon with H_2O_2

Aiming to verify the effects of oxygen-containing groups, WPAC was oxidized with H_2O_2 under SK, US and MW heating. After oxidation the mixtures were washed with 1% NaOH to neutral pH. In all runs, the obtained WPAC samples after filtration were oven dried at 110°C overnight. The specific modification methods are described below:

(1) Modification with SK

Firstly, the effect of H_2O_2 concentration and oxidation time was investigated in oxidation process. 0.5 g of WPAC (hereafter noted as C) was oxidized with H_2O_2 (12% or 35%, 15 mL) and shaken with 450 rpm at 25°C for 4 h or 24 h. The oxidization process was designated as O, thus the oxidized samples with various

concentrations of H_2O_2 and reaction time under SK were labelled as $CO_{12\%,\ 4h}$-SK, $CO_{12\%,\ 24h}$-SK, $CO_{35\%,\ 4h}$-SK, and $CO_{35\%,\ 24h}$-SK, respectively.

(2) Modification with US

An ultrasonic horn (20 kHz) was applied for the US treatment. 0.5 g of WPAC was added in 15 mL of 12% H_2O_2 and the mixture was sonicated at 250 W (25°C) for 0.5 and 1 h. The oxidized samples under US were noted as $CO_{12\%,\ 0.5h}$-US and $CO_{12\%,\ 1h}$-US.

(3) Modification under MW heating

A SynthWave (2.45 GHz) was applied for the MW treatment. 0.5 g of WPAC was added in 15 mL of 12% H_2O_2 and then the mixtures were processed by MW heating at 90°C for 0.25 and 0.5 h. These oxidized samples under MW heating were listed as $CO_{12\%,\ 0.25h}$-MW and $CO_{12\%,\ 0.5h}$-MW.

6.2.4 Modification under microwave calcination

ACs was calcined with MW-heating to convert surface oxygen-containing groups for observing the variation of adsorption performance toward antibiotics.

(1) MW calcination

A high-temperature MicroSynth (2.45 GHz) was applied for the treatment. 1 g of AC was put in Nickel crucibles, which was continuously filled with N_2 (16 NL h^{-1} of flow rate). After 30 min of gas flow, the temperature was ramped from 25°C to 500°C or 600°C with 12 min, and then maintained at 500°C for 3 min, 8 min, 15 min, or 600°C for 3 min at N_2 atmosphere. The MW calcination was indicated as MWC, thus the samples modified with MW calcination were noted as $C_{500°C,\ 3min}$-MWC, $C_{500°C,\ 8min}$-MWC, $C_{500°C,\ 15min}$-MWC, and $C_{600°C,\ 3min}$-MWC.

(2) Combination of MW calcination/H_2O_2 oxidation

0.5 g of WPAC obtained under the above MW calcination (MicroSynth) was added in 15 mL of 12% H_2O_2 and the mixture was processed by MW heating (SynthWave) at 90°C for 15 min. The combined modification method was designated as MWC/H_2O_2.

6.2.5 Adsorption of antibiotics onto activated carbons

In typical runs, 10 mg of the pristine or modified ACs were added in 50 mL of approximately 50 mg L^{-1} antibiotics solutions, and then the mixture was shaken with 450 rpm at 25°C for 4 h.

After adsorption, all the samples were filtered and dried at 110°C for 4 h. The residual concentration of antibiotics in the aqueous filtrate was determined by a UV–vis spectrometer. The q_e and *AE* expressing adsorption performance of ACs were calculated according to equations (3) and (4). All experiments are duplicated and errors were shown by the difference between the higher measured value and the average value. If the errors are not visible in Figures, they are smaller than the symbols representing the average values.

6.3 Results and discussion

6.3.1 Adsorption efficiencies of different antibiotics on pristine wood powder activated carbon

The *AE* values of MAR, SMMX, CEF, OXY and DS on 5-50 mg of WPAC in aqueous solutions were studied. The results are compared and shown in Fig. 6.2.

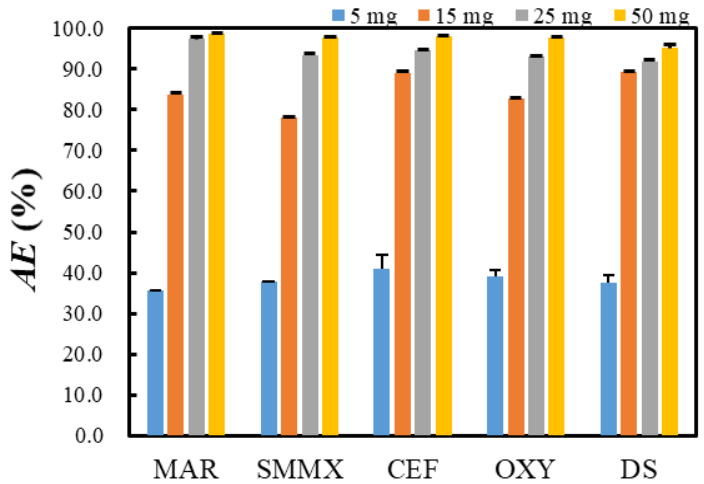

Fig. 6.2 Effect of WPAC amount on *AE* values of various antibiotics

(Adsorption conditions: 5-50 mg of pristine WPAC in approximately 50 mL, 50 mg L^{-1}MAR, SMMX, CEF, OXY and DS aqueous solutions, shaken with 450 rpm at 25°C for 4 h)

As depicted in Fig. 6.2, the *AE* values of MAR, SMMX, CEF, OXY and DS increased from 36% to 99%; from 38% to 98%; from 41% to 98%; from 39% to 97%; from 37% to 95%, respectively, as WPAC amounts increased from 5 to 50 mg. It indicated larger amount of WPAC efficiently absorbed MAR from aqueous solution. The results coincide with the statement that the adsorption performance is significantly affected by surface area, the number of available active sites and surface functional groups [307].

In this study, the modification of ACs by various methods was performed to improve their adsorption performance helping to better understand the features of adsorption mechanism, while the consumption of ACs can be reduced.

6.3.2 Effect of oxidation by H_2O_2 on wood powder activated carbon modification and adsorption

The effects of H_2O_2 concentration and oxidation time, were investigated to verify the enhancement of the oxidation modification on performance of WPAC toward MAR, and the results are shown in Fig. 6.3.

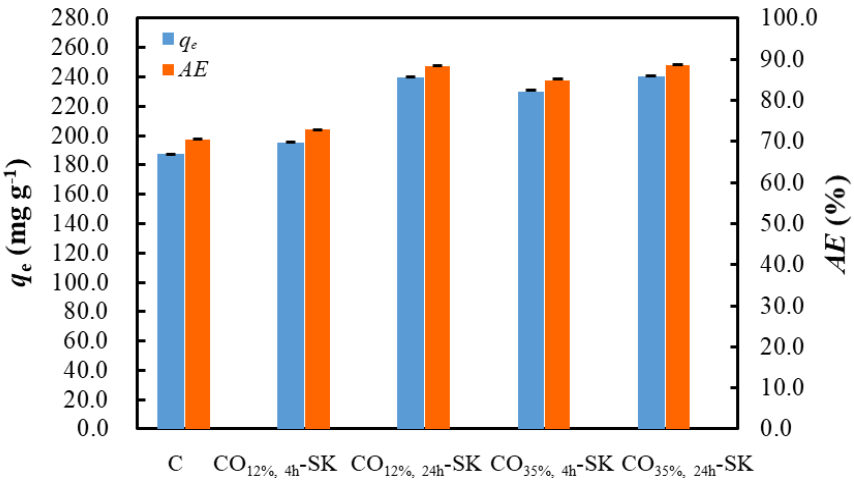

Fig. 6.3 Effect of oxidation by H_2O_2 with SK on adsorption performance to MAR
(Modification conditions: 0.5 g of WPAC in 15 mL of 12% or 35% H_2O_2 shaken with 450 rpm at 25°C for 4 h or 24 h; Adsorption conditions: 10 mg of ACs in 50 mL of 50 mg L^{-1} MAR solution shaken with 450 rpm at 25°C for 4 h)

As shown in Fig. 6.3, as with the pristine WPAC, the oxidation process enhanced the adsorption performance of q_e and *AE* values toward MAR. In details,

compared to $CO_{12\%,\ 4h}$-SK, the higher q_e and *AE* values of MAR onto $CO_{35\%,\ 4h}$-SK were observed, since the increasing H_2O_2 concentration promoted the surface oxidation of WPAC in 4 h. While comparing these two samples of $CO_{12\%,\ 24h}$-SK and $CO_{35\%,\ 24h}$-SK, the similar adsorption performance to MAR were observed, because the reaction time of 24 h is long enough for the surface oxidation by H_2O_2 even at low concentration. It suggests that the different degrees of oxidation with H_2O_2 could introduce the oxygen surface complexes. Meanwhile, the oxidation affects the physicochemical properties of ACs [308]. The sample modified with 12% H_2O_2 for 24 h presented higher adsorption performance than the sample obtained in 4 h, indicating that the efficient oxidation with low concentration H_2O_2 requires longer time. However, the samples oxidized in 4 h or 24 h of oxidation time with high concentration H_2O_2 (35%) exhibited the similar adsorption performance, suggesting that the efficient oxidation with high concentration H_2O_2 is achieved in a shorter time.

6.3.3 Effect of sonication on wood powder activated carbon modification and adsorption

Sonication often enhances chemical reactivity [309]. In this study, WPAC was oxidized with H_2O_2 under US of 0.5 and 1 h and the adsorption performance of modified ACs toward MAR is depicted in Fig. 6.4.

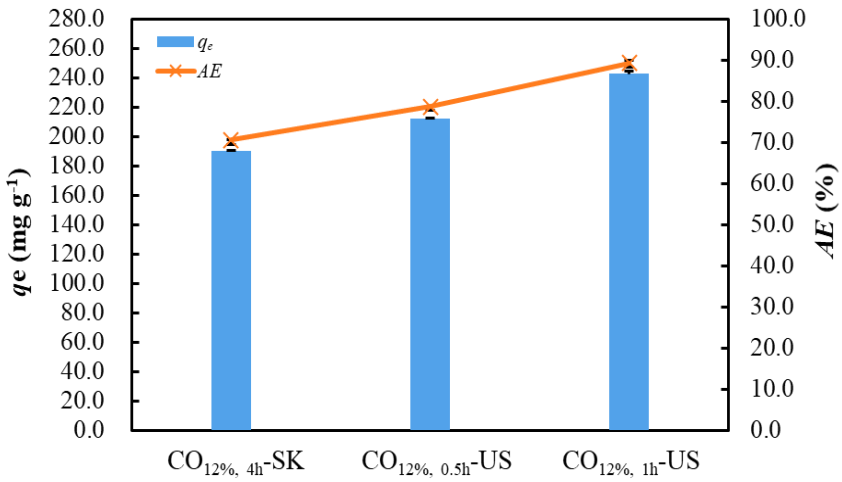

Fig. 6.4 Effect of oxidation time with US on adsorption performance of modified ACs (Modification conditions: 0.5 g of WPAC in 15 mL of 12% H_2O_2 sonicated with 250 W at 25°C for 0.5 and 1 h)

WPAC modified with oxidation under US exhibited more efficient adsorption performance toward MAR when compared with $CO_{12\%,\ 4h\text{-}SK}$. As shown in Fig. 6.4, sonication remarkably accelerates the oxidation of surface groups and shortens oxidation time. In addition, the adsorption performance of the modified WPAC was improved as the sonication time extended.

6.3.4 Effect of microwave heating on wood powder activated carbon modification and adsorption

MW heating has been proven to enhance various types of oxidation processes [310]. In this study, the effects of oxidation time (0.25 and 0.5 h) with MW heating on the adsorption performance of WPAC toward MAR were investigated and the results are shown in Fig. 6.5.

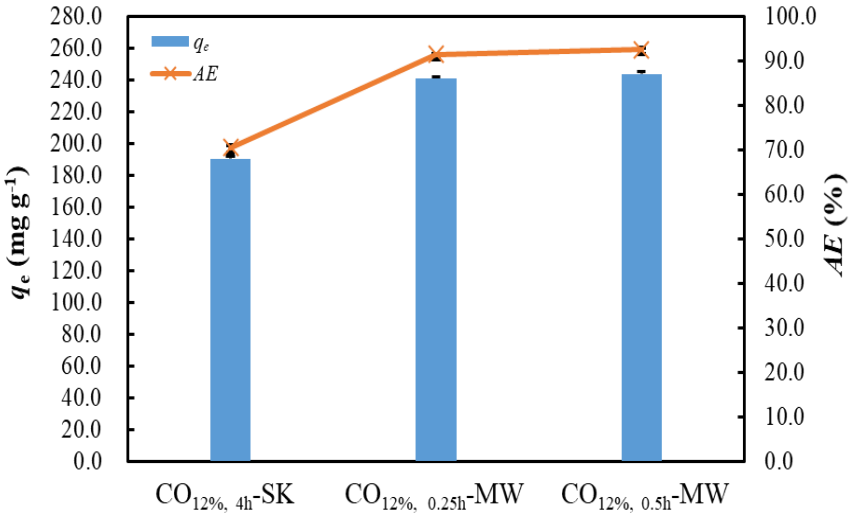

Fig. 6.5 Effect of oxidation time with MW heating on adsorption performance

(Modification conditions: 0.5 g of WPAC in 15 mL of 12% H_2O_2 processed with MW heating at 90°C for 0.25 and 0.5 h)

As shown in Fig. 6.5, the significant higher q_e and *AE* values on the oxidized sample were achieved at 90°C for 0.25 or 0.5 h MW heating, compared with the oxidized samples with SK at 25°C for 4 h. It revealed that the reaction temperature obviously affects the oxidation rate, while the time of MW heating very slightly influence the adsorption performance of modified WPAC. It indicates that MW heating exhibited very high efficiency toward the surface oxidation of ACs, which is

consistent with our previous studies [136]. MW irradiation can significantly affect the physical and chemistry properties of carbons.

6.3.5 Comparison of adsorption performance among activated carbons modified by shaking, sonication and microwave

WPAC was oxidized with H_2O_2 under SK, US and MW to compare the role of various enabling technologies. The modification conditions are summarized in Table 6.2. The results are compared and shown in Fig. 6.6.

Table 6.2 Modification conditions for oxidation of AC with H_2O_2 under SK, US and MW

Oxidation methods	Conditions
C	10 g of WPAC oven dried at 110°C overnight
C/SK with H_2O or H_2O_2	15 mg of WPAC in 15 mL H_2O or H_2O_2shaken with 450 rpm at 25°C for 24 h, 1% NaOH washed to neutral, oven dried at 110°C overnight
C/US with H_2O or H_2O_2	15 mg of WPAC in 15 mL of 12% H_2O or H_2O_2 sonicated with 20 kHz at 25°C for 1 h, 1% NaOH washed to neutral, oven dried at 110°C overnight
C/MW with H_2O or H_2O_2	15 mg of WPAC in 15 mL of 12% H_2O or H_2O_2 heated at 25°C for 0.5 h, 1% NaOH washed to neutral, oven dried at 110°C overnight

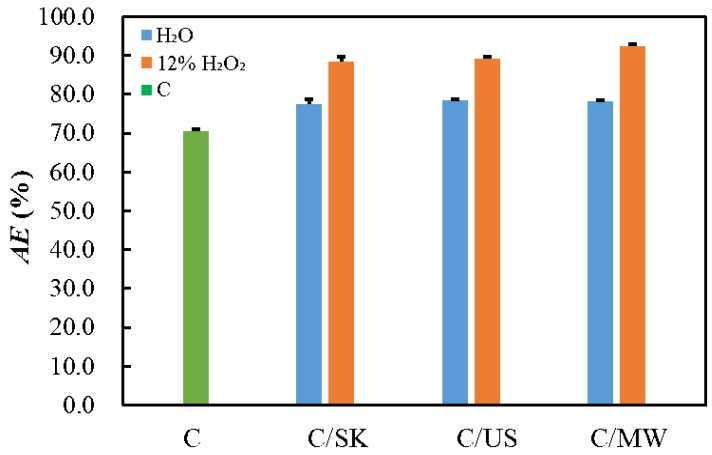

Fig. 6.6 Comparison of adsorption efficiencies of MAR among WPAC oxidized with H_2O_2 under various enabling technologies

(Modification conditions: 0.5 g of WPAC in 15 mL of 12% H_2O_2 stirred with SK with 450 rpm for 24 h, sonicated at 25°C for 1 h, and heated with MW at 90°C for 0.25 h)

Washing with deionized water can remove ash and some soluble substances present in the carbon [311]. Thus, *AE* values of MAR onto WPACs washed with deionized water using SK, US and MW increase to the extent, as shown in Fig. 6.6. Comparison with washing samples, oxidized samples presented more efficient adsorption performance toward MAR. The highest *AE* values were achieved with the samples processed with MW heating.

6.3.6 Effect of microwave calcination on wood powder activated carbon modification and adsorption

MW irradiation is a viable technology for the modification of ACs due to the direct absorption toward MW [312]. In this study, WPAC was calcined at 500°C and 600°C for 3-15 min with MW and the results are shown in Fig. 6.7.

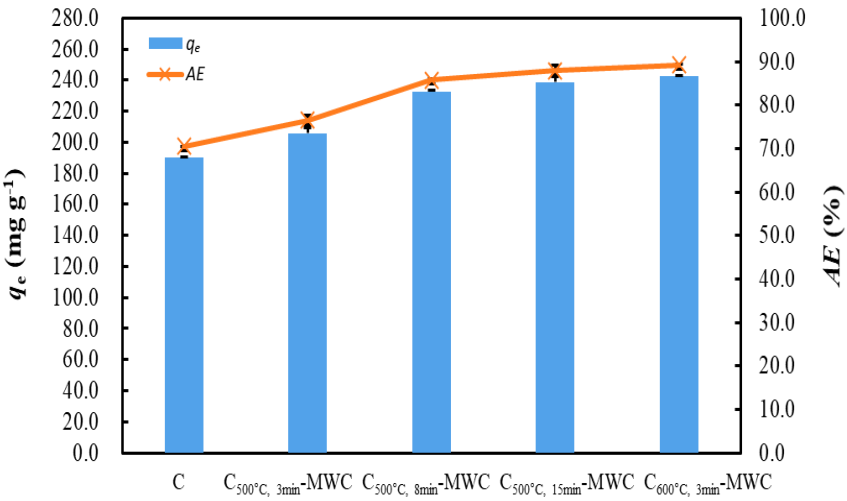

Fig. 6.7 Effect of MW calcination on adsorption performance

(Modification conditions: 1 g of WPAC in crucibles heated under MW at 500°C for 3, 8 and 15 min, or at 600°C for 3 min with 10 NL h^{-1} N_2 flow rate; Adsorption conditions: 10 mg of WPAC in 50 mL of 50 mg L^{-1} MAR solution shaken with 450 rpm at 25°C for 4 h)

As depicted in Fig. 6.7, the q_e and *AE* values of MAR remarkably increased by the modification of WPAC using MW calcination, as compared to 70.5% of *AE* value and 190.3 mg g^{-1} of q_e value onto the pristine WPAC. The adsorption performance of WPACs modified at 500°C was improved progressively with the calcination time.

The *AE* values onto $C_{500°C,\ 15min}$-MWC, and $C_{600°C,\ 3min}$-MWC both reached to *ca.*

89%, indicating that time and temperature both are critical to modify the surface functional groups, surface area and pore volumes, which is consistent with previous studies [100, 136].

6.3.7 Effect of combination of microwave calcination and oxidation with H_2O_2 on wood powder activated carbon modified and adsorption

Oxygen-containing groups play an important role in the adsorption process. The functional groups can be decomposed or converted into the form of CO or CO_2 under MW calcination [94]. In order verify possibility of further modification after MW calcination and change oxygen-containing groups, WPAC was modified with MW calcination followed by oxidation with H_2O_2. The results are shown in Fig. 6.8.

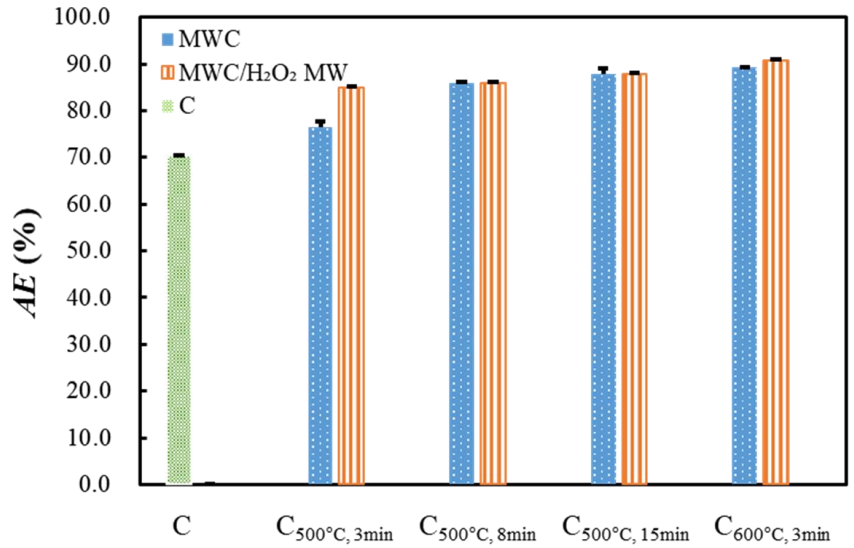

Fig. 6.8 Effect of combined MW calcination and oxidation with H_2O_2 on adsorption performance

(Modification conditions: 1 g of WPAC in crucibles heated under MW at 500°C for 3 min, 8 min, 15 min, and at 600°C for 3 min with 10 NL h^{-1} N_2 flow rate; or 0.5 g of WPAC obtained after MWC treatment, added in 15 mL of 12% H_2O_2 and the mixture heated under MW at 90°C for 15 min)

As we seen in Fig. 6.8, the *AE* value (84.8%) of MAR onto WPAC modified with MWC/H_2O_2 at 500°C for 3 min is higher than that (76.6%) onto the sample modified with MWC at 500°C for 3 min. While the samples were calcined at 500°C for 8 min, 15 min and 600°C for 3 min followed by oxidation, the *AE* values slightly

increased. Furthermore, the *AE* values are very close onto WPACs modified by MWC and MWC/H_2O_2 at 500°C for 8-15 min and 600°C for 3 min. It indicates that once the oxygen-containing groups were completely decomposed, the surface of ACs cannot be further modified by oxidation.

6.3.8 Effect of microwave calcination on various activated carbon modification and adsorption

In order to verify the adaptation of MW calcination, different commercial ACs were modified with MW calcination at 600°C for 3 min. The *AE* values of MAR onto samples modified by MW calcination are shown in Fig. 6.9.

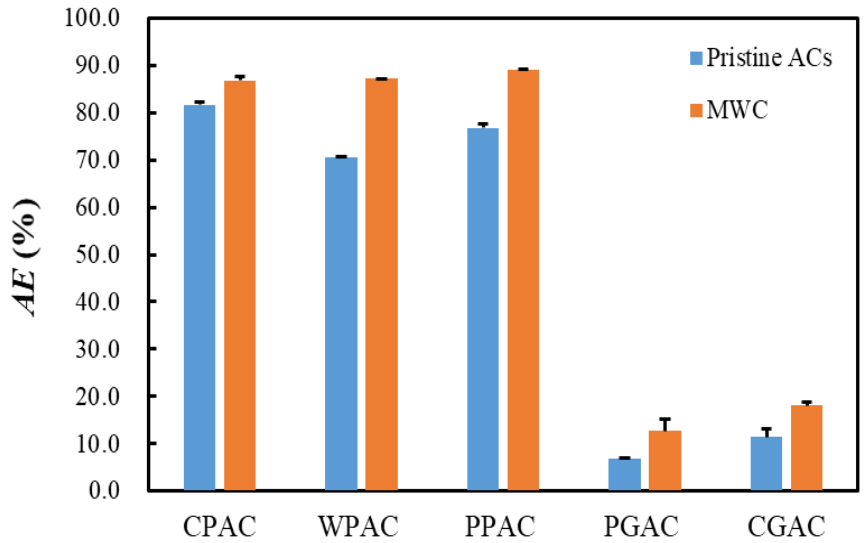

Fig. 6.9 Adsorption efficiencies of MAR onto various ACs modified by MW calcination (Modification conditions: 1 g of WPAC in crucibles heated under MW at 600°C for 3 min with 10 NL h^{-1} N_2 flow rate; Adsorption conditions: 10 mg of ACs in 50 mL of 50 mg L^{-1} MAR solution shaken with 450 rpm at 25°C for 4 h)

As shown in Fig. 6.9, various ACs after MW calcination presented much higher *AE* values for MAR compared with pristine ACs. It indicates that the oxygen-functional groups were decomposed under MW calcination, but the physical properties were improved. Among the granular PGAC and CGAC samples with MW calcination exhibited greatly enhancement of *AE* values from 19.3% to 35.0% and 31.4% to 50.0%, respectively. Thus, MW calcination was an appropriate method for both modification of PACs and GACs to improve their performance.

References

[285] Sapkota, A., Sapkota, A. R., Kucharski, M., Burke, J., McKenzie, S., Walker, P., Lawrence, R. Aquaculture practices and potential human health risks: current knowledge and future priorities. Environment International, 34(2008) 1215-1226.

[286] Kummerer, K. Antibiotics in the aquatic environment–a review–part I. Chemosphere, 75 (2009) 417–434.

[287] Sarmah, A. K., Meyer, M. T. Boxall, A. B. A global perspective on the use, sales, exposure pathways, occurrence, fate and effects of veterinary antibiotics (VAs) in the environment. Chemosphere, 65 (2006) 725–759.

[288] Peng, B., Chen, L., Que, C., Yang, K., Deng, F., Deng, X., Wu, M. Adsorption of antibiotics on graphene and biochar in aqueous solutions induced by π-π interactions. Scientific Reports, 6(2016) 31920-31930.

[289] Luo, Y., Mao, D., Rysz, M., Zhou, Q., Zhang, H., Xu, L., JJ Alvarez, P. Trends in antibiotic resistance genes occurrence in the Haihe River, China. Environmental Science & Technology, 44(2010) 7220-7225.

[290] Schenck, F. J., Callery, P. S. Chromatographic methods of analysis of antibiotics in milk. Journal of Chromatography A, 812(1998) 99-109.

[291] Albright, J. L., Tuckey, S. L., Woods, G. T. Antibiotics in milk-a review. Journal of Dairy Science, 44(1961) 779-807.

[292] Wang, G., Wu, T., Li, Y., Sun, D., Wang, Y., Huang, X., Liu, R. Removal of ampicillin sodium in solution using activated carbon adsorption integrated with H_2O_2 oxidation. Journal of Chemical Technology & Biotechnology, 87(2012) 623-628.

[293] Xiang, Y., Xu, Z., Wei, Y., Zhou, Y., Yang, X., Yang, Y., Zhou, Z. Carbon-based materials as adsorbent for antibiotics removal: Mechanisms and influencing factors. Journal of Environmental Management, 237(2019) 128-138.

[294] Fu, H., Li, X., Wang, J., Lin, P., Chen, C., Zhang, X., Suffet, I. M. Activated carbon adsorption of quinolone antibiotics in water: Performance, mechanism, and modeling. Journal of Environmental Sciences, 56(2017) 145-152.

[295] Ahmed, M. J. Adsorption of quinolone, tetracycline, and penicillin antibiotics from aqueous solution using activated carbons. Environmental Toxicology and Pharmacology, 50(2017) 1-10.

[296] Kwiatkowski, J. F. Activated Carbon: Classifications. Properties and Applications, 2011, 239-266.

[297] Bonanni, A., Ambrosi, A., Pumera, M. On Oxygen-Containing Groups in Chemically Modified Graphenes. Chemistry-A European Journal, 18(2012) 4541-4548.

[298] Shen, W., Li, Z., & Liu, Y. (2008). Surface chemical functional groups modification of porous carbon. Recent Patents on Chemical Engineering, 1(2008) 27-40.

[299] Figueiredo, J. L., Pereira, M. F., Freitas, M. M., Órfão, J. J. Characterization of active sites on carbon catalysts. Industrial & Engineering Chemistry Research, 46(2007) 4110-4115.

[300] Villacañas, F., Pereira, M. F. R., Órfão, J. J., Figueiredo, J. L. Adsorption of simple aromatic compounds on activated carbons. Journal of Colloid and Interface Science, 293(2006), 128-136.

[301] Cho, H. H., Smith, B. A., Wnuk, J. D., Fairbrother, D. H., Ball, W. P. Influence of surface oxides on the adsorption of naphthalene onto multiwalled carbon nanotubes. Environmental Science & Technology, 42(2008) 2899-2905.

[302] Faria, P. C. C., Órfão, J. J. M., Figueiredo, J. L., Pereira, M. F. R. Adsorption of aromatic compounds from the biodegradation of azo dyes on activated carbon. Applied Surface Science, 254(2008) 3497-3503.

[303] Ania, C. O., Pelayo, J. G., Bandosz, T. J. Reactive adsorption of penicillin on activated carbons. Adsorption, 17(2011) 421-429.

[304] Sheng, G. D., Shao, D. D., Ren, X. M., Wang, X. Q., Li, J. X., Chen, Y. X., Wang, X. K. Kinetics and thermodynamics of adsorption of ionizable aromatic compounds from aqueous solutions by as-prepared and oxidized multiwalled carbon nanotubes. Journal of Hazardous Materials, 178(2010) 505-516.

[305] Kurniawan, T. A., Lo, W. H. Removal of refractory compounds from stabilized landfill leachate using an integrated H_2O_2 oxidation and granular activated carbon (GAC) adsorption treatment. Water Research, 43(2009) 4079-4091.

[306] Dorival-García, N., Zafra-Gómez, A., Cantarero, S., Navalón, A., Vílchez, J. L. Simultaneous determination of 13 quinolone antibiotic derivatives in wastewater samples using solid-phase extraction and ultra performance liquid chromatography–tandem mass spectrometry. Microchemical Journal, 106(2013) 323-333.

[307] Q.S. Liu, P. Wang, S.S. Zhao, W. Zhang, Treatment of an industrial chemical wastewater using a granular activated carbon adsorption-microwave regeneration process. Journal of Chemical Technology & Biotechnology, 87 (2012) 1004–10.

[308] Moreno-Castilla, C., Ferro-Garcia, M. A., Joly, J. P., Bautista-Toledo, I., Carrasco-Marin, F., Rivera-Utrilla, J. Activated carbon surface modifications by nitric acid, hydrogen peroxide, and ammonium peroxydisulfate treatments. Langmuir, 11(1995) 4386-4392.

[309] Hua, I., Hoffmann, M. R. Optimization of ultrasonic irradiation as an advanced oxidation technology. Environmental Science & Technology, 31(1997) 2237-2243.
[310] Han, D. H., Cha, S. Y., Yang, H. Y. Improvement of oxidative decomposition of aqueous phenol by microwave irradiation in UV/H_2O_2 process and kinetic study. Water Research, 38(2004) 2782-2790.
[311] Jia, Y. F., Thomas, K. M. Adsorption of cadmium ions on oxygen surface sites in activated carbon. Langmuir, 16(2000) 1114-1122.
[312] Guo, J., Lua, A. C. Preparation of activated carbons from oil-palm-stone chars by microwave-induced carbon dioxide activation. Carbon, 38(2000) 1985-1993.

Chapter 7: Adsorptive Removal of Veterinary Antibiotics from Milk Using Activated Carbon

Abstract

The present study aims to remove the residual veterinary antibiotic-MAR from milk with ACs in batch and flow systems to meet the MRL. Different types (granule and powder) and amounts of ACs were studied. In batch mode, 50 mg of commercial MGAC with 1083 m^2 g^{-1} of S_{BET} exhibited the superior adsorption performance for 20 mL of 1.0 µg mL^{-1} MAR-spiked milk. 93.7% of *RE* and 0.063 µg mL^{-1} of MAR residue were achieved. In flow mode, 325 mL of 1.0 µg mL^{-1} MAR-spiked milk was efficiently purified through 500 mg of MGAC in a glass column (1 cm I.D.) and 93.4% of *RE* and 0.066 µg mL^{-1} of MAR residue were attained at the end. The flow process can handle 1.6 times higher in q_e than that in batch mode. In summary, MAR can be efficiently, economically and conveniently removed using ACs adsorption from milk, despite the presence of competition adsorption of impurities. The adsorption with flow mode paves the way for the removal of residual antibiotics in milk.

7.1 Introduction

Antibiotics are extensively used in dairy cattle for the treatment of diseases involving bacterial infections, particularly mastitis. Mastitis is the most prevalent disease in cattle and most of the veterinary treatment of dairy cattle involves intramammary infusion of antibiotics to control mastitis [313]. The inappropriate and prohibited veterinary drugs used by negligence or fraud lead to the presence of antibiotics residues in milk, especially at an early stage of lactation [313, 314]. In order to reduce milk resource waste and environmental risk, antibiotics-polluted milk must be collected and treated to obtain qualified or antibiotic-free milk. Thus the purified milk can be reused to feed calves. As mentioned in Section 6.1, MAR is a new fluoroquinolone antibiotic and the maximal MAR concentration in milk after the first administration was observed to be 1.024 µg mL^{-1} [315], which greatly exceeds 0.075 µg mL^{-1} of MRL regulated by European Union Council Regulation 2377/90 [316].

The adsorptive removal of antibiotics from wastewaters [294, 295, 317] and detection of residual antibiotics in milk [288] have been well studied. Adsorption with ACs is considered as an effective and low-cost method for removal of

antibiotics from a few to several hundred µg ml^{-1} in water or wastewater [294, 295, 318]. However, little is known about the adsorptive removal of residual antibiotics in milk by using ACs. In our previous study, the adsorption of IOP in aqueous solutions via ACs in flow mode was much more effective treatment process in comparison with batch mode [284].

Several methods were reported for the detection of antibiotics in milk samples. The most popular method is HPLC hyphenated with different detection systems, e.g. UV, FD, MS, MS/MS [288, 318-325]. In the present study, HPLC with UV detector was chosen to analyze antibiotics in milk samples before and after adsorption [326]. The aims of this study is to remove the residual MAR from milk with ACs in batch and flow systems to meet the MRLs.

7.2 Experimental

7.2.1 Milk samples

Raw milk was purchased from the local markets (Leichter Genuss, Netto, Regensburg, Germany). The milk was stored at 4°C until use. At room temperature, 100 µL of 100 mg mL^{-1} MAR stock solution was put into 100 mL of Mill-Q water to give 100 µg mL^{-1} MAR aqueous solution, which was then diluted into 1.0 µg mL^{-1} with commercial milk.

7.2.2 Adsorption process in batch and flow mode

In batch mode, 50-1000 mg of MGAC and MPAC were put in 20 mL of 1.0 µg mL^{-1} MAR-spiked milk and stirred with 700 rpm at 25°C for 4 h.

In flow mode, 0.5 g of MGAC was filled in a glass column (23 × 1.0 cm I.D.), which corresponded to a 1 cm bed height. The MAR-spiked milk (1 µg mL^{-1}) passed through the MGAC column at 0.5 mL min^{-1} of flow rate. Aliquots (25 or 50 mL interval) of the processed milk were periodically collected at the outlet.

All experiments are duplicated and errors were shown by the difference between the higher measured value and the average value. If the errors are not visible in Figures, they are smaller than the symbols representing the average values. The *RE* value in batch is calculated as equation (4) and the cumulative

loaded amount in flow is calculated as equation (5).

7.2.3 Analytical methods

Milk or antibiotic-spiked milk samples were mixed with acetonitrile (1:1, v/v) and then centrifuged with 14000 rpm for 30 min to remove protein before HPLC/UV analysis. The procedures of milk sample pretreatment for HPLC/UV analysis are depicted in Fig. 7.1. The HPLC was performed using a Waters HPLC system comprising two Waters 515 HPLC samples, a Water 717 plus auto-sampler, a Waters 2487 UV/VIS-Detector, and the Water Empower 3 software. The column used was a KnauerEurospher C18-Column (100 Å, 250 × 4.6 mm). The mobile phases were the mixture of 0.1% of trifluoroacetic acid (TFA, 70%) and acetonitrile (ACN, 30%), which was delivered at a flow rate of 0.8 mL min^{-1}. 50.0 or 150.0 µL of samples was injected and the column was maintained at the room temperature with 60 min detection time.

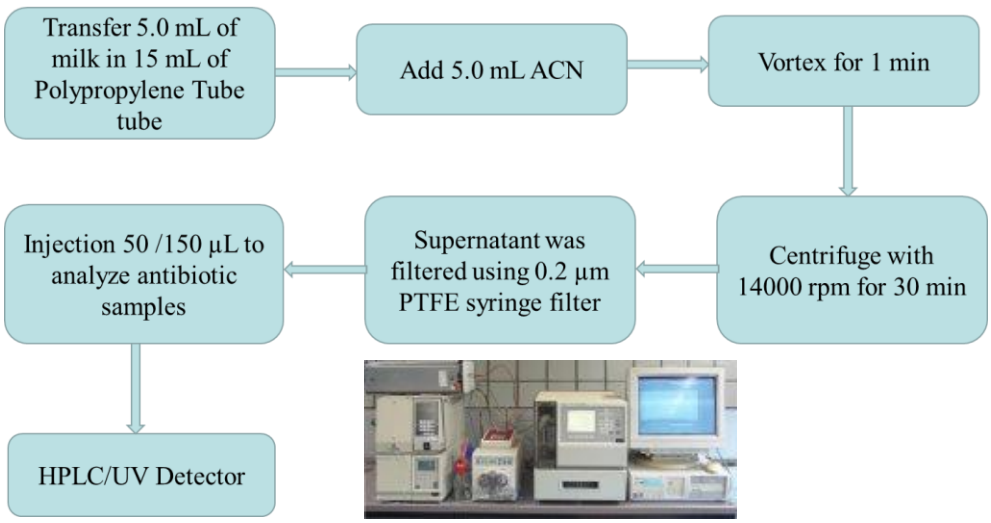

Fig. 7.1 Scheme of HPLC/UV analytical procedures for milk samples

7.3 Results and discussion

7.3.1 Recovery studies

100 µg mL^{-1} of MAR stock solution was prepared with Mill-Q water and then stored at 4°C in the dark. The working solutions of 0.001 to 1 µg mL^{-1} MAR were

obtained by diluting the stock solution before use. The calibration curve was drawn according to the peak areas (*A*) vs concentration of MAR (*C*). As a result, the equation of MAR calibration curve is shown as: $A=333333C+477$, $R^2=0.9997$. The recovery efficiency of pretreatment for the MAR-spiked milk was calculated by the ratio of measurement concentration and spiked concentration after deproteinization. The recovery efficiencies of MAR at various concentration in spiked milk are average of three replicates and listed in Table 7.1. As we seen in Table 7.1, the sample pretreatment exhibited good recovery efficiency and repeatability from RSD values.

Table 7.1 Recovery efficiencies of deproteinization for MAR-spiked milk

MAR-spiked milk after deproteinization (μg mL^{-1})	Recovery efficiency (%)	Relative standard deviation (RSD, %)
1.0	98.7	1.0
0.5	99.8	2.2
0.25	96.9	4.3
0.05	88.9	5.0

7.3.2 Adsorption of marbofloxacin with spiked milk by batch mode

In order to reduce the consumption of ACs, the effect of different MGAC dosages on *RE* was examined and the results are illustrated in Fig. 7.2.

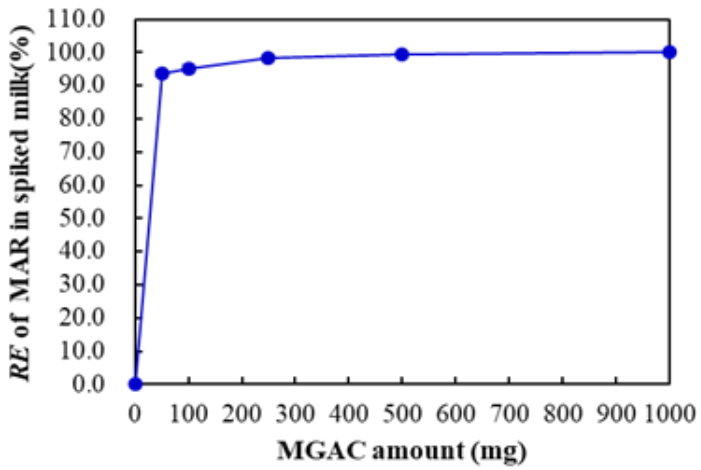

Fig. 7.2 Adsorption of MAR with spiked milk on MGAC

(Adsorption conditions: 50-1000 mg of MGAC in 20 mL of 1.0 μg mL^{-1} MAR-spiked milk and stirred with 700 rpm at 25°C for 4 h)

As shown in Fig. 7.2, *RE* values increased for MAR-spiked samples with the increased amount of MGAC. 93.7%, 95.5%, 98.4%, 99.3% and 100% of *RE*s were achieved with 50, 100, 250, 500 and 1000 mg of MGAC, respectively, and the corresponding residual concentrations were 0.063, 0.045, 0.016, 0.007, and 0.000 μg mL^{-1}, respectively. Obviously, 50 mg MGAC is sufficient for the purification of 20 mL of 1.0 μg mL^{-1} MAR-spiked milk. With other commercial MPAC, 96.8% and 99.1 % of *REs* were obtained using 100 mg and 250 mg of AC amount, respectively, which corresponds to 0.032 and 0.009 μg mL^{-1} of residual concentrations. All of purified samples after adsorption via MGAC and MPAC met the MRL in milk [316].

7.3.3 Adsorption of marbofloxacin with spiked milk by flow system

Adsorption with flow mode is able to handle large volume with high *RE*. Flow mode can provide useful technical support for future industrial applications [284]. The *RE*s of MAR with cumulative volume of MAR-spiked milk is shown in Fig. 7.3.

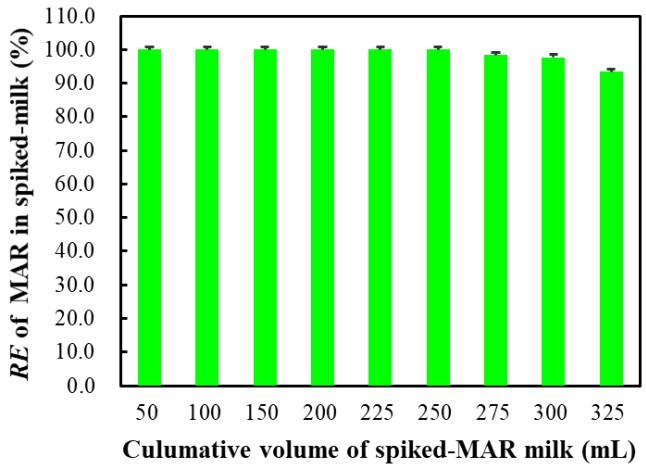

Fig. 7.3 Dependence of *RE* of MAR on the passed volume of spiked milk in flow mode
(Adsorption conditions: 325 mL of 1 μg mL^{-1} MAR-spiked milk passed through a 0.5 g MGAC package column at 0.5 mL min^{-1} (Periodical sampling: 25 or 50 mL aliquots))

As shown in Fig. 7.3, 325 mL of MAR-spiked milk was efficiently purified through the MGAC column and *RE* can reach to 93.4% at the end, corresponding to 0.066 μg mL^{-1} of residual concentration, which meets the MRL of MAR in milk. The load of MAR from the spiked milk onto MGAC was calculated to be 648 MAR/g MGAC. In summary, the purification capacity in the flow mode is 1.6 times higher than that with the batch mode.

References

[313] Priyanka, S. P., Sheoran, M. S., and Ganguly, S. Antibiotic residues in milk a serious public health hazard. Journal of Environment and Life Sciences, 2(2017) 99-102.

[314] European Medicines Agency, Marbofloxacin: Summary report (1)–Committee for Veterinary Medicinal Products, European Public MRL Assessment Report No. EMEA/MRL/079/96-FINAL, 1996.

[315] Schneider, M., Vallé, M., Woehrlé, F., and Boisrame, B. Pharmacokinetics of marbofloxacin in lactating cows after repeated intramuscular administrations and pharmacodynamics against mastitis isolated strains. Journal of Dairy Science, 87 (2004) 202-211.

[316] Aresta, A., Cotugno, P., Zambonin, C. Determination of ciprofloxacin, enrofloxacin, and marbofloxacin in bovine urine, serum, and milk by microextraction by a packed sorbent coupled to ultra-high performance liquid chromatography. Analytical Letters, 52 (2018) 1-13.

[317] Kim, S. H., Shon, H. K., and Ngo, H. H. Adsorption characteristics of antibiotics trimethoprim on powdered and granular activated carbon. Journal of Industrial and Engineering Chemistry, 16 (2010) 344-349.

[318] Bruno, F., Curini, R., Corcia, A. D., Nazzari, M., Samperi, R. Solid-phase extraction followed by liquid chromatography-mass spectrometry for trace determination of β-lactam antibiotics in bovine milk. Journal of Agricultural and Food Chemistry, 49(2001) 3463-3470.

[319] Cinquina, A. L., Roberti, P., Giannetti, L., Longo, F., Draisci, R., Fagiolo, A., Brizioli, N. R. Determination of enrofloxacin and its metabolite ciprofloxacin in goat milk by high-performance liquid chromatography with diode-array detection: Optimization and validation. Journal of Chromatography A, 987(2003) 221-226.

[320] Khosrokhavar, R., Hosseini, M. J., Amini, M., Pirali-Hamedani, M., Ghazi-Khansari, M., Bakhtiarian, A. Validation of an analytical methodology for determination of oxytetracycline residue in milk by HPLC with UV detection. Toxicology Mechanisms and Methods, 18(2008) 351-354.

[321] Samanidou, V. F., Tsochatzis, E. D., Papadoyannis, I. N. HPLC determination of cefotaxime and cephalexine residues in milk and cephalexine in veterinary formulation. Microchimica Acta, 160(2008) 471-475.

[322] Chung, H. H., Lee, J. B., Chung, Y. H., Lee, K. G. Analysis of sulfonamide and quinolone antibiotic residues in Korean milk using microbial assays and high performance liquid chromatography. Food Chemistry, 113(2009) 297-301.

[323] Mahmood, A. H., Medley, G. A., Grice, J. E., Liu, X., Roberts, M. S. Determination of trovafloxacin and MBXbofloxacin in sheep plasma samples by HPLC using UV detection. Journal of Pharmaceutical and Biomedical Analysis, 62 (2012) 220-223.

[324] Nebot, C., Regal, P., Miranda, J. M., Fente, C., Cepeda, A. Rapid method for quantification of nine sulfonamides in bovine milk using HPLC/MS/MS and without using SPE. Food Chemistry, 141(2013) 2294-2299.

[325] Montesano, C., Vannutelli, G., Gregori, A., Ripani, L., Compagnone, D., Curini, R., Sergi, M. Broad screening and identification of novel psychoactive substances in plasma by high-performance liquid chromatography–high-resolution mass spectrometry and post-run library matching. Journal of Analytical Toxicology, 40(2016) 519-528.

[326] Aziz, E. A. A., El-Nabtity, S. M., El Barawy, A. A. M., Saleh, M. A. Determination of marbofloxacin residues in Rabbit Tissues by HPLC. Zagazig Veterinary Journal, 45(2017) 39-46.

Chapter 8: Conclusions and Perspectives

The serious environmental problems caused by pharmaceuticals and other organic pollutants, require the development of efficient and economic technologies for industrial wastewater treatment. Thus, the potential application of specific ACs as adsorbents in highly polluted wastewaters was investigated in this study. The related compounds include COD, PP at high concentration in industrial CW, IOP and phenols in aqueous solutions, antibiotics in aqueous solution and milk. Meanwhile, the regeneration and reuse of adsorbent, as well as the recovery of adsorbates were investigated. Moreover, the ACs were modified to improve their adsorption performance. On the basis of above studies, the mechanisms of adsorption/desorption were illustrated.

The industrial CW was efficiently purified by using the hybrid method of flocculation and adsorption. As pre-treatment, a large fraction of organic matter, such as UV_{254}, COD, PP, TS, TDS and TSS, was removed by using flocculation. The residual organic matters were further removed by adsorption with ACs. As a result, the cooperative flocculation/adsorption has been demonstrated to be an effective and economical method. In order to reduce the consumption of adsorbent and disposal of used adsorbent, the spent ACs were regenerated with MW calcination. The regenerated ACs were robust and permitted five recycles equally. Predictably, this simple and scalable process could afford a promising treatment method for other industrial wastewaters containing high concentration organic matter, such as food processing, brewing and farming industries, etc.

The wastewater containing pharmaceuticals at high concentration should be treated to reduce the discharge of pollutants, simultaneously recovery of high-value pharmaceuticals. In this study, IOP, as model ICAs, was efficiently recovered using simple adsorption/desorption process. In traditional concept, the desorption of adsorbates from ACs is often troublesome. To meet this challenge, hydrophilic IOP loaded onto the ACs was efficiently eluted using either methanol or ethanol and the regenerated ACs by elution were reused for five cycles in a flow mode. Given the benefits of the adsorption/desorption processes, such as simple operations and low-costs, the results of this research could be extended to the extraction of other high-value substances such as contrast agents, drugs and bioactive ingredients.

Phenols are considered priority organic pollutants and often used as model compound for the technology development of wastewater treatment. The adsorptive removal of phenols on ACs is easily achieved, however, the desorption of phenols is still an attractive challenge. The efficient desorption of phenols from ACs with preferable solvents (Lewis basic solvents, acetic acid, and alcohols) and most co-solvents with 0.4% urea (aq) or 3% NH_3 (aq) was achieved, and the flow mode provided complete desorption and regeneration of ACs. The results indicates the basicity, polarity, and hydrogen bonds synergistically affect phenols desorption. It also demonstrated that phenols adsorption is a reversible physical process, clearly showing the feasibility of phenols desorption with proper solvents. This result was also verified by comparison of DRIFT spectra and porosity properties among pristine, loaded and eluted ACs. Overall, our procedure paves the way to eliminate secondary pollution, recover valuable compounds, reuse ACs, as well as reduce the treatment costs. These achievements could open new applications of adsorption/desorption of organic pollutants from industrial wastewaters.

In order to enhance the adsorption performance toward antibiotics such as MAR, WPAC were modified by using MW calcination and oxidation with H_2O_2 under SK, US and MW heating. After the oxidation under SK, *AE* of MAR onto WPAC increased from 70.5% to 88.3%. US or MW heating accelerated the oxidation, but slightly rise *AE* values into 89.3% and 92.5%, respectively. As compared to the oxidation, *AE* of MAR onto modified WPAC reached 89.2% using MW calcination at 600°C for 3 min. Moreover, various ACs were modified with same MW calcination, resulting in greatly enhanced adsorption performance toward MAR. It concludes that the physicochemical properties of ACs collaboratively affect the adsorption performance. Accordingly, the content of oxygen-functional groups, BET, etc. among the pristine and modified ACs should be compared in future, while the improved adsorption performance of ACs should be verified by the adsorption of other antibiotics or organic contaminants. From an economic view, the higher performance of modified ACs can reduce the consumption of adsorbents and the treatment cost.

The adsorptive removal of organic pollutants can not only be applied in wastewater treatment, but also extended to the purification of polluted milk. In the present study, 93.7% of *RE* for 20 mL of 1 μg mL^{-1} MAR-spiked milk onto 50 mg

MGAC was achieved in batch mode, although the competitive adsorption of impurities existed in milk. The resulting residual concentration was 0.063 μg mL^{-1}, which meets the MRL of MAR in food. MPAC exhibited a comparable adsorption performance. By using a flow mode, 325 mL of 1 μg mL^{-1} MAR-spiked milk was efficiently purified via 500 mg MGAC column. 93.4% of *RE* was achieved and the corresponding residual concentration was 0.066 μg mL^{-1}. Thus the flow mode with MGAC showed higher capacity (648 μg MAR/g MGAC) as compared to the batch mode (375 μg MAR/g MGAC). Moreover, in the adsorption process, the composition and nutritional properties of the milk could not be affected. It is the outstanding benefits of the adsorption process: (1) Despite of the presence of competition adsorption of impurities in milk, ACs still exhibited the superior adsorption performance for MAR; (2) The composition and nutritional properties of the milk after the adsorption could be remained. Other antibiotics in polluted-milk could be removed using the above method in future.

To completely implement the adsorption/desorption processes in the future, the following investigations are proposed:

(1) Characterization of modified ACs to verify the mechanism of enhanced performance;

(2) The competitive adsorption treatment the industrial wastewaters of containing different pollutants;

(3) Preparation and application of novel porous carbonaceous materials using enabling technologies;

(4) Comparison with other porous materials for developing more superior adsorbents.

Appendix

1. Refereed Journal Publications

First author research articles:

[1] **Ge, X.**, Wu, Z., Manzoli, M., Jicsinszky, L., Wu, Z., Nosyrev, A. E., Cravotto, G. Adsorptive recovery of Iopamidol from aqueous solution and parallel reuse of activated carbon: batch and flow study. *Industrial & Engineering Chemistry Research*, 58(2019) 7284-7295.

[2] **Ge, X.**, Wu, Z., Cravotto, G., Manzoli, M., Cintas, P., Wu, Z. Cork wastewater purification in a cooperative flocculation/adsorption process with microwave-regenerated activated carbon. *Journal of Hazardous Materials*, 360 (2018) 412-419.

[3] **Ge, X.**, Wu, Z., Manzoli, M., Wu, Z., Cravotto, G., Feasibility and mechanism of desorption of phenolic compounds from activated carbons. *Industrial & Engineering Chemistry Research*, 2020. (Minor revision)

Co-author research articles:

[1] Liu, P., Wu, Z., **Ge, X.**, Yang, X. Hydrothermal synthesis and microwave-assisted activation of starch-derived carbons as an effective adsorbent for naphthalene removal. *RSC Advances*, 9(2019) 11696-11706.

[2] He, X., Wu, Z., Sun, Z., Wei, X., Wu, Z., **Ge, X.**, Cravotto, G. A novel hybrid of β-cyclodextrin grafted onto activated carbon for rapid adsorption of naphthalene from aqueous solution. *Journal of Molecular Liquids*, 255(2018) 160-167.

[3] Ardebili, S. M. S., **Ge, X.**, Cravotto, G. Flow-mode biodiesel production from palm oil using a pressurized microwave reactor. *Green Processing and Synthesis*, 8(2019) 8-14.

2. Conferences

Oral Communications

[1] **Ge, X.**, Wu, Z., Cravotto, G. Adsorptive recovery of pharmaceutical from

aqueous solution and reuse of activated carbon. Merck & Elsevier Young Chemist Symposium, Rimini, Italy, 2018.

[2] Cravotto, G., **Ge, X.**, Moran Plata, M., Martina, K. Harnessing cavitational effects toward achieving green process intensification. 3rd Asia Oceania Sonochemical Society Conference, Chennai, India, 2017.

Poster Communications

[1] **Ge, X.**, Wu. Z., Kunz, W., Alessandro, B., Cravotto, G., Adsorptive removal of marbofloxacin from milk using activated carbons. 16th International Conference on Environmental Science and Technology, Rhodes, Greece, 2019.

[2] **Ge, X.**, Wu, Z., Manzoli, M., Cravotto, G., Wu, Z., Adsorption of *p*-nitrophenol from aqueous solution on activated carbon and desorption assisted by enabling technologies. 7th European Chemical Society, Liverpool, United Kingdom, 2018.

[3] Wu, Z., Alessandro, B., **Ge, X.**, Giancarlo, C. Marbofloxacin degradation using sonication and ozonation in water. 4th Meeting of the Asia-Oceania Society of Sonochemistry, Nanjing University, Nanjing, China, 2019.

[4] Wu, Z., Wang, W., Li. W., Qiu, Z., Liu, P., Wu, Z., **Ge, X.**, Treatment of an organic chemical wastewater by combination of hydrodynamic cavitation and ozonation at a pliot scale. 16th European Society of Sonochemistry, Besancon, France, 2018.

[5] Calcio Gaudino, E., Grillo. G., **Ge, X.**, Cravotto, G., Process intensification in biodiesel production under non-conventional technique. 4th International Congress on Catalysis for Biorefineries, Lyon, France 2017.

Ge, X., Wu, Z., Cravotto, G., Manzoli, M., Cintas, P., Wu, Z. Cork wastewater purification in a cooperative flocculation/adsorption process with microwave-regenerated activated carbon. *Journal of Hazardous Materials*, 360(2018) 412-419.

Journal of Hazardous Materials 360 (2018) 412–419

Contents lists available at ScienceDirect

Journal of Hazardous Materials

journal homepage: www.elsevier.com/locate/jhazmat

Cork wastewater purification in a cooperative flocculation/adsorption process with microwave-regenerated activated carbon

Xinyu Ge[a], Zhilin Wu[a,b], Giancarlo Cravotto[a,*], Maela Manzoli[a], Pedro Cintas[c], Zhansheng Wu[d]

[a] Dipartimento di Scienza e Tecnologia del Farmaco, University of Turin, Turin 10125, Italy
[b] Nanjing Institute of Environmental Science of the Ministry of Environmental Protection of China, Nanjing, China
[c] Departamento de Química Orgánica e Inorgánica and IACYS-Unidad de Química Verde Desarrollo Sostenible, Universidad de Extremadura, 06006 Badajoz, Spain
[d] School of Chemistry and Chemical Engineering, Shihezi University, Shihezi 832003, China

GRAPHICAL ABSTRACT

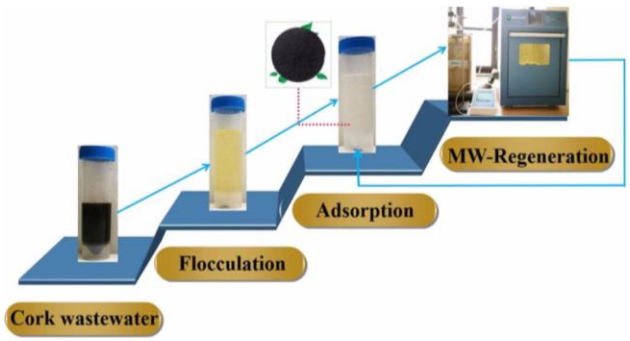

ARTICLE INFO

Keywords:
Cork wastewater
Flocculation
Adsorption
Activated carbon
Microwave-assisted regeneration

ABSTRACT

The aim of this work is to investigate a novel cork wastewater (CW) purification method that combines flocculation/adsorption with the microwave assisted regeneration of coconut powder activated carbon (CPAC). The flocculation treatment made use of $FeSO_4{\cdot}7H_2O$/NaOH and provided high removal efficiency, as shown by the observed values of UV_{254} (90%), chemical oxygen demand (COD, 86%), polyphenols (PP, 81%),total solid (TS, 40%), total suspended solid (TSS, 62%), and total dissolved solid (TDS, 18%). After the flocculation and filtration, CPAC was used to further remove left TSS, TDS and dissolved organics. The effects of CPAC amount, pH value and adsorption time have been studied. It was found that 250 mg is the optimum CPAC amount for the treatment of 50 mL CW at pH 3.5 for 10 min. Overall process effectiveness can be summarised as follows: UV_{254} (100%), COD (98%), PP (100%), TS (58%), TSS (93%), and TDS (24%), while the characteristic colour of the CW completely disappeared. The microwave regenerated CPAC can undergo five runs without appreciable losses in removal efficiency. Predictably, this simple and scalable process could afford a promising treatment method for other industrial wastewaters with high content of organic matters such as PP, phenolic acids and tannins.

* Corresponding author at: Dipartimento di Scienza e Tecnologia del Farmaco, University of Turin, Via P. Giuria 9, I-10125 Turin, Italy.
E-mail address: giancarlo.cravotto@unito.it (G. Cravotto).

Ge, X., Wu, Z., Manzoli, M., Jicsinszky, L., Wu, Z., Nosyrev, A. E., Cravotto, G. Adsorptive recovery of Iopamidol from aqueous solution and parallel reuse of activated carbon: batch and flow study. I*ndustrial & Engineering Chemistry Research*, 58(2019) 7284-7295.

I&EC research
Industrial & Engineering Chemistry Research

Article

Cite This: *Ind. Eng. Chem. Res.* 2019, 58, 7284−7295

pubs.acs.org/IECR

Adsorptive Recovery of Iopamidol from Aqueous Solution and Parallel Reuse of Activated Carbon: Batch and Flow Study

Xinyu Ge,[†] Zhilin Wu,[†,‡] Maela Manzoli,[†] László Jicsinszky,[†] Zhansheng Wu,[§] Alexander E. Nosyrev,[∥] and Giancarlo Cravotto*[,†,∥]

[†]Department of Drug Science and Technology and NIS - Centre for Nanostructured Interfaces and Surfaces, University of Turin, Via P. Giuria 9, Turin 10125, Italy

[‡]Nanjing Institute of Environmental Sciences of the Ministry of Ecology and Environment of China, Jiangwangmiao Street 8, Nanjing 210042, China

[§]School of Chemistry and Chemical Engineering, Shihezi University, Beisilu Street. 280, Shihezi 832003, China

[∥]Institute of Translational Medicine and Biotechnology, First Moscow State Medical University (Sechenov), 8 Trubetskayaul, Moscow 109807, Russia

Supporting Information

ABSTRACT: This study demonstrates the adsorptive recovery of high-concentration Iopamidol (IOP) from aqueous solution. IOP is a highly valuable X-ray iodinated contrast agent (ICA), and the reuse of the adsorbent activated carbon (AC) is via elution with alcohol. Of the adsorbents selected, coconut powder AC (CPAC) displayed the best adsorption performance for IOP. The results of batch investigation into adsorption kinetics, isotherms, activation energy, and thermodynamic calculations support the occurrence of a physisorption process. The adsorption mechanism has been determined using the intraparticle diffusion model. A Boyd plot has revealed that IOP adsorption onto CPAC was mainly governed by particle diffusion. CPAC also exhibited excellent adsorptive performance toward IOP, which was efficiently eluted and recovered using methanol in a semicontinuous flow system. Moreover, the spent CPAC was efficiently regenerated and reused in five adsorption/desorption cycles. The characterization of CPAC samples by SEM, DRIFT, and TGA shows that IOP is absorbed onto CPAC, leading to significant decreases in the BET surface area and pore volume and shift of the pore diameter. $\pi-\pi$, donor−acceptor complex, van der Waals, and hydrogen-bond interactions are governed by the IOP adsorption. Hydrogen-bond interactions between IOP and alcohols play a crucial role in the desorption process. IOP was completely eluted, and the surface properties of CPAC were recovered after elution in the flow system. This study demonstrates that many benefits can be achieved from adsorption/desorption processes, such as those in wastewater treatment and the recovery of valuable compounds, as adsorbent recycling simplifies the operations and reduces treatment costs.

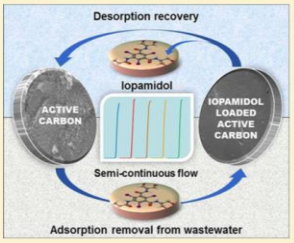

7th European Chemical Society, Liverpool, United Kingdom, 2018.

EuCheMS European Chemical Sciences

7th EuCheMS Chemistry Congress | LIVERPOOL UK 26–30 August 2018

Adsorption of *p*-Nitrophenol from Aqueous Solution on Activated Carbon and Desorption Assisted by Enabling Technologies

Xinyu Ge[1], Zhilin Wu[1], Maela Manzoli[1], Giancarlo Cravotto[1*], Zhansheng Wu[2]

Abstract

The *p*-nitrophenol (PNP) removal has been extensively investigated. Adsorption by activated carbon (AC) is one of the most efficient and used method. Nowadays, the regeneration of spent AC is a challenge for reusing and the recovery of PNP. In this study, AC was characterized by BET, SEM, FTIR, etc. The adsorption removal efficiency, kinetic and isotherm were investigated, and PNP desorption by solvent extraction under stirring, ultrasound (US) and microwave (MW) was performed studying in parallel the mechanism.

Coconut Powder Activted Carbon (CPAC)

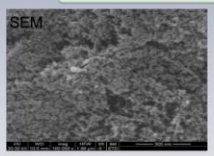

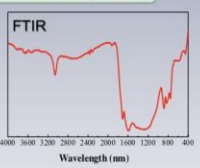

High BET surface area (1952 m^2/g), large pore volume (micropore volume 1.76 cm^3/g, mesopores volume 1.57 cm^3/g), a variety of functional groups.

Adsorption of PNP on CPAC

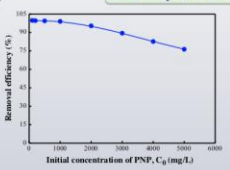

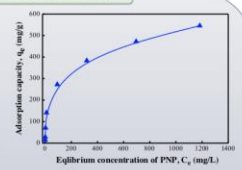

Liquid Phase Parallel Synthesizer
Heidolph Synthesis, Italy

- CPAC amount 350 mg, solution volume 50 mL, adsorption time 10 min at pH 5, vibration speed 450 rpm, temperature 30 °C. (UV/Vis analysis)
- As initial concentrations increase, the removal efficiencies decrease.
- The adsorption isotherm was fitted well by Langmuir isotherm.

Orthoganol array test: desorption of PNP

Group number	Solvents	Volume (mL)	Temperature (°C)	Desorption efficiency (DE, %)
1	Methanol	3	30	60.5
2	Methanol	6	45	65.1
3	Methanol	10	60	70.4
4	Ethanol	3	45	66.4
5	Ethanol	6	60	92.4
6	Ethanol	10	30	94.7
7	2% NaOH	3	60	32.6
8	2% NaOH	6	30	30.5
9	2% NaOH	10	45	62.3
$\bar{A}_1$	65.33	53.17	61.90	
$\bar{A}_2$	84.50	62.67	64.60	
$\bar{A}_3$	41.80	75.80	65.13	
R	42.70	22.63	3.233	

Note: R is the range of $\bar{A}_1$, $\bar{A}_2$ and $\bar{A}_3$ representing the impact extent or importance of one factor.

- PNP amount on CPAC: 141.4 mg/g; CPAC amount: 100 mg
- In terms of R value, solvent is the most critical factor.
- PNP was efficiently desorbed in ethanol.

Role of ultrasound and microwave on desorption

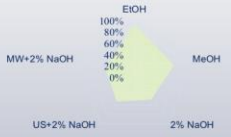

CPAC amount 100 mg; solvent volume 10 mL, desorption time 15 min, vibration speed 450 rpm, temperature 30 °C. (HPLC analysis). Enhanced desorption efficiency were 8% by US at 30 °C and 10%-19% by MW at 100 °C.

Mechanism of adsorption and desorption

CPAC structure

[4]

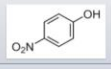

Monolayer surface adsorption
Physical adsorption

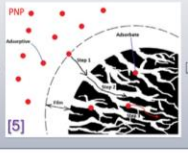

[5]

Desorption in Solvent

Similar polarity between adsorbent and solvent, role of hydrogen bonds, mechanical effect of US, dielectric heating effect.

Acknowledgements & References

The authors thank the University of Turin (Ricerca Locale 2016-2017) and the Junta de Extremadura and Fondo Europeo de Desarrollo Regional (Research grant IB16167) for financial support.

[1] X.Y. Ge, Z.S. Wu, Cravotto, G., et al. *J. Ind. Eng. Chem.* 39(2016) 27-36.
[2] X.Y. Ge, Z.S. Wu, Z.L. Wu, Cravotto, G., et al. *J. Taiwan Inst. Chem. Eng.* 64(2016) 235-243.
[3] X.Y. Ge, Z.S. Wu, Z.L. Wu, Cravotto, G., et al. *Chem. Eng. Process* 91(2015) 67-77.
[4] http://www.aquapuredepot.com/img/category/description/ENPRESS_LIT_ONE.pdf.
[5] K.L. Tan, B.H. Hameed, *J. Taiwan Inst. Chem. Eng.* 74 (2017) 25-48.

* E-mail of the corresponding author: giancarlo.cravotto@unito.it

Conclusion

- ✓ Due to high surface area, pore volume and pore size, CPAC presented high adsorption capacity for PNP.
- ✓ Langmuir model indicates monomolecular layer.
- ✓ The adsorption process for PNP was controlled by intraparticle diffusion, following Fickian mechanism of diffusion.
- ✓ Loaded-PNP was efficiently desorbed in ethanol.
- ✓ Ultrasonic and microwave can enhance efficiency of 2% NaOH desorption.

UNIVERSITÀ DEGLI STUDI DI TORINO

DSTF Dipartimento di Scienza e Tecnologia del Farmaco UNIVERSITÀ DI TORINO

[1]Dipartimento di Scienza e Tecnologia del Farmaco, University of Turin, Torino 10125, Italy,
[2]School of Chemistry and Chemical Engineering, Shihezi University, Shihezi 832003, China.

16th International Conference on Environmental Science and Technology, Rhodes, Greece, 2019.

CEST 2019 16th International Conference on Environmental Science and Technology
CEST2019, 4-7 September 2019, Rhodes, Greece

Adsorptive Removal of Marbofloxacin from Milk using Activated Carbons

Ge Xinyu,[1] Wu Zhilin,[1] Kunz Werner,[2] Alessandro Barge,[1] Carvotto Giancarlo[1,*]
[1]Dipartimento di Scienza e Tecnologia del Farmaco, University of Turin, Via Pietro Giuria 9, Turin 10125, Italy.
[2]Department of physical Chemistry, University of Regensburg, Universitaetsstr. 31, Regensburg 93053, Germany.

Introduction

- **Background:** Antibiotics are extensively used in dairy cattle for the treatment of diseases involving bacterial infections, particularly mastitis [1]. The inappropriate and prohibited veterinary drugs used by negligence or fraud lead to the presence of antibiotics residues in milk, especially at an early stage of lactation. Marbofloxacin (MAR) is a new fluoroquinolone antibiotic [1, 2].
- **Aims:** To remove the residual MAR from milk with various activated carbons (ACs) in batch and flow systems to meet the maximum residue limits (MRLs, 0.075 μg/mL).
- **Perspective:** The purified milk can be reused to feed calves.
- **Innovative:** New adsorptive method for removal of antibiotics in milk [3].

Methods

1. Batch mode: 50 mg of AC was added in 20 mL of 1 μg/mL MAR-spiked milk and stirred at room temperature.

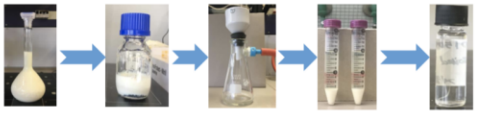

Fig. 1 Sample preparation and adsorption process in batch mode

2. Flow mode: 0.5 g CGAC was filled in 1.0 cm×23 cm column about 1 cm and used for adsorption of 1 μg/mL MAR-spiked milk with 0.5 mL/min.

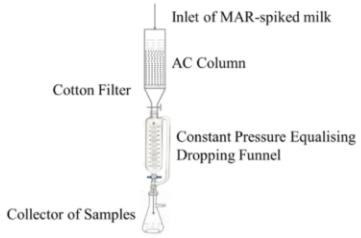

Fig. 2 Adsorption setup in flow mode [4]

3. Deproteinization: milk sample/ACN (1:1, v/v) , centrifugation 30 min.

4. HPLC/UV analysis: mobile phase of 0.1% of TFA (70%) and ACN (30%); flow rate: 0.8 mL/min; injection volume: 50 μL; column temperature: 25 °C, detection time: 60 min.

Results

1. Adsorption of MAR in spiked milk in batch mode

Table 1 The effect of AC amounts for adsorption of MAR

Amount of CGAC (mg)	MAR removal efficiency (RE, %)	Residual concentration (RC, μg/mL)
50	93.7	0.063
100	95.5	0.045
250	98.4	0.016
500	99.3	0.007
1000	100	0

Note: Commercial Granular Activated Carbon (CGAC)

In batch mode, 93.7% of RE and 0.063 μg/mL of MAR residue were achieved with 50 mg CGAC in 20 mL milk to meet the MRLs. Additionally, 99.1 % of RE was achieved with 250 mg of Commercial Powder AC (CPAC), which corresponds to 0.009 μg/mL of RC.

2. Adsorption of MAR in spiked milk in flow mode

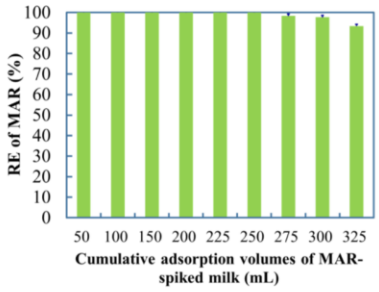

Fig. 3 Dependence of RE of MAR on the passed volume of spiked milk

In flow mode, 325 mL of 1 μg/mL MAR-spiked milk was efficiently purified through 500 mg CGAC in column and 93.4% of RE and 0.066 μg/mL of MAR residue were attained for meeting the MRLs.

Conclusions

Pollutant MAR was efficiently, economically and conveniently removed from milk using ACs, despite of the presence of obvious competition adsorption of impurities. Significant high amount of spiked milk (1.6 times higher in volume) was purified by flow process as compared with batch mode. The flow adsorption with ACs paves the way for the removal of antibiotics in milk.

References

1. Priyanka, S.P., et al., J. Environ. Eng. Sci., 2017, 2: 99-102.
2. European Medicines Agency, 1996.
3. Peng, B. , et al., Sci. Rep-UK, 2016, 6: 31920.
4. Ge, X.Y., et al., Ind. Eng. Chem. Res., 2019, 58 (17): 7284-7295.

Acknowledgements

The authors gratefully acknowledge financial support from University of Turin (Ricerca Locale 2018-2019) and thank Apl. Prof. Rainer Muller, Dr. Theresa, Dr. Marcel from University of Regensuburg.

* E-mail of the corresponding author: giancarlo.cravotto@unito.it

Resume

University of Turin,
Via Pietro Giuria 9, Turin, 10125, Italy

Xinyu GE
xge@unito.it; +39-3272805099

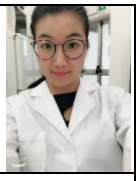

Education

Doctoral student in Natural Sciences and Innovative Technologies

2016.10- 2020.05	Department of Drug Science and Technology, Doctoral School in Nature Sciences and Innovative Technologies, University of Turin, Turin, Italy. Thesis: Process development for the adsorption/desorption of pharmaceuticals and other organic pollutants from industrial wastewater. Supervisor: Prof. Giancarlo Cravotto (University of Turin).

Postgraduate student in Environmental Chemical Engineering

2013.09- 2016.06	Department of Environmental Chemical Engineering, Shihezi University, Shihezi, China. Thesis: Microwave-assisted modification of coal-based activated carbons and application for polycyclic aromatic hydrocarbons (PAHs) from aqueous solution: adsorption properties and mechanism. Supervisor: Prof. Zhansheng Wu (Shihezi University).

Bachelor student in Applied Chemistry

2009.09- 2013.06	Department of Applied Chemistry, Shihezi University, Shihezi, China. Thesis: Preparation of coal-based activated carbons via microwave irradiation for the adsorption of naphthalene. Supervisor: Prof. Zhansheng Wu (Shihezi University).

Professional Skills and Competence

Experimental Skills	- Proficient in literatures, reviews and normal laboratory techniques; - Enable to prepare and modify porous carbon materials by microwave-assisted method; - Adsorptive recovery of valuable compounds from wastewaters using a flow mode; - Regeneration of spent activated carbons with solvents elution, microwave heating and ultrasonic technologies; - Purification of wastewaters highly polluted with PAHs, polyphenols, phenols, pharmaceuticals, as well as antibiotics-polluted milk by adsorption or hybrid technologies; - General analytical methods of materials, such as SEM, TEM, XPS, XRD, FTIR, DRIFTS, BET, TGA, HPLC/UV, UV/Vis, COD, polyphenol, total suspended solids (TSS), total dissolved solids (TDS), and total solids (TS).
Technical Skills	- Specialized software: Origin, ChemDraw, JabRef, SpectraGraph, XPS peak, Microsoft Office.
Linguistic Skills	- English: College English Test-Six, China (452/710, qualified); College English Test-Four, China (493/710, qualified); - During my doctoral studies in Italy, I developed strong academic communication skills in reading, listening, speaking and writing.